NTNU
Innovation and Creativity

Stability Analysis of EKF - based Attitude Determination and Control

Karianne Knutsen Tønne

Master of Science in Engineering Cybernetics
Submission date: May 2007
Supervisor: Jan Tommy Gravdahl, ITK

Norwegian University of Science and Technology
Department of Engineering Cybernetics

Problem Description

The thesis covers the topics of attitude determination and control for the planned ESMO spacecraft. The Extended Kalman Filter (EKF) is to be used for attitude determination.

Assignments:

• Investigate the concept of nonlinear separation principle

• Analyze the stability properties of the Extended Kalman Filter (EKF) in general and apply this to an attitude determination system for ESMO

• Analyze the stability properties of attitude controllers for ESMO

• Analyze the stability of the combined attitude control/determination system

• Simulate the attitude control/determination system

Assignment given: 08. January 2007
Supervisor: Jan Tommy Gravdahl, ITK

Stability analysis of EKF - based attitude determination and control

Karianne Knutsen Tønne
kariannetonne@gmail.com

May 31, 2007

Preface

This work is the concluding part of the Master Degree at Norwegian University of Technology and Science (NTNU), Department of Engineering Cybernetics. The assignment was given and developed by Jan Tommy Gravdahl in co-operation with the Norwegian SSETI team at Narvik University College.

Great thanks to all my fellow students at GG48 for a very positive and supporting environment, and for all the good advices on how to use LaTex. Also great thanks to my adviser Jan Tommy Gravdahl for his support and guidance throughout this project.

May 31, 2007

Karianne Knutsen Tønne

Abstract

This thesis is a part of the SSETI (Student Space Exploration Technology Initiative) project, where students from several universities around Europe work together with the European Space Agency (ESA) with designing, building, testing and launching an Earth-Moon satellite orbiter (European Student Moon Orbiter (ESMO).

A satellite model with reaction wheels placed in tetrahedron was deduced in a preliminary study together with an extended Kalman filter to estimate the attitude from star measurements.

The stability and convergence properties of this system are studied in this thesis. Previous studies on the convergence of extended Kalman filter are presented and a proof of exponentially convergence of a system with extended Kalman filter is given and used to prove that ESMO with the extended Kalman filter converges exponentially.

The most recent work and different methods to apply a nonlinear separation principle is presented. Three feedback controllers with proof of global asymptotic stability (GAS) is then introduced and implemented on ESMO. Based upon the global asymptotic stability of the feedback controllers, and the proof that the extended Kalman filter works as an exponentially observer, a nonlinear separation principle is deduced. The closed loop system can then be stated globally asymptotically stable based upon the deduced separation principle.

The closed loop with the three different controllers is then simulated in Simulink for varying gains and different reference steps. The three controllers show stable characteristic as the theory implies. The robust controller shows best tracking and estimation properties, it is very accurate, simple, robust and adaptable to environmentally changes, and is therefore proposed as the most suitable controller for ESMO.

Contents

Chapter 1

Introduction

This thesis is a study of attitude determination using extended Kalman filter, stability and feedback control for the ESMO satellite, in co-operation with SSETI educational program in ESA. The main subject is to continue the work done previously on attitude determination by implementing feedback control and prove stability of the feedback loop.

1.1 SSETI Project

The European Space Agency (ESA) decided in 2000 to create a project that would make students around Europe actively involved in real space missions. The result was the Student Space Exploration and Technology Initiative (SSETI). Since then, the association has grown and involves more than 21 different Universities across Europe in 12 different nations.

The main goal of the SSETI is to motivate today's students to work in the fields of science and space technology, by giving them hands on experience with real space missions.

The satellite projects with SSETI are being designed, modeled, constructed and tested at a distributed level. This means that every university participating get responsibility for the construction of one subsystem. ESA contributes with the coordination between all the participants by offering news and ftp servers and IRC meetings. They also arrange two workshops every year where all the teams meet up presents their work and discuss further action, as well as getting valuable advices and inputs from experts at ESA.

The mission structure for the SSETI program is given:

Mission 0	SSETI Express	Launching: 2005
Mission 1	ESEO - Earth Orbiter	Launching: 2008
Mission 2	ESMO - Moon Orbiter	Launching: 2011
Mission 3	ESMR - Moon Rover	Launching: unknown

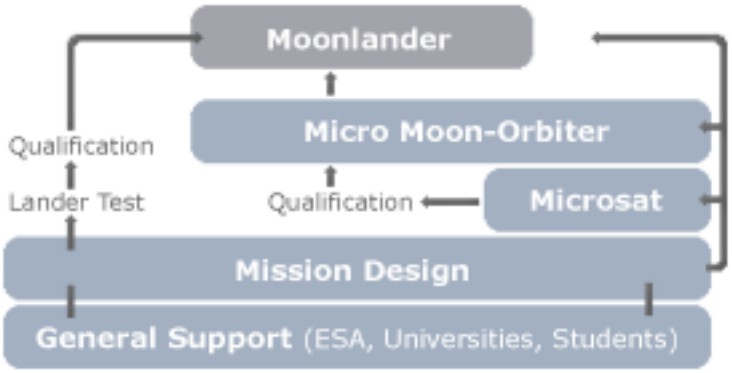

Figure 1.1: Project plan

So far, the SSETI Express is the only one launched, and the mission proved to be successful. The ESEO is already come very far in the design and construction, and is planned launched late 2008. The ESMO satellite is still only in a very early design stage.

1.1.1 SSETI Express and ESEO

The SSETI Express was almost a rescue operation for the whole SSETI project. Both motivation and ambition started slowly to fade as the complexity of the ESEO's submodules proved to be time consuming, and progressed very slowly. By taking advantage of all the work done so far, the SSETI Express was created and launched only eighteen months after the birth of the project. The success of SSETI Express motivated the students and once again the enthusiasm for student space community rose. All the experience gained from this mission is used in the ESEO and ESMO and all future student satellite projects.

The SSETI Express had several task to employ on its flight. Three educational student CubeSat pico-satellites from Japan, Germany and Norway were brought as passengers, and released in low-earth orbits. This is the first time in the history that a spacecraft is used to place other satellites into earth orbit. The other mission objectives for this flight was to take picture of the earth and function as a radio transponder for global amateur radio community, and at the same time, act as a test-bed and demonstrator for the ESEO hardware.

The SSETI Express was launched 27th of October 2005. The mission had a prema-

ture ending, most likely a failure in the electrical power system on board prevented the spacecraft from re-charging its batteries. The project was still concluded a success as two of its main missions were fulfilled successfully.

Figure 1.2: SSETI Express

The ESEO (European Student Earth Orbiter) is still under construction and is scheduled to be launched in late 2008. It is far more complex then the previous SSETI Express and the mission objectives for this satellite are more extensive than that for the Express. The plan is to launch ESEO directly into a geo-stationary orbit using the Ariane 5 launch vehicle. This is called a piggyback launch as the satellite starts the journey with one main passenger and up to seven other micro satellites. This method is used to limit and spread the enormous cost of a spacecraft launch over several participants. The nominal mission shall end 28 days after separation from launcher. ESEO is suppose to test a propulsion system for orbit manoeuvres. It is also going to deploy integrated radiation dosimeters within OBDH nodes and central PC Box to monitor radiation dosage during mission, and take picture of the moon to increase the enthusiasm for the third and fourth SSETI missions to the moon.

1.1.2 ESMO - European Student Moon Orbiter

ESMO is the 3rd SSETI satellite mission and is also a big milestone in the history of space missions, as it will be the first student satellite orbiting the moon. It is only in the early design stages, but by using previous knowledge from ESEO and SSETI Express, it will hopefully be able to meet the launch date set in late 2011.

The mission objectives for this satellite are as before to give students the opportunity to get hands-on experience on actual spacecrafts and educate young people to a career in the European space industry. The more technical assignments during its

life in orbiting the moon, will be to take picture of the moon, 3D mapping of lunar surfaces and measure variation in lunar radiation and gravity.

1.1.3 ESMR - European Student Moon Rover

The ESMR is SSETI biggest dream and ambition as it one day hopes to be able to successfully land on the moon. The vehicle is planned to be a rover capable of moving around on the moon surface.

1.2 Previous work done on ESMO

The ESMO mission is SSETI's third student satellite mission and is only in its starting face yet. The Norwegian team has responsibility for the control system, and a few studies on this has already been performed.

Both Lund and Simonsen (Narvik 06) studied the dynamics and attitude determination for the ESMO satellite. In [1], a very good mathematical model based upon values from ESEO, is derived for the ESMO satellite. While in [2], this model is linearized and used together with a discrete Kalman filter to determine attitude for the ESMO satellite. Although some assumptions are made, a good and to some degree realistic result is achieved where the KF removes noise from the measurements and estimate the state with high accuracy.

In the preliminary studies to this thesis [3], attitude determination is taken one step further by implementing extended Kalman filter on the previous derived ESMO model. The accuracy of the attitude determination is here tested for one and two star sensors and for different sampling frequencies. The result from the simulations here, shows that double star sensor with highest possible sampling frequency gives the most accurate response, although more computational power is needed. Even so, for single star sensor and medium frequency, the error in estimated state is still within the required accuracy of 0.01°.

1.3 Motivation and goals

The motivation for this thesis is to be a part of a larger team, designing, building, testing and then launching a real satellite moon-orbiter. The ESMO is the third and so far most complex and challenging mission for the SSETI. The demand for an accurate and robust determination and control system to decide and control the attitude is huge as to be able to manoeuvre the satellite into desired working points

The goal for this thesis is to implement a feedback controller on the previous developed attitude determination system, and thereafter prove that the overall closed-loop system is globally asymptotically stable. Since the system is nonlinear and

depending on state estimation from an extended Kalman filter, the main objective for this thesis will be to prove that a nonlinear separation principle yields for the system.

1.4 Outline of this thesis

Chapter 2

In this chapter, mathematical background and notation is given, followed by a section where the satellite dynamics of ESMO is derived. Discretizing of the nonlinear model is also done here, together with linearizing and a short presentation of the extended Kalman filter with the filter equation in discrete form are presented. All the work in this chapter was also derived in the preliminary studies to this thesis. [3]

Chapter 3

Three feedback controllers are introduced here, a short presentation of PD control, both nonlinear and linear case and a robust controller are shortly presented, followed by a brief discussion.

Chapter 4

In chapter 4 basic nonlinear stability notation and terms are given. Different types of stability are briefly presented followed by the most important Lyapunov stability tool used later in the thesis.

Chapter 5

The linear separation principle is proved generally in this chapter together with stability analysis of the linearized ESMO attitude determination system given in [2].

Chapter 6

Quite a lot of work is done previous in establishing a nonlinear separation principle, and some of the most important work is presented in this chapter. Also, the most evident work done on stability and convergence of the extended Kalman filter is introduced here.

Chapter 7

In this chapter the convergence of the extended Kalman filter proposed for ESMO is established. It is also seen here that EKF can behave as an exponential observer for ESMO.

Chapter 8

Proof of stability of the proposed controllers can be found in this chapter. Based upon this and the exponentially convergent observer, a nonlinear separation principle for the feedback loop combining ESMO dynamics, EKF and controller is proposed her as the main result of this thesis.

Chapter 9

Implementation and simulation of the feedback loop is carried out in this chapter. All the controllers are being simulated for different gains and its properties are discussed corresponding with the needs of ESMO.

Chapter 10

Conclusion, recommendations and further work are proposed her.

Chapter 2

Attitude determination on ESMO

2.1 Notations and definitions

To be able to study the arts of attitude determination, there are some basic definitions and notations which are important to be familiar with. In this section some ways of representing satellite motion and attitude as vectors, reference frames and rotation matrices will be illustrated. The symbols and definitions presented in this section will be used extensively throughout this thesis.

2.1.1 Vectors

Vectors are used to represent forces, torques, velocity and accelerations. The vector can be represented by its magnitude and its direction; this is called a coordinate free vector representation. The vector can also be expressed in terms of coordinates in different reference frames, i.e. in the Cartesian coordinate frame. If the Cartesian coordinate frame is defined by three orthogonal unit vectors $\vec{i}$, $\vec{j}$ and $\vec{k}$ along the x_1, x_2 and x_3 axis. The vector can be represented as:

$$\vec{v} = v_1\vec{i} + v_2\vec{j} + v_3\vec{k} \tag{2.1}$$

And further on as a coordinate vector:

$$\mathbf{v}^a = \begin{bmatrix} v_1 \\ v_2 \\ v_3 \end{bmatrix} \tag{2.2}$$

The subscript a denotes the coordinate frame $\mathbf{v}$ is expressed in.

There are some mathematical definitions that are quite useful to be familiar with

when using vectors in representing attitude. The scalar or dot product in terms of coordinate vectors:

$$\vec{u} \cdot \vec{v} = \begin{bmatrix} v_1 & v_2 & v_3 \end{bmatrix} \begin{bmatrix} u_1 \\ u_2 \\ u_3 \end{bmatrix} = u_1 v_1 + u_2 v_2 + u_3 v_3 = \mathbf{u}^T \mathbf{v} \tag{2.3}$$

The vector cross product with reference to the Cartesian i, j, k frame:

$$\vec{u} \times \vec{v} = \begin{vmatrix} \vec{i} & \vec{j} & \vec{k} \\ u_1 & u_2 & u_3 \\ v_1 & v_2 & v_3 \end{vmatrix} = (u_2 v_3 - v_2 u_3)\vec{i} + (v_1 u_3 - u_1 v_3)\vec{j} + (u_1 v_2 - v_1 u_2)\vec{k} = \begin{pmatrix} u_2 v_3 - v_2 u_3 \\ v_1 u_3 - u_1 v_3 \\ u_1 v_2 - v_1 u_2 \end{pmatrix} \tag{2.4}$$

The *skew-symmetric* form of the vector $\mathbf{u}$ is introduced by [4] as:

$$\mathbf{u}^{\times} = \mathbf{S}(u) := \begin{pmatrix} 0 & -u_3 & u_2 \\ u_3 & 0 & -u_1 \\ -u_2 & u_1 & 0 \end{pmatrix} \tag{2.5}$$

2.1.2 Rotation matrices

Vector Coordinate Transformation

As showed earlier in this section, vectors can be represented in different coordinate frames. In order to work with several vectors presented in different frames, a method for transforming a vector into different coordinate frames is needed. This is achievable by using rotation matrix:

$$\mathbf{v}^a = \mathbf{R}_b^a \mathbf{v}^b \tag{2.6}$$

where $\mathbf{R}_b^a$ is the rotation matrix from a to b.

The rotation matrix is therefore a tool to transform vector represented in one frame to another while preserving the vector length. It also describes the orientation between two reference frames and rotates a vector within a reference frame. Some properties about the rotation matrix are important to mention.

- $\mathbf{R}_b^a \mathbf{R}_a^b = \mathbf{I} \Leftrightarrow \mathbf{R}_b^a = (\mathbf{R}_a^b)^{-1}$
- $\det \mathbf{R}_b^a = 1$
- $\mathbf{R} | \mathbf{R} \in R^{3\times 3}$

All these properties need to be fulfilled for the matrix to be a rotation matrix.

It can also be useful to know the differential equation of the rotation matrix.

$$\dot{R}_b^a = R_b^a S(\omega_{ab}^a) = R_b^a \times \omega_{ab}^a \tag{2.7}$$

Where the $S(\cdot)$ denotes the skew symmetric matrix.

Composite rotations are rotations between several frames. A rotation from frame a to frame c is performed by a rotation from a to b, and then b to c.

$$\mathbf{v}^a = \mathbf{R}_b^a \mathbf{R}_c^b$$

Simple rotations

A plane or a simple rotation is a single rotation about a fixed axis. There are a total of three simple rotations. Rotation ϕ around x-axis, θ around the y-axis and ψ around the z-axis.

$$\mathbf{R}_x(\phi) = \begin{pmatrix} 1 & 0 & 0 \\ 0 & cos\phi & -sin\phi \\ 0 & sin\phi & cos\phi \end{pmatrix} \tag{2.8}$$

$$\mathbf{R}_y(\theta) = \begin{pmatrix} cos\theta & 0 & sin\theta \\ 0 & 1 & 0 \\ -sin\theta & 0 & cos\theta \end{pmatrix} \tag{2.9}$$

$$\mathbf{R}_z(\psi) = \begin{pmatrix} cos\psi & -sin\psi & 0 \\ sin\psi & cos\psi & 0 \\ 0 & 0 & 1 \end{pmatrix} \tag{2.10}$$

Angle axis

The rotation matrix R_b^a can be described as a rotation θ about a unit vector $\vec{k}$. This is referred to as angle axis parameterization. The rotation matrix will then be expressed as:

$$R_b^a = \mathbf{R}_k \equiv cos\theta \mathbf{I} + \mathbf{k}^{\times} sin\theta + \mathbf{k}\mathbf{k}^T(1 - cos\theta) \tag{2.11}$$

2.2 Attitude

There are two main representations used in attitude determination which are important to be familiar with in order to analyse the mathematics behind attitude determination and control. These two representations are Euler angles and Euler parameters or quaternions.

2.2.1 Euler angles

It is possible to use the rotation matrix $\mathbf{R}_b^a$ to describe the attitude of a spacecraft through the unit vectors of the body attached to it. A total of nine parameters will come out of it (3x3 matrix). Because of the demand for orthogonality in the matrix, six constraint needs to be fulfilled, leading to only three independent parameters describing the rotation. The Euler angles represent a set of these three parameters that can be used to describe the attitude of a rigid body. The Euler angles consist of three independent-simple rotations that take the fixed frame and make it coincide with the body. The rotation matrix is then given as a composite of rotations about the x, y and z- axis. The composite of rotations is not fixed; there are several combinations that work well. I.e the roll, pitch and yaw composite also known as the Bryan's angles which is combined of a rotation ψ around the z-axis, rotation θ around the y-axis and rotation ϕ around the x-axis. This can also be described as a 3 2 1 rotation matrix. Other examples of combinations are the Cordan angles (1 2 3) and the original Euler angle combination (3 1 3). An example of the Bryan angles is shown below:

$$\mathbf{R} = \mathbf{R}_z(\psi)\mathbf{R}_y(\theta)\mathbf{R}_x(\phi) \tag{2.12}$$

where the $\mathbf{R}_z(\psi)$, $\mathbf{R}_y(\theta)$ and the $\mathbf{R}_x(\phi)$ is given by equation (2.8), (2.9) and (2.10) which leads to

$$\mathbf{R}_b^a = \begin{bmatrix} c\theta c\psi & s\theta s\phi s\psi - c\phi s\psi & s\theta c\phi c\psi + s\phi s\psi \\ c\theta s\psi & s\theta s\phi c\psi + c\phi c\psi & s\theta c\phi s\psi - s\phi c\psi \\ -s\theta & c\theta s\phi & c\theta c\phi \end{bmatrix} \tag{2.13}$$

There are some pro's and con's with this representation. The positive aspects are that it is physically intuitive and there are no redundant parameters. On the negative side, Euler angles suffers from singularities at given orientations. I.e the Bryan angles is singular at $\theta = \pm 90\,\text{deg}$ and creates a gimball lock at this angle, or in other words, one of the angles will be cancelled out so that only two independent angles remains.

2.2.2 Euler parameters and Quaternion

Euler parameters where introduced by Euler in 1770 and is basically the same as what Hamilton devised as quaternion in 1843, they only differs in notation. A

quaternion is by definition a complex number with one real part and three imaginary parts. The real part in Euler angles is denoted by η, while the complex number is given by a vector of three ϵ. η and ϵ is defined by an angle axis parameter θ and a vector $\mathbf{k}$.

$$\eta = cos\frac{\theta}{2} \tag{2.14}$$

$$\boldsymbol{\epsilon} = \boldsymbol{k}sin\frac{\theta}{2} \tag{2.15}$$

The rotation θ around the axis is given by the unit vector $\mathbf{k}$. Extension to the complex numbers (η, ϵ_1, ϵ_2, ϵ_3) is bounded by the constraint:

$$\eta^2 + \boldsymbol{\epsilon} \cdot \boldsymbol{\epsilon} = \eta^2 + \boldsymbol{\epsilon}^T\boldsymbol{\epsilon} = \cos^2\frac{\theta}{2} + sin^2\frac{\theta}{2} = 1 \Leftrightarrow \epsilon_1^2 + \epsilon_2^2 + \epsilon_3^2 + \eta^2 = 1 \tag{2.16}$$

By representing the attitude in this manner, it will not suffer from singularities, as with the Euler angles representation. It gives a rational expression of the rotation matrix as opposed to the angle-axis representation which is in trigonometrical terms.

By using some trigonometrical tricks and the above definition of Euler parameters, we can deduce a rotation matrix based on Euler parameters. Note that:

$$sin\theta = 2sin\frac{\theta}{2}cos\frac{\theta}{2} \tag{2.17}$$

$$cos\theta = cos^2\frac{\theta}{2} - sin^2\frac{\theta}{2} = 2cos^2\frac{\theta}{2} - 1 = 1 - 2sin^2\frac{\theta}{2} \tag{2.18}$$

By using this in equation (2.11)

$$\mathbf{R}_k = (2cos^2\frac{\theta}{2} - 1)\mathbf{I} + 2sin\frac{\theta}{2}cos\frac{\theta}{2} \cdot \mathbf{k}^\times + 2sin^2\frac{\theta}{2}\mathbf{k}\mathbf{k}^T \tag{2.19}$$

Next step is to apply the definition of Euler parameter in the above equation. It is used that

$$\eta^2 = cos^2\tfrac{\theta}{2},\ \boldsymbol{\epsilon}^T\boldsymbol{\epsilon} = sin^2\tfrac{\theta}{2},\ \eta\boldsymbol{\epsilon}^\times = sin\tfrac{\theta}{2}cos\tfrac{\theta}{2}$$

the rotation matrix can now be expressed as

$$\boldsymbol{R}(\eta, \boldsymbol{\epsilon}) = (2\eta^2 - 1)\mathbf{I} + 2\eta\boldsymbol{\epsilon}^\times + 2\boldsymbol{\epsilon}^T\boldsymbol{\epsilon} \tag{2.20}$$

$$= \mathbf{I} + 2\eta\boldsymbol{\epsilon}^\times + 2\boldsymbol{\epsilon}^\times\boldsymbol{\epsilon}^\times \tag{2.21}$$

The total rotation matrix on component form will then be:

$$R(\eta,\epsilon)=\begin{bmatrix}\eta^2+\epsilon_1^2-\epsilon_2^2-\epsilon_3^2 & 2(\epsilon_1\epsilon_2-\eta\epsilon_3) & 2(\epsilon_1\epsilon_3+\eta\epsilon_2)\\ 2(\epsilon_1\epsilon_2+\eta\epsilon_3) & \eta^2-\epsilon_1^2+\epsilon_2^2-\epsilon_3^2 & 2(\epsilon_2\epsilon_3-\eta\epsilon_1)\\ 2(\epsilon_1\epsilon_3-\eta\epsilon_2) & 2(\epsilon_2\epsilon_3+\eta\epsilon_1) & \eta^2-\epsilon_1^2-\epsilon_2^2+\epsilon_3^2\end{bmatrix} \tag{2.22}$$

By defining the Euler parameter as quaternions $Q=\begin{bmatrix}\eta\\ \epsilon\end{bmatrix}$ it is possible to use all the mathematical tools for quaternions on the system. I.e the quaternion product:

$$Q=\begin{bmatrix}\eta\\ \epsilon\end{bmatrix}\otimes\begin{bmatrix}\eta\\ \epsilon\end{bmatrix}=\begin{bmatrix}\eta^2+\epsilon^T\epsilon\\ -\epsilon^\times\epsilon\end{bmatrix} \tag{2.23}$$

$$Q^TQ=\eta^2+\epsilon^T\epsilon=1 \tag{2.24}$$

Rotations by quaternion are done in [4].If $R=R_e(\eta,\epsilon)$ is the rotation matrix corresponding to the Euler parameters η and ϵ. $\mathbf{v}\in R^3$. $\mathbf{Rv}$ is then either the coordinate vector of the vector $\mathbf{v}$ in some other frame, or the rotation of vector $\mathbf{v}$. The transformation $\mathbf{Rv}$ can then be achieved with Euler parameters and quaternion product:

$$\begin{bmatrix}0\\ \mathbf{Rv}\end{bmatrix}=\begin{bmatrix}\eta\\ \epsilon\end{bmatrix}\otimes\begin{bmatrix}0\\ \mathbf{v}\end{bmatrix}\otimes\begin{bmatrix}\eta\\ -\epsilon\end{bmatrix} \tag{2.25}$$

$$=\begin{bmatrix}\eta\epsilon^T\mathbf{v}-\eta\epsilon^T\mathbf{v}-\epsilon^T\epsilon^\times\mathbf{v}\\ \eta^2\mathbf{v}+2\eta\epsilon^\times\mathbf{v}+\epsilon\epsilon^T\mathbf{v}+\epsilon^\times\epsilon^\times\mathbf{v}\end{bmatrix} \tag{2.26}$$

$$=\begin{bmatrix}0\\ (\mathbf{I}+2\eta\epsilon^\times+2\epsilon^\times\epsilon^\times)\mathbf{v}\end{bmatrix} \tag{2.27}$$

2.3 Coordinate, Reference frames and Transformation between frames

A reference frame is a coordinate system in which a system is observed. It consists of a set of axis, relative to which an observer can measure position and motion of all points in a system, in addition to the orientation of all objects in the frame. There are basically two types of reference frames: inertial and non inertial.

2.3.1 Reference Frames

Inertial reference frames

The inertial reference system is a coordinate system in which Newton's first and second laws are valid. It can translate at a constant velocity, but it does not rotate, and its origin moves with constant velocity along a straight line. An object within

the frame only accelerates when a physical force is applied. The earth is usually used as an inertial reference frame, but the sun or the moon could also be treated as inertial systems. By defining the moon as an inertial reference system, the origin of the frame will coincide with the centre of the moon. The axes will be placed as shown in the figure 2.1.

Non - inertial reference frames

Non inertial reference frames accelerates and/or rotates without appropriate force applied. Newton's second law does not hold in non inertial reference frames. There are several frames worth mentioning in this section.

Earth centred Earth fixed frame / Moon centred Moon fixed
As with the Inertial frame, this frame has its origin at the centre of the earth, but the axis rotates relative to the inertial frame with an angular rotation ω_e which is equal the rotation of the whole inertial system (Earth rotation when it is fixed to earth).

Orbital moving frame The orbital reference frame rotates in a polar orbit over the geographical poles of the earth (or in this case the moon) with an angular velocity ω_0 relative to the chosen inertial frame. The z-axis points toward the origin of the inertial frame, x-axis points toward the tangent of the orbit while the z-axis is orthogonal with the orbit and completes the right hand rule. The attitude is now described by the roll, pitch and yaw angles around the x, y and z axis respectively, and relative to the orbit frame. Denoted by O.

Body frame
The body frame is also a moving reference frame but in contrast to the two other moving frames, this frame is fixed to the vessel. The origin of the frame is placed in the centre of mass of the vehicle or object. The z-axis still points toward the origin of chosen inertial frame, while x and z-axis are defined according to the right hand coordinate system along the symmetrical axis. The deviation between the orbit frame and the body frame describes the satellite attitude. Denoted by B. See figure 2.1.

2.3.2 Frame transformation

In this section, the frames and transformations used in this thesis will be provided. It should be noted that one assumption that will be applied for the satellite system is that it is not influenced by any other gravity forces than the one from the moon. I.e. it is assumed that the influence of gravity from moon and sun is neglectable compared to the moon gravity. The moon will also be looked upon as a non accelerating isolated system. This makes it possible to view the moon as a inertial reference frame for the satellite. Instead of the well known term of ECI and ECEF

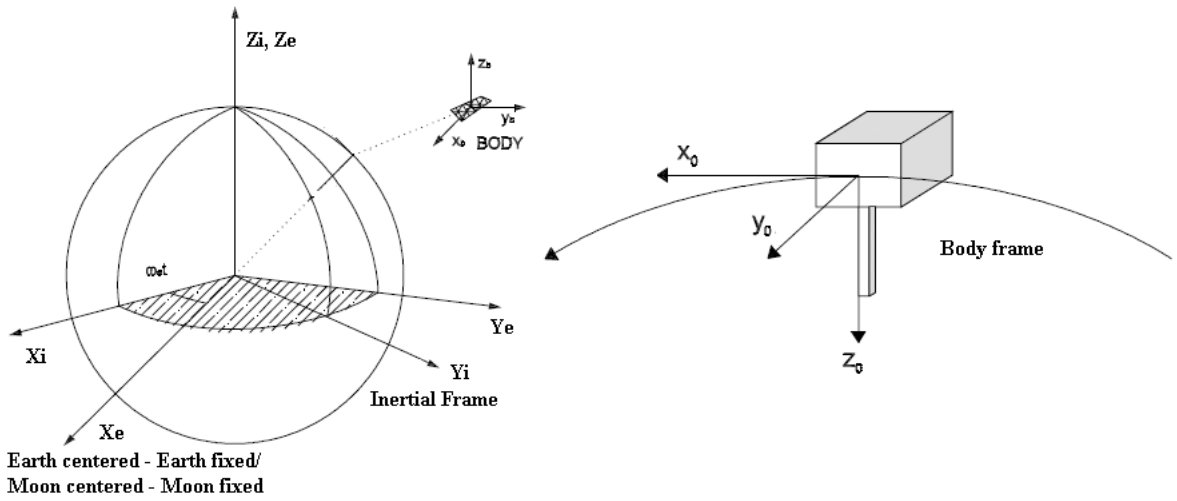

Figure 2.1: Reference frames

(Earth centred inertial and Earth centred earth fixed), MCI (Moon centred inertial) and MCMF (moon centred, moon fixed) description will be used, where each of the new terms have the same characteristics as respectively ECI and ECEF.

Non inertial to inertial (MCMF to MCI)

The MCMF has as explained earlier, most of the same properties as the MCI, but since its axis are fixed to the moon, it will rotate with the moon with the angular velocity:

$$\begin{aligned} &\text{Moons rotational period} = 27.32166\text{days/rev} = 2.66199626 \cdot 10^{-6}\text{rad/s} \\ &\Rightarrow \omega_{ie} = \frac{2\pi}{2.66199626 \cdot 10^{-6}} = 2.6617 \cdot 10^{-6}\text{rad/s} \end{aligned} \tag{2.28}$$

and therefore it is not an inertial reference frame. There is a time varying rotation $\alpha = \omega_{ie}$t around the z_i axis, the transformation from moon fixed reference to inertial will therefore be

$$R_e^i = R_{zi}(\alpha) = \begin{bmatrix} cos\alpha & -sin\alpha & 0 \\ sin\alpha & cos\alpha & 0 \\ 0 & 0 & 1 \end{bmatrix} \tag{2.29}$$

Inertial to orbital frame (MCI to orbit)

The transformation from inertial coordinates to orbital coordinates is depending on the satellites orbit. It is decided that the ESMO shall be in a polar radius, but the altitude is still not decided but will be assumed to be 200km. In this transformation

there will be a time varying rotation about ω_0 about the y_i axis and a 180° constant rotation about the x_i axis. The rotation matrix from inertial frame to orbit will therefore be

$$R_i^o = R_{x,\pi} \cdot R_{y,\mu} = \begin{bmatrix} cos\mu & -1 & sin\mu \\ 0 & -1 & 0 \\ sin\mu & 0 & -cos\mu \end{bmatrix} \tag{2.30}$$

where $\mu = \beta_0 + \omega_0 \mathrm{t}$, β_0 is the drop angle and the t is the time since last 0° passing.

ω_0 is given by looking at the forces acting on the satellite. There are centripetal acceleration and gravitational acceleration. For the satellite to maintain orbit, these accelerations needs to be equal.

$$m\frac{V_0^2}{R} = \frac{GMm}{R^2} \Rightarrow V_0^2 = \frac{GM}{R} \tag{2.31}$$

$$\text{the orbit velocity is } V_0 = \omega_0 R \Rightarrow (R\omega_0)^2 = \frac{GM}{R} \tag{2.32}$$

$$\Rightarrow \omega_0 = \sqrt{\frac{GM}{R^3}} \tag{2.33}$$

Orbital to body

It is the body coordinates that is the final goal in the frame transformation as the attitude measurements and reference values will be defined in this reference system. The rotation matrix in Euler angles given in equation (2.13) can be used to express this transformation, but because of problems with singularities it is advisable to use the Euler parameters instead, and the rotation matrix is therefor given as

$$R_o^b = R(\eta, \epsilon) = \begin{bmatrix} \eta^2 + \epsilon_1^2 - \epsilon_2^2 - \epsilon_3^2 & 2(\epsilon_1\epsilon_2 - \eta\epsilon_3) & 2(\epsilon_1\epsilon_3) + \eta\epsilon_2 \\ 2(\epsilon_1\epsilon_2 - \eta\epsilon_3) & \eta^2 - \epsilon_1^2 + \epsilon_2^2 - \epsilon_3^2 & 2(\epsilon_2\epsilon_3) + \eta\epsilon_1 \\ 2(\epsilon_1\epsilon_3 - \eta\epsilon_2) & 2(\epsilon_2\epsilon_3) + \eta\epsilon_1 & \eta^2 - \epsilon_1^2 - \epsilon_2^2 + \epsilon_3^2 \end{bmatrix} \tag{2.34}$$

the colonnes in (2.34) are the directional cosines. $R_o^b = \begin{bmatrix} \mathbf{c}_1^b & \mathbf{c}_2^b & \mathbf{c}_3^b \end{bmatrix}$.

2.4 Sensor

The sensors are the satellite tools for getting information from the environment around. They use information from stars, sun, earth, magnetic field or a combination, to determine the attitude of the satellite. These sources are used as reference points for the satellite, and thus give the satellite attitude relative to the chosen reference sources or reference vectors. Since attitude determination is independent

of the position, the magnitude of this vector will not be important. The attitude sensors measure the orientation of given reference vectors in a frame referenced to the satellite.

2.4.1 Star Sensor

The stars are available all over the sky and hence provide orbit independent and always available references and therefor, the stars are superior to any other available attitude reference in space. A star sensor measure star coordinates in the satellite frame and compare these coordinates with an on board star catalogue, which then provide well defined 3-axis attitude representation. The attitude can be determined within arc seconds. The Euler parameters are most often used as representation when using star sensor. These are directly comparable with the satellite attitude and therefore no extra modeling is required.

There are three main types of star sensors; scanner, gimball and fixed head tracker. The star scanner uses the vehicle motion to search the sky for known stellar configuration. The gimball star tracker is a mechanical device to search for stars while the fixed head star tracker apply an electronic searching device, tracking and identifying stars over a limited field of view (FoV). For this configuration it is very important with some kind of sun shading to avoid the sun from interfering with the search.

The star sensor is the most accurate attitude sensor, but it is also known to have some major disadvantages. It is complex and in great need of a powerful computer processing unit. This makes the sensor both heavier and more expensive. It is also known to have very poor operation range and unable to operate as the operating rate becomes larger than about 10 deg/min. These huge disadvantages have to some extend been overcome in the recent years. The Danish Technical University developed in 2001 a new and very much improved star sensor called μASC. It is a development from the previous and at that time revolutionary Advanced Stellar Compas (ASC). The μASC is both small, light and has an operating range that exceeds all previous attempts on developing star sensors.

2.4.2 Star sensor modeling

The star sensor can easily be modeled by using the true attitude from a satellite model with added noise.[5]

$$\mathbf{q}_{star} = \mathbf{q} \otimes \mathbf{q}_n \tag{2.35}$$

where $\mathbf{q}$ is the actual attitude taken from a nonlinear model, and $\mathbf{q}_n$ is star sensor noise represented as Euler parameters. The sensor noise can be modeled by using random function in Matlab with limitation parameters, and it is possible to use several star sensors to see how the estimation is affected by several measurements,

though for simplicity, only one star sensor will be used in this thesis.

It will be assumed that the μASC are used in the sensor modeling. The properties of the sensor are therefor; mass 450gr, accuracy of 1 arc sec, attitude rate up to 99.999% and a update rate of max 20Hz. One arcsecond equals 0.000278° which in turns gives us following Euler parameters

$$\mathbf{q}_a \approx \begin{bmatrix} 1 \\ 2.4 \cdot 10^{-6} \\ 2.4 \cdot 10^{-6} \\ 2.4 \cdot 10^{-6} \end{bmatrix} \tag{2.36}$$

This is used further on to model the star sensor as [6]

$$\mathbf{q}_n = \begin{bmatrix} \sqrt{1 - \|\epsilon_\mathbf{n}\|^2} \\ \epsilon_\mathbf{n} \end{bmatrix} \tag{2.37}$$

$\epsilon_\mathbf{n}$ is Gaussian white noise with expected value

$$\mathbf{E}\left[\epsilon_{n,i}^2\right] = \sigma_{\epsilon_{n,i}}^2 \text{ , for i} = 1, 2, 3 \tag{2.38}$$

where

$$\sigma_{\epsilon_{n,i}}^2 = 2.4 \cdot 10^{-6} \tag{2.39}$$

It can be useful to model the measurement noise as additive and this can be expressed on component form as [6]

$$\mathbf{v}_{star} = \begin{bmatrix} \eta\eta_n - \epsilon^T\epsilon - \eta \\ \eta\epsilon + \eta_n\epsilon + \mathbf{S}(\epsilon)\epsilon_n - \epsilon \end{bmatrix} \tag{2.40}$$

from (2.40) the covariance matrix can be calculated

$$\mathbf{E}\left[\mathbf{v}_{star}^2\right] = \sigma_{\mathbf{v}_{star}}^2 = \begin{bmatrix} \eta E\left[\eta_n^2\right] - \epsilon^T\left[\epsilon_n^2\right] - \eta \\ \eta\left[\epsilon_n^2\right] + \left[\eta_n^2\right]\epsilon + \mathbf{S}(\epsilon)\left[\epsilon_n^2\right] - \epsilon \end{bmatrix} \tag{2.41}$$

By assuming that $\eta_n = \sqrt{1 - \|\epsilon_n\|^2} \approx 1 \Rightarrow E\left[\eta_n^2\right]$, (2.41) can be reduced to

$$\sigma_{\mathbf{v}_{star}}^2 = \begin{bmatrix} \epsilon^T\left[\epsilon_n^2\right] \\ \eta\left[\epsilon_n^2\right] + \mathbf{S}(\epsilon)\left[\epsilon_n^2\right] \end{bmatrix} \tag{2.42}$$

The measurment noise matrix will then be given as

$$\mathbf{R}_k = diag(\sigma_{v_{2,k-1}}^2 \ \sigma_{v_{3,k-1}}^2 \ \sigma_{v_{4,k-1}}^2) \tag{2.43}$$

2.5 Mathematical Model of ESMO

2.5.1 Eulers equation of motion

The second fundamental law of rigid body dynamics states that the time derivative of angular momentum is equal to the applied torque. The Euler equation of motion gives the total moment applied to the body B from the external environment

$$\mathbf{I}\dot{\omega}_b + \omega_b \times (\mathbf{I}\omega_b) = \mathbf{M}_b \tag{2.44}$$

Where $\mathbf{M}_b$ is the applied torque on the body, the gravity torque and the actuator/reaction wheel torque. Total equation of motion will then be on the form

$$\mathbf{I}\dot{\omega}^b_{ib} = -\omega^b_{ib} \times (\mathbf{I}\omega^b_{ib}) + \tau^b_g + \tau^b_c \tag{2.45}$$

Where τ^b_g represents the torque applied to the satellite because of gravity and the τ^b_c will be the torque applied by the controllers i.e actuators and reaction wheels.

It is necessary to express the equation of motion in reference to the orbit frame instead of the inertial frame. To do this, some transformation between frames must be performed.

$$\omega^b_{ib} = \omega^b_{io} + \omega^b_{ob} = \mathbf{R}^b_o\omega^o_{io} + \omega^b_{ob} \tag{2.46}$$

$\mathbf{R}^b_o$ is the rotation matrix from orbit to body frame expressed in equation (2.34) , ω^b_{ob} is the angular velocity vector of the body frame relative the orbit frame and the ω^o_{io} is the constant rotation of the orbit relative the inertial frame given by

$$\omega^o_{io} = \begin{bmatrix} 0 & -\omega_0 & 0 \end{bmatrix}^T \tag{2.47}$$

ω_0 is defined in equation (2.33).

The derivative of equation (2.46) will also be useful

$$\dot{\omega}^b_{ib} = \frac{\delta}{\delta t}(\mathbf{R}^b_o\omega^o_{io} + \omega^b_{ob}) = (\dot{\mathbf{R}}^b_o\omega^o_{io} + \dot{\omega}^b_{ob}) = \dot{\omega}^b_{ob} - \mathbf{S}(\omega^b_{ob})\mathbf{R}^b_o\omega^o_{io} \tag{2.48}$$

By using this in the equation of motion (2.45), the motion can now be expressed in body relative to orbit frame.

$$\dot{\omega}^b_{ob} = (\mathbf{I^b})^{-1}\left[-(\mathbf{S}(\omega^b_{ob} + \mathbf{R}^b_o\omega^o_{io})\mathbf{I^b}(\omega^b_{ob} + \mathbf{R}^b_o\omega^o_{io})) + \tau^b_g + \tau^b_c\right] + \mathbf{S}(\omega^b_{ob})\mathbf{R}^b_o\omega^o_{io} \tag{2.49}$$

2.5.2 Actuator Dynamics

The control torque applied to the satellite in this thesis will be generated by reaction wheels. The reaction wheels are assumed placed in a tetrahedron structure as investigated by [1] for the ESMO satellite. In this structure, the reaction wheels are placed in the vertexes of a tetrahedron shape as can be seen in fig 2.2.

The advantages of placing the reaction wheels in this configuration is that it introduce redundancy to the system, i.e, if one wheel fails, the other three wheels will still be running and keeping the satellite three-axis stable. Also, by having four wheels working at the same time, the total torque will be greater and the angular velocity on each wheel can be reduced. This will then give expanded lifetime for each reaction wheel because of reduced wear.

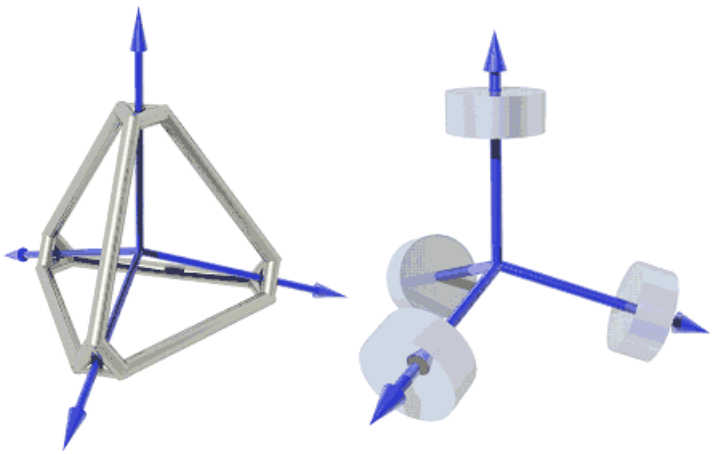

Figure 2.2: Tetrahedron configuration

According to [6] the resulting torque can be derived

$$\boldsymbol{\tau}_c^b = -S(\boldsymbol{\omega}_{ib}^b)\mathbf{A}\mathbf{I}_w(\boldsymbol{\omega}_w + \mathbf{A}^T\boldsymbol{\omega}_{ib}^b) \tag{2.50}$$

$$\dot{\boldsymbol{\omega}}_w = (\boldsymbol{I}_w)^{-1}\boldsymbol{\tau}_w - \mathbf{A}^T\dot{\boldsymbol{\omega}}_{ib}^b \tag{2.51}$$

Equation (2.46) inserted in (2.50) and the derivative from (2.48) in (2.51) leads to

$$\boldsymbol{\tau}_c^b = -S(\boldsymbol{R}_o^b\boldsymbol{\omega}_{io}^o + \boldsymbol{\omega}_{ob}^b)\mathbf{A}\mathbf{I}_w(\boldsymbol{\omega}_w + \boldsymbol{A}^T(\boldsymbol{R}_o^b\boldsymbol{\omega}_{io}^o + \boldsymbol{\omega}_{ob}^b)) \tag{2.52}$$

$$\dot{\boldsymbol{\omega}}_w = (\mathbf{I}_w)^{-1}\boldsymbol{\tau}_w - \mathbf{A}^T(\dot{\boldsymbol{\omega}}_{ob}^b - S(\boldsymbol{\omega}_{ob}^b)\mathbf{R}_o^b\boldsymbol{\omega}_{io}^o) \tag{2.53}$$

2.5.3 Gravity Gradient

The satellite will at all times be influenced by the gravity of the planets nearby, mostly the sun, earth and the moon. The gravity influence of the moon will though

be very much larger than the gravity influence by both sun and earth which therefor can be neglected.

Newtons laws states that a mass M in a distance R from a mass m, where $\mu = MG$, attracts each other with a force

$$F = \mu_g \frac{m}{R^2} \vec{R} \tag{2.54}$$

The gravitational force $\mathbf{dF}_i$ acting on a mass element $\mathbf{dm}_i$ located at a position R_i from the body center of the satellite is [5]

$$dF_i = -\mu_{gi} \frac{R_i}{R_i^3} dm_i \tag{2.55}$$

Gravity torque about the satellites geometric center due to the force dF_i at position r_i relative to the geometric center of the satellite is

$$d\vec{\tau}_{gi} = r_i \times dF_i \tag{2.56}$$

which leads to following expression for the gravity torque

$$\tau_g^b = 3\omega_0^2 C_3 \times \mathbf{I}^b C_3 \tag{2.57}$$

where C_3 is the third column of the rotation matrix in equation (2.34) and ω_0 is given in equation (2.33).

2.5.4 Kinematics

The kinematic part of the model describing rotation of rigid body, gives the time derivative of the parameterization of the rotation matrix as a function of angular velocity. The kinematic differential equations are exact models with no uncertainties and no approximations involved [4]. The kinematic differential equation for the Euler parameters are

$$\dot{\eta} = -\frac{1}{2} \boldsymbol{\epsilon}^T \boldsymbol{\omega}_{ob}^b \tag{2.58}$$

$$\dot{\boldsymbol{\epsilon}} = \frac{1}{2} (\eta \mathbf{I} + S(\boldsymbol{\epsilon})) \boldsymbol{\omega}_{ob}^b \tag{2.59}$$

2.6 Overall mathematical model

The mathematical model of the nonlinear system can be summarized to [6]

$$\dot{\mathbf{x}} = \begin{bmatrix} \dot{\eta} \\ \dot{\boldsymbol{\epsilon}} \\ \dot{\boldsymbol{\omega}}^b_{ob} \\ \dot{\boldsymbol{\omega}}_w \end{bmatrix} = \mathbf{f}(\mathbf{x}, \tau_{\mathbf{w}}, t) + \mathbf{E}w \tag{2.60}$$

where $\mathbf{w}$ is process noise, $\mathbf{E}$ is process noise matrix and $\mathbf{f}(\mathbf{x}, \tau_{\mathbf{w}}, t)$ is given as

$$\mathbf{f} = \begin{bmatrix} -\frac{1}{2}\boldsymbol{\epsilon}^T\boldsymbol{\omega}^b_{ob} \\ \frac{1}{2}(\eta\mathbf{I} + S(\boldsymbol{\epsilon}))\boldsymbol{\omega}^b_{ob} \\ (\mathbf{I}^b)^{-1}(-(S(\boldsymbol{\omega}^b_{ob} + \mathbf{R}^b_o\boldsymbol{\omega}^o_{io})\mathbf{I}^b(\boldsymbol{\omega}^b_{ob} + \mathbf{R}^b_o\boldsymbol{\omega}^o_{io})) + \boldsymbol{\tau}^b_g + \boldsymbol{\tau}^b_c - \boldsymbol{\tau}_w) + S(\boldsymbol{\omega}^b_{ob})\mathbf{R}^b_o\boldsymbol{\omega}^o_{io} \\ (\mathbf{I}_w)^{-1}\boldsymbol{\tau}_w - \mathbf{A}^T(\dot{\boldsymbol{\omega}}^b_{ob} - S(\boldsymbol{\omega}^b_{ob})\mathbf{R}^b_o\boldsymbol{\omega}^o_{io}) \end{bmatrix} \tag{2.61}$$

where $\boldsymbol{\tau}^b_c$ and $\boldsymbol{\tau}^b_g$ is

$$\boldsymbol{\tau}^b_c = -S(\mathbf{R}^b_o\boldsymbol{\omega}^o_{io} + \boldsymbol{\omega}^b_{ob})\mathbf{A}\mathbf{I}_w(\boldsymbol{\omega}_w + \mathbf{A}^T(\mathbf{R}^b_o\boldsymbol{\omega}^o_{io} + \boldsymbol{\omega}^b_{ob})) \tag{2.62}$$

$$\boldsymbol{\tau}^b_g = 3\omega_0^2 C_3 \times \mathbf{I}^b C_3 \tag{2.63}$$

$$\boldsymbol{\tau}_w = \text{control torque} \tag{2.64}$$

$\mathbf{A}$ is the wheels configuration/allocation matrix, I_w is the reaction wheels inertia given in Appendix A, C_3 is the third column of the rotational matrix R^b_{ob} 2.34.

2.7 Linearization

A linearization of the nonlinear satellite model is necessary for use in an extended Kalman filter. The states to be determined are the angular velocity w^b_{ob} and the quaternions $\mathbf{q}$. The linearizartion is done by [6] and [5]. The liner matrix $\mathbf{F}_k$ can be separated into attitude and velocity such that $\mathbf{F}_k$ is on the form

$$\mathbf{F}_k = \begin{bmatrix} \mathbf{F}_{att} \\ \mathbf{F}_{vel} \end{bmatrix} = \begin{bmatrix} \frac{\delta \dot{\boldsymbol{q}}}{\delta x_1} \cdots \frac{\delta \dot{\mathbf{q}}}{\delta x_7} \\ \frac{\delta \dot{\boldsymbol{\omega}}^{\boldsymbol{b}}_{\boldsymbol{ob}}}{\delta x_1} \cdots \frac{\delta \dot{\boldsymbol{\omega}}^{\boldsymbol{b}}_{\boldsymbol{ob}}}{\delta x_7} \end{bmatrix} \tag{2.65}$$

$$= \begin{bmatrix} 0 & -\frac{1}{2}\omega^b_{ob,x} & -\frac{1}{2}\omega^b_{ob,y} & -\frac{1}{2}\omega^b_{ob,z} & -\frac{1}{2}\epsilon_1 & -\frac{1}{2}\epsilon_2 & -\frac{1}{2}\epsilon_3 \\ \frac{1}{2}\omega^b_{ob,x} & 0 & -\frac{1}{2}\omega^b_{ob,z} & \frac{1}{2}\omega^b_{ob,y} & \frac{1}{2}\eta & \frac{1}{2}\epsilon_3 & -\frac{1}{2}\epsilon_2 \\ \frac{1}{2}\omega^b_{ob,y} & \frac{1}{2}\omega^b_{ob,z} & 0 & -\frac{1}{2}\omega^b_{ob,x} & -\frac{1}{2}\epsilon_3 & \frac{1}{2}\eta & \frac{1}{2}\epsilon_1 \\ \frac{1}{2}\omega^b_{ob,z} & -\frac{1}{2}\omega^b_{ob,y} & \frac{1}{2}\omega^b_{ob,x} & 0 & \frac{1}{2}\epsilon_2 & -\frac{1}{2}\epsilon_1 & \frac{1}{2}\eta \\ b_{11} & b_{12} & b_{13} & b_{14} & b_{15} & b_{16} & b_{17} \\ b_{21} & b_{22} & b_{23} & b_{24} & b_{25} & b_{26} & b_{27} \\ b_{31} & b_{32} & b_{33} & b_{34} & b_{35} & b_{36} & b_{37} \end{bmatrix}_{x=x^*} \tag{2.66}$$

All the elements b_{ij} can be found in Appendix A.

Linearization of the system with respect to the input gives us the **B** matrix.

$$\mathbf{B}_k = \begin{bmatrix} \mathbf{0} \\ -(\mathbf{I}^b)^{-1} \end{bmatrix} \tag{2.67}$$

2.8 Discrete system

The system matrix on discrete form will be

$$z_{k+1} = f(z_k, x_k) + E_k w_k \tag{2.68}$$
$$y_k = h(z_k) + G_k v_k \tag{2.69}$$

w_k and v_k is process and measurement noise respectively. $h(z_k)$ is in this case only a linear function of the measurement matrix,while the system state $f(z_k, x_k)$ is approximated by a Taylor expansion the linearised system matrix F_k and Γ_k

$$\phi_k = I + F_k \Delta T + \frac{1}{2} F_k^2 \Delta^2 + \frac{1}{3!} F_k^3 \ldots \tag{2.70}$$
$$\Gamma_k = (\mathbf{I}\Delta t + \frac{1}{2}\mathbf{F}_k^2 \Delta t^2)\mathbf{B}_k \tag{2.71}$$

so that the discrete system is on the form

$$f(z_k, x_k) = \phi_k z_k + \Gamma_k \tau_{w,k} \tag{2.72}$$
$$h(z_k) = H_k z_k \tag{2.73}$$

With a state estimator (in this case extended Kalman filter) given as

$$\hat{z}_{k+1} = f(\hat{z}_k, x_k) + K_k(y_k - h(\hat{z}_k)) \tag{2.74}$$
$$f(\hat{z}_k, x_k) = \phi_k \hat{z}_k + \Gamma_k \tau_{w,k} \tag{2.75}$$

Estimation error is defined as

$$\xi_k = z_k - \hat{z}_k \tag{2.76}$$

this will then give

$$\begin{aligned} \xi_{k+1} &= z_{k+1} - \hat{z}_{k+1} \\ &= (f(z_k, x_k) + E_k w_k) - (f(\hat{z}_k, x_k) + K_k(y_k - h(\hat{z}_k))) \\ &= \phi_k z_k + E_k w_k - \phi_k \hat{z}_k - K_k(H_k z_k - H_k \hat{z}_k + D_k v_k) \\ &= (I + F_k \Delta T + \frac{1}{2} F_k^2 \Delta T^2 + \frac{1}{!3} F_k^3 \Delta T^3 \ldots)(z_k - \hat{z}_k) - H_k C_k (z_k - \hat{z}_k) \\ &+ E_k w_k - K_k D_k v_k \\ &= (F_k - K_k H_k)\xi_k + \varphi(z_k, \hat{z}_k, x_k) + E_k w_k - K_k D_k v_k \end{aligned} \tag{2.77}$$

with the functions

$$\varphi(z_k, \hat{z}_k, x_k) = (I + \frac{1}{2}F_k^2\Delta T^2 + \frac{1}{!3}F_k^3\Delta T^2 \ldots)(z_k - \hat{z}_k) \tag{2.78}$$

$$\chi(z_k, \hat{z}_k) = 0 \text{ since } h(z_k) \text{ is linear.} \tag{2.79}$$

2.9 Extended Kalman Filter on ESMO

The Linearized Kalman filter (LKF) and the extended Kalman filter (EKF) where introduced as approximations to the optimal linear estimation in order to derive a filter for nonlinear systems. LKF and EKF work in quite a similar way, the only difference being that LKF linearize the system matrices around a nominal predetermined trajectory while the EKF linearize around the filter's estimated trajectory which is update for every time step. It is the extended Kalman filter which will be the center of attention in this analysis.

The EKF constructs a linear system that approximates the nonlinear system near the current best estimate, it is assumed that process and observations are linear on the scale of the error in the estimated state. The validity of this assumptions are secured by re-linearization about each new state [7]. The filter equations are given as

$$K_k = P_k^- H_k^T (H_k P_k^- H_k^T + R_k)^{-1} \tag{2.80}$$

$$\hat{x}_k = \hat{x}_k^- + K_k(Z_k - H_k\hat{x}_k^-) \tag{2.81}$$

$$P_k = (I - K_k H_k)P_k^-(I - K_k H_k)^T + K_k R_k K_k^T \tag{2.82}$$

$$\hat{x}_k^- = \hat{\Phi}_k\hat{x}_k + \Gamma_k\tau_{w,k} \tag{2.83}$$

$$P_{k+1}^- = \hat{\Phi}_k\hat{P}_k\hat{\Phi}_k^T + E_k Q_k E_k^T \tag{2.84}$$

where

$$\Phi_k = e^{\mathbf{F_k\Delta t}} \approx \mathbf{I} + \mathbf{F}_k\Delta t + \frac{1}{2}\mathbf{F}_k^2\Delta t^2 \tag{2.85}$$

$$\mathbf{\Gamma}_k = (e^{\mathbf{F_k\Delta t}} - \mathbf{I})\mathbf{F}_k^{-1}\mathbf{B}_k \approx (\mathbf{I}\Delta t + \frac{1}{2}\mathbf{F}_k^2\Delta t^2)\mathbf{B}_k \tag{2.86}$$

R_k is the measurement noise matrix given by (2.43) and E_k and Q_k are constant modelling and processing noise matrix given in (A.6) and (A.5).
The EKF cannot as the linear KF, guarantee optimality or convergence, but it has still proved to be very useful and solve many nonlinear problems successfully.

When using EKF, the nonlinearity can be either in the process model, the observation model or both. The recursive loop is divided into the same phases as for the simple KF, but introduces some complexities in addition. See Figure 2.3

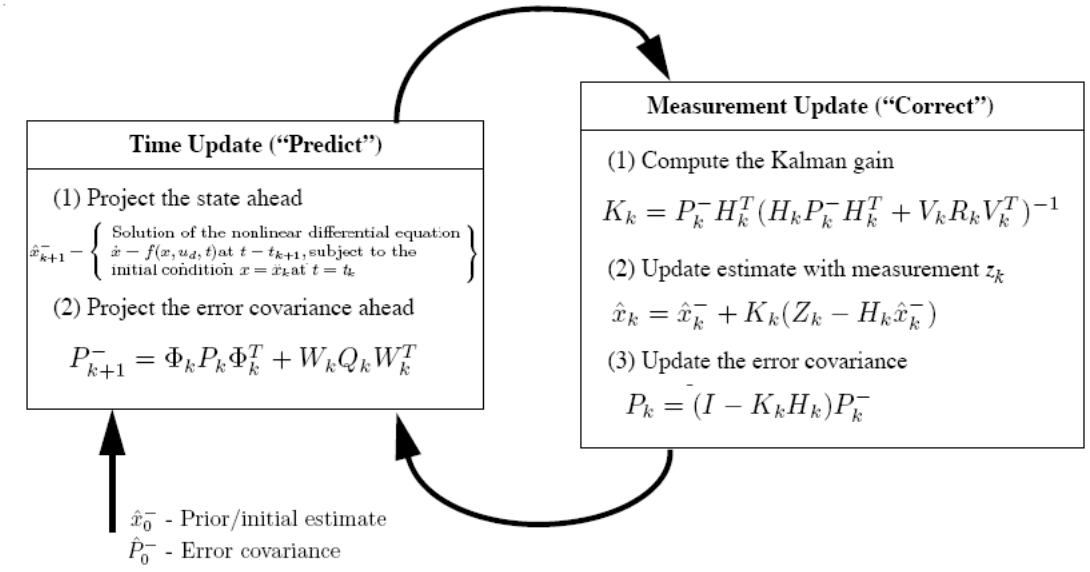

Figure 2.3: Extended Kalman filter loop

Chapter 3

Introduction to Feedback control and controllers

3.1 Controllers for ESMO

To control ESMO, active control around the z-axis is feasible. The control torque acting on the satellite is generated from change in spin of the reaction wheels.

3.1.1 PD Controller

One simple stabilizing controller is a regular PD controller. The impact a PD - controller has on the system is that for high frequencies, it lifts the phase and hence stabilizes the system and raise the bandwidth, wich in turn quickens the control of the system. For low frequencies, the PD - controller acts as a regular P-gain controller.

The PD-controller, proposed for ESMO with the estimated state as input to the controller, is given as

$$u_k = k(\hat{x}) = \tau_{w,k} = K_p A^{\diamond} \Delta\hat{\epsilon} + K_d A^{\diamond} \Delta\hat{\omega}^b_{ob} \tag{3.1}$$

$$\Delta\hat{\omega}^b_{ob} = \omega^b_{ob,ref} - \hat{\omega}^b_{ob} \tag{3.2}$$

$$\Delta\hat{\epsilon} = \epsilon_{ref} - \hat{\epsilon} \tag{3.3}$$

$$\tag{3.4}$$

$A^{\diamond}$ is the pseudo inverse of A given by $A^{\diamond} = A^T(AA^T)^{-1}$. Its purpose is to distribute the calculated input to the four reaction wheels.

Reference value for $\omega^b_{ob,ref} = 0$ such that $\Delta\hat{\omega}^b_{ob} = -\hat{\omega}^b_{ob}$, this is because it is desirable that the angular velocity goes toward zero after the desired attitude is reach. Derivative and proportional gains are found through simulations and testing.

3.1.2 Model Dependent PD controller

It is also possible to derive a model dependent PD - control law for the satellite. The reason for this is to provide both good tracking performances also in the cases where high gains are not possible. This is done by incorporating the structure of the model in the control law. A suggestion to a model dependent controller is given in [8] as

$$\boldsymbol{\tau} = k_p \boldsymbol{\epsilon} - k_d \boldsymbol{\Delta\omega} + \boldsymbol{I}\frac{d\omega_{ob}^b}{dt} + \omega_{ob}^b \times \boldsymbol{I}\omega_{ob}^b \tag{3.5}$$

3.1.3 Robust controller

Many of today's controllers are theoretically excellent and gives optimal response in shielded environment and when not interpreted by disturbance, modelling errors or changes in the system or the environment. They are engineered to give the best possible performance for the least possible cost. The emphasis on optimality often overshadows the robust aspects and the controller will fail as soon as noise or changes in the environment or system appears. Robust control makes sure that the controller work well even if the system differs from the employed model and tolerate errors in system model. An robust controller is given by [9] as

$$u = -\frac{1}{2}\left[(\boldsymbol{\epsilon} \times \boldsymbol{\epsilon} + \eta \boldsymbol{I})G_p + \gamma(1-\eta)\boldsymbol{I}\right]\boldsymbol{\epsilon} - G_r\boldsymbol{\omega} \tag{3.6}$$

G_r and G_p are 3×3 symmetric positive definite matrices and γ is a positive scalar.

3.2 Discussion

There are some properties worth mentioning for the above controllers. The PD - controller generally introduce a stabilizing affect on system because of the phase lift, the controller can therefore be characterized as a stable controller. When the PD controller is applied independent of the system model it stabilizes the system in general, but it does not always provide good response for systems when high gains cannot be applied. For these cases it is necessary to incorporate some structure from the system model in the control law.

The equilibriums and stability characteristic are not mentioned in this chapter as it will be thoroughly investigated in later chapters. Generally, what can be mentioned about stability for system where quaternion are used to represent attitude is that it is difficult to prove global stability as there necessarily will be two equilibrium points. When $\epsilon = 0$ both $\eta = \pm 1$ will make $R = I$. These equilibrium points have different stability properties which need to be analyzed. The convergence will be local to one of the two, and the issue in establishing global stability will be to decide or force the system to only one of the equilibriums, if not, only local stability can be determined.

Chapter 4

Basic stability theory for nonlinear systems

In this chapter some basic but very important theorems, tools and definition for nonlinear stability analysis will be presented. The theory is taken from [10] and will be used extensively throughout the rest of this thesis.

4.1 Notation and basic terms

Some basic terms and notations need to be introduced.

4.1.1 Norms and spaces

The term space or Euclidean space is often used in control system analysis. The definition of an Euclidean space is a space in which Euclid's axioms and definitions apply; a metric space that is linear and finite-dimensional. It consists of all numbers denoted by R. The set of all n-dimensional vectors $x = \begin{bmatrix} x_1 & x_2 & \dots & x_n \end{bmatrix}$ where the elements of x are real numbers defines the n-dimensional Euclidean space denoted by R^n.

Vector and matrix norms are other definition that needs to be introduced before any stability theorems can be presented. The norm $\|x\|$ of a vector x is a real valued function with the following properties

- $\|x\| \geq 0 \; \forall \; x \in R^n$ and $\|x\| = 0$ only if $x = 0$
- $\|x + y\| \leq \|x\| + \|y\| \; \forall \; x, y \in R$ triangle inequality
- $\|\alpha x\| = |\alpha| \|x\| \; \forall \; \alpha \in R$, $x \in R^n$

The P norm is equal to

$$\|x\|_p = (|x_1|^p + \cdots + |x_n|^p)^{1/p} \;\; 1 \leq p < \infty \tag{4.1}$$

The most common p-norms are the

- Infinity norm: $\|x\|_\infty = \max_i |x_i|$
- One norm: $\|x\|_1 = |x_1| + \cdots + |x_n|$
- Euclidean norm: $\|x\|_2 = (|x_1|^2 + \cdots + |x_n|^2)^{1/2}$

The last important properties for vector norms is known as Holders Inequality

$|x^T y| \leq \|x\|_p \|y\|_q$, $\frac{1}{p} + \frac{1}{q} = 1 \; \forall x, y \in R^n$

The norms of matrices can also be convenient to be familiar with. If a matrix A of real numbers defines a linear mapping $Y = Ax$ from $R^n \rightarrow R^m$ the following norms will yield

- P norm: $\|A\|_p = \sup_{x \neq 0} \frac{\|Ax\|_p}{\|x\|_p} = \max_{\|x\|_p = 1} \|Ax\|_p$
- One norm: $\|A\|_1 = \max_j \sum_{i=1}^m |a_{ij}|$
- Euclidean norm: $\|A\|_2 = \left[\lambda_{\max}(A^T A)\right]^{1/2}$
- Infinity norm: $\|A\|_\infty = \max_i \sum_{j=1}^n |a_{ij}|$

4.1.2 Definiteness and uniqueness

A few definitions need to be considered before stability can be studied. One of the most important tools used in the stability proof in the following sections are the definitions of Positive definite functions and matrices.

Definition 4.1.1 ***Positive Definite Function****: A scalar function $f(x)$, is said to be positive definite if $f(x) > 0 \; \forall \; x$ and $f(x) = 0$ if and only if $x = 0$.*

Definition 4.1.2 ***Positive Semi Definite Function****: A scalar function $f(x)$, is said to be positive semi definite if $f(x) \geq 0 \; \forall \; x$ and $f(x) = 0$ if and only if $x = 0$.*

Definition 4.1.3 ***Negative Definite Function****: A scalar function $f(x)$, is said to be negative definite if $-f(x)$ is positive definite.*

Positive definite matrices are another property very valuable in control system theory.

Definition 4.1.4 ***Positive Definite Matrix****: A $n \times n$ matrix, $Q = Q^T$, is positive definite if, for all $x \in R^n$, the function $f(x) = x^T Q x$ is positive definite. A positive definite matrix has the following properties:*

1. *All eigenvalues are positive real*
2. *Eigenvectors are orthogonal*
3. *Can be Cholesky factorized to $Q = P^T P$ for some matrix P.*

The Lipschitz condition ensures existence and uniqueness of a function and is used in many theorems and proof. A function is Lipschtiz if $f(t, x)$ satisfies the inequality

$$\|f(t, x) - f(t, y)\| \leq L\|x - y\| \tag{4.2}$$

for alle (t, x) and (t, y) in some neighborhood of (t_0, x_0)

4.2 Types of stability and convergence

There are several types of stability for both linear and nonlinear systems. In this section a short introduction to requirements of each of the typical stability classes in nonlinear system theory will be given. For a feedback loop system, convergence only imply that the error between reference and output goes to zero, it does not guarantee anything of the behaviour of the response before reaching steady state. Stability on the other hand, implies both convergence to zero and predicted behaviour of the overall response. A stable system error will stay within the set for all times, while when only convergence is established, the error might move outside the bounded set at some point before converging. Stability implies convergence, while convergence does not imply stability. It should also be mentioned that in most cases convergence will be a satisfactory result for the system as the only requirement is for the steady state error to be zero.

Since satellite attitude determination is dependent of time, it is natural to present the stability requirements for non autonomous systems in the following subsections. Nonlinear system stability is basically studied in a Lyapunov sense, where Lyapunov's methods are used to determine behaviour of the system. With Lyapunov analysis, the systems are being studied by looking at the stability behaviour of the systems equilibrium points. There are several useful methods and many constraints that must be fulfilled to state the different kinds of stability. The system is said to be:

- Stable if for each $\epsilon > 0$ there is a $\delta = \delta(\epsilon, t_0) > 0$ s.t

$$\|x(t_0)\| < \delta \Rightarrow \|x(t)\| < \epsilon, \forall\ t \geq t_0 \geq 0 \tag{4.3}$$

- Uniformly stable if for each $\epsilon > 0$ there is a $\delta = \delta(\epsilon) > 0$ independent of t_0 s.t

$$\|x(t_0)\| < \delta \Rightarrow \|x(t)\| < \epsilon, \forall\ t \geq t_0 \geq 0 \tag{4.4}$$

- Unstable if it is not stable
- Asymptotically stable if it is stable, and there exists a positive constant $c = c(t_0)$ s.t $x(t) \to 0$ as $t \to \infty\ \forall \|x(t_0)\| < 0$
- Uniformly asymptotically stable if it is uniformly stable and there exists a constant c independent of t_0 such that for all $\|x(t_0)\| < c$, $x(t) \to 0$ as $t \to \infty$ uniformly in t_0. That is, for each $\eta > 0$ there is a $T = T(\eta)$ s.t

$$\|x(t)\| < \eta, \forall, t \geq t_0 + T(\eta), \forall\ \|x(t_0)\| < 0 \tag{4.5}$$

- Globally uniformly asymptotically stable if it is uniformly stable, $\delta(\epsilon)$ can be chosen to satisfy $\lim_{\epsilon \to \infty} \delta(\epsilon) = \infty$ and for each pair of positive constants η, c, $\exists\ T = T(\eta, c) > 0$ s.t

$$\|x(t)\| < \eta, \forall\ t \geq t_0 + T(\eta, c)\ \forall\ \|x(t_0)\| < c \tag{4.6}$$

- Exponentially stable if there exist positive constants c, k and λ s.t

$$\|x(t)\| \leq k\|x(t_0)\|e^{-\lambda(t-t_0)}, \forall\ \|x(t_0)\| < c \tag{4.7}$$

- Globally exponentially stable if (4.7) is satisfied for any initial state $x(t_0)$.

4.3 Stability tools and Theorems

The main tool for testing stability of nonlinear systems is Lyapunov's theorems. It is more general than other test as it does not depend on testing roots or eigenvalues, but the behaviour of the system. Lyapunov's direct and indirect methods are of Lyapunov's most famous stability tests and a short description of these methods follows in the next sections.

4.3.1 Direct Lyapunov

The direct Lyapunov method involves finding a positive definite function, somehow depending on the system that satisfies certain criteria. The most difficult part of Lyapunov's direct method is finding this function.

Theorem 4.3.1 ***Lyapunovs Direct method:*** *Let $x = 0$ be an equilibrium point of $\dot{x} = f(x)$ and $D \subset R^n$ be a domain containing $x = 0$. Let $V : D \to R$ be a continuously differentiable function such that*

$$V(0) = 0 \text{ and } V(x) > 0 \text{ in } D - \{0\} \tag{4.8}$$

$$\dot{V}(x) \leq 0 \text{ in } D \tag{4.9}$$

Then, x = 0 is stable. Moreover if

$$\dot{V}(x) < 0 \text{ in } D - \{0\} \tag{4.10}$$

then x=0 is asymptotically stable.

The condition $\dot{V}(x) \leq 0$ implies that when a trajectory crosses a Lyapunov surface $V(x) = c$, it moves inside the set $\Omega_c = \{x \in R^n | V(x) \leq x\}$ and can never come out again. When $\dot{V} < 0$ the trajectory moves from one Lyapunov surface to an inner surface with smaller c. When $\dot{V}(x) \leq 0$ there are no guarantees that the trajectory will approach the origin, but it can be concluded that the system is stable as the trajectory will remain inside a closed surface.

To ensure global Lyapunov stability, another constraint is added to the direct Lyapunov method. From before

1. the function V(x) must be positive definite
2. the time derivative of the function $\dot{V}(x)$ must be negative definite

   and the last property to ensure global stability is

3. the function V(x) must be radially unbounded. I.e $V(x) \to \infty$ as $x \to 0$.

The last condition makes sure that no matter how far away from the origin you are, the system will converge to the origin.

4.3.2 Indirect Lyapunov

The second method of Lyapunov is the indirect Lyapunov method. In this method conditions are given for establishing stability of the origin as an equilibrium point for nonlinear system by investigating the stability of the linearized system. This method does not require a Lyapunov function, which as mentioned previously, often can be very difficult to find.

Theorem 4.3.2 ***Lyapunov's indirect method****: Let x=0 be an equilibrium point for the nonlinear system*

$$\dot{x} = f(x) \tag{4.11}$$

where $f : D \to R^n$ is continuously differentiable and D is a neighborhood of the origin. Let

$$A = \frac{\partial f}{\partial x}(x)\bigg|_{x=0} \tag{4.12}$$

Then,

1. *The origin is asymptotically stable if* $Re\lambda_i < 0$ *for all eigenvalues of A.*
2. *The origin is unstable if* $Re\lambda_i > 0$ *for one or more of the eigenvalues of A.*

What should be noted is that this theorem does not say anything about the case where $Re\lambda_i = 0$. In this case the linearization fails to determine the stability.

Another theorem states exponential stability of non autonomous systems based on the above indirect Lyapunov method

Theorem 4.3.3 ***Exponential stability****: Let* $x = 0$ *be an equilibrium point for the nonlinear system*

$$\dot{x} = f(t, x) \tag{4.13}$$

where $f : [0, \infty) \times D \rightarrow R^n$ *is continuous differentiable,* $D = \{x \in R^n | \|x\|_2 < r\}$*, and the Jacobien matrix* $[\partial f / \partial x]$ *is bounded and Lipschitz in D, uniformly in t. Let*

$$A(t) = \frac{\partial f}{\partial x}(t, x)\bigg|_{x=0} \tag{4.14}$$

Then, the origin is an exponentially stable equilibrium point for the nonlinear system if it is an exponentially stable equilibrium point for the linear system

$$\dot{x} = A(t)x \tag{4.15}$$

4.3.3 Theorems and tools

Region of attraction

The region of attraction is a term that indicates how far from the origin the trajectory can be, and still converge to the origin as $t \rightarrow \infty$. Let $\phi(t, x)$ be a solution that starts at $x_0 = 0$, $t = 0$, then the region of attraction will be the set of all points x s.t $\phi(t, x)$ is defined $\forall\ t \geq 0$ and $\lim_{t \rightarrow \infty} \phi(t, x) = 0$

Invariant set

M is an invariant set with respect to $f(x)$ if $x(0) \in M\ \forall\ t \in R$ makes $x(t) \in M$. If a solution belongs to M at some time instant, then it belongs to M for all future and past time. A solution is positive invariant if it is invariant for all $t \geq 0$.

La Salle's Invariance Principle

Let $\Omega \subset D$ be a compact set that is positive invariant with respect to $f(x)$. Let $V : D \rightarrow R$ be continuously differentiable function s.t $\dot{V}(x) \leq 0$ in Ω. Let E be the set of all points in Ω where $\dot{V}(x) = 0$. Let M be the largest invariant set in E. Then every solution starting in Ω approaches M as $t \rightarrow \infty$.

Corollary 4.3.4 *Let $x = 0$ be an equilibrium point. Let $V : D \to R$ be a continuous differentiable radially unbounded, positive definite function s.t $\dot{V}(x) \leq 0$ for all $x \in R^n$. Let $S = \{x \in R^n | \dot{V}(x) = 0\}$ and suppose that no solution can stay identically in S other than the trivial solution $x(t) \equiv 0$. Then the origin is globally asymptotically stable.*

Corollary 4.3.5 *Let $x = 0$ be an equilibrium point. Let $V : R^n \to R$ be a continuous differentiable positive definite function on a domain D containing $x = 0$ s.t $\dot{V}(x) \leq 0$ in D. Let $S = \{x \in D | \dot{V}(x) = 0\}$ and suppose that no solution can stay identically in S other than the trivial solution $x(t) \equiv 0$. Then the origin is asymptotically stable.*

This principle relaxes the negative definiteness constraint on the Lyapunov function as it extends Lyapunovs results in three different directions

- Estimate of the region of attraction
- Can be used when there is an equilibrium set instead of equilibrium point
- V(x) does not have to be positive definite

Barbalat's Lemma

The above invariance theorem shows that the trajectory approaches the largest invariant set in E, where E is the set of all points in Ω where $\dot{V}(x) = 0$. This is a very good theorem for autonomous systems, but come to nonautonomous system it can be very difficult to find a set E for the system as $\dot{V}(t, x)$ is a function of both x and t. This would be easier to state if it can be shown that

$$\dot{V}(t, x) \leq -W(x) \leq 0$$

The set E can be defined as the set of points where $W(x) = 0$. The Barbalat lemma is both used in proof for theorem that states this, and on its own

Lemma 4.3.6 ***Barbalat**: Let $\phi : R \to R$ be an uniformly continuous function on $[0, \infty)$. Suppose that $\lim_{t\to\infty} \int_0^t \phi(\tau)d\tau$ exists and is finite. Then, $\phi(t) \to 0$ as $t \to \infty$.*

Chapter 5

Stability for linear KF and feedback control

5.1 In general: Separation principle

The closed loop of a system does not necessarily apply the same properties as the open loop system, it is therefor necessary to design a feedback law that stabilizes the closed loop. When the system output states cannot be measured, an observer can be applied to estimate these states. When combining a feedback loop and an observer, the system properties might change. It is therefor important to properly investigate the overall characteristic of the system when either closing a loop or combining observer and feedback in a loop, to assure that the system remains stable. For linear system this can be done quite simply by applying the principle of separation.

The principle of separation, also known as the certainty equivalence principle or separation theorem, states that for a controller designed by using an observer and a constant-gain state feedback matrix, the observer gain and the state-feedback gain can be designed separately. The overall closed loop system eigenvalues are the union of the observer eigenvalues and the state-feedback eigenvalues alone, and each part can therefore be designed separate.

In other words, if a model is constructed by designing an observer and feeding back the state estimate through a constant matrix, the closed loop eigenvalues are those of the observer along with those that would have been present if no observer where used and the feedback had been applied to the actual plant states.

5.1.1 Proof of the separation theorem for linear systems

Given the system

$$\dot{x} = Ax + Bu + w \tag{5.1}$$
$$y = Cx + v \tag{5.2}$$

with the simple feedback law controller

$$u = -K\hat{x}(t) \tag{5.3}$$

where $\hat{x}(t)$ is the estimated states from an observer designed as a Kalman filter, given by

$$\dot{\hat{x}} = A\hat{x} + Bu + L(y - C\hat{x}) \tag{5.4}$$
$$L = \Sigma C^T R^{-1} \tag{5.5}$$
$$A\Sigma + \Sigma A^T + Q_0 - \Sigma C^T R_0^{-1} C\Sigma = 0 \tag{5.6}$$

The system can now be written as

$$\begin{bmatrix} \dot{x} \\ \dot{\hat{x}} \end{bmatrix} = \begin{bmatrix} A & -BK \\ LC & A - BK - LC \end{bmatrix} \cdot \begin{bmatrix} x \\ \hat{x} \end{bmatrix} \tag{5.7}$$

To prove system stability of the combined Kalman filter and feedback loop gain, the eigenvalues of (5.7) must be in the left hand plane. This is not obvious from the matrix. By state space transforming the system it is possible to look at the system in a different way.

$$\begin{bmatrix} x \\ \hat{x} \end{bmatrix} = P \begin{bmatrix} z \\ \hat{z} \end{bmatrix} \ , P = \begin{bmatrix} I_n & 0_n \\ I_n & -I_n \end{bmatrix} \ , P = P^{-1} \tag{5.8}$$

$$\Downarrow$$

$$\begin{bmatrix} z \\ \hat{z} \end{bmatrix} = \begin{bmatrix} I_n & 0_n \\ I_n & -I_n \end{bmatrix} \begin{bmatrix} x \\ \hat{x} \end{bmatrix} = \begin{bmatrix} x \\ x - \hat{x} \end{bmatrix} = \begin{bmatrix} x \\ \tilde{x} \end{bmatrix} \tag{5.9}$$

By using $\hat{x} = x - \tilde{x}$ in equation (5.7), a new representation of the closed loop state space will be

$$\begin{bmatrix} \dot{x} \\ \dot{\tilde{x}} \end{bmatrix} = \begin{bmatrix} A - BK & -BK \\ 0 & A - LC \end{bmatrix} \cdot \begin{bmatrix} x \\ \tilde{x} \end{bmatrix} \tag{5.10}$$

With this new representation, two important facts are worth mentioning

1. The system eigenvalues are invariant during a state transformation. That means, the eigenvalues of (5.7) are equal the eigenvalues of (5.10).

2. The system matrix in (5.10) is block-triangular (the elements of the matrix are matrices).

The characteristic of a block-triangular matrix is that the eigenvalues of the matrix are equal the eigenvalues of the matrices along the diagonal. This means that the eigenvalues of the closed loop system will be the union of the observer eigenvalues (Kalman filter poles) (A - LC) and the controller poles (A - BK) which can be designed independently. The feedback gain K is a design parameter and the poles of the controller can therefore be chosen arbitrary and the Kalman filter gain L is the optimal observer gain and thereby always stable, and hence, the separation principle is proved and system stability can be guaranteed.

5.2 Stability of linear ESMO model with feedback

A linear model of ESMO was presented in section by Simonsen in [2] where the discrete model is as follows

$$\mathbf{x}_k = \mathbf{A}\mathbf{x}_{k-1} + \mathbf{B}\mathbf{u}_k + w_{k-1} \tag{5.11}$$
$$\mathbf{Z}_k = \mathbf{H}\mathbf{x}_k + \mathbf{v}_k \tag{5.12}$$

The Kalman filter gives following equation for the estimate of the state

$$\hat{\mathbf{x}}_k = \mathbf{A}\hat{\mathbf{x}}_{k-1} + \mathbf{B}\mathbf{u}_k + K_k(Z_k - H\hat{x}_{k-1}) \tag{5.13}$$

K_k is the Kalman filter gain which minimizes the mean-square estimation error. A simple control law $u_k = -L\hat{x}_{k-1}$ is used as feedback controller for the system. By applying this control law to the (5.11) and (5.13), the system becomes

$$\begin{bmatrix} x_k \\ \hat{x}_k \end{bmatrix} = \begin{bmatrix} A & -BL \\ K_kH & A - BL - K_kH \end{bmatrix} \begin{bmatrix} x_{k-1} \\ \hat{x}_{k-1} \end{bmatrix} \tag{5.14}$$

By using the transformation illustrated in (5.9), the system matrix can be rearranged to the more convenient block-triangular shape

$$\begin{bmatrix} x_k \\ \tilde{x}_k \end{bmatrix} = \begin{bmatrix} A - BL & -BL \\ 0 & A - K_kH \end{bmatrix} \begin{bmatrix} x_{k-1} \\ \tilde{x}_{k-1} \end{bmatrix} \tag{5.15}$$

For the linearized ESMO model with feedback, the eigenvalues of (5.15) needs to be in the LHP to be stable. Since the system matrix is block triangular, the eigenvalues of the overall system is equal the eigenvalues of the matrices on the diagonal which is the eigenvalues of the feedback controller and the Kalman filter respectively. The eigenvalues are then determined by

$$\det(\lambda I - (A - BL)) = 0 \tag{5.16}$$
$$\det(\lambda I - (A - K_kH)) = 0 \tag{5.17}$$

where

$$\mathbf{A} = \begin{bmatrix} 1 & T & 0 & 0 & 0 & 0 \\ -4\omega_0^2\sigma_x & 1 & 0 & 0 & 0 & \omega_0(1-\sigma_x)T \\ 0 & 0 & 1 & T & 0 & 0 \\ 0 & 0 & -3\omega_0^2\sigma_y T & 1 & 0 & 0 \\ 0 & 0 & 0 & 0 & 1 & T \\ 0 & -\omega_0(1-\sigma_z) & 0 & 0 & -\omega_0^2\sigma_z T & 1 \end{bmatrix}$$

$$= \begin{bmatrix} 1 & 0.02 & 0 & 0 & 0 & 0 \\ -4.6e-7 & 1 & 0 & 0 & 0 & 1e-5 \\ 0 & 0 & 1 & 0.02 & 0 & 0 \\ 0 & 0 & -1.5e-7 & 1 & 0 & 0 \\ 0 & 0 & 0 & 0 & 1 & 0.02 \\ 0 & -1.16e-5 & 0 & 0 & 6.5e-8 & 1 \end{bmatrix}$$

$$\mathbf{B} = \begin{bmatrix} 0 & 0 & 0 \\ \frac{T}{2I_x} & 0 & 0 \\ 0 & 0 & 0 \\ 0 & \frac{T}{2I_y} & 0 \\ 0 & 0 & 0 \\ 0 & 0 & \frac{T}{2I_z} \end{bmatrix} = \begin{bmatrix} 0 & 0 & 0 \\ 0.0025 & 0 & 0 \\ 0 & 0 & 0 \\ 0 & 0.0022 & 0 \\ 0 & 0 & 0 \\ 0 & 0 & 0.0029 \end{bmatrix}$$

L is the control gain which is chosen arbitrary so that $\det(\lambda I - (A - BL)) = 0$ gives eigenvalues in LHP and therefore stable. L is chosen in [2] by pole placement with following stable poles p = [-1 -0.5 -1 -0.5 -1 -0.5], and gives following control gain matrix

$$L = \begin{bmatrix} 60000 & 1400 & 0 & 0 & 0 & 0.0040 \\ 0 & 0 & 68182 & 1591 & 0 & 0 \\ 0 & -0.0040 & 0 & 0 & 51724 & 1207 \end{bmatrix}$$

H = I and K_k is the Kalman filter gain. According to [11], the solution of the Kalman filter equation is uniformly asymptotically stable no matter what the initial conditions are as long as the system is stochastically controllable and observable. The Kalman filter gain is calculated from the Riccati equation and given by

$$P_k^- = AP_{k-1}A^T + Q_k \tag{5.18}$$
$$P_k = (I - K_k H)P_k^- \tag{5.19}$$
$$K_k = P_k^- H^T (HP_k^- H^T + R_k)^{-1} \tag{5.20}$$

Bounded Q, R and A will guarantee stochastic controllability and observability for the system.

Stability by use of separation principle is thereby proved for the linear ESMO case.

Chapter 6

Stability of EKF and nonlinear Separation Principle

6.1 Separation Principle for nonlinear systems

It is an easy task to show that the separation principle holds for linear systems. The overall closed loop system eigenvalues will be the union of the observer eigenvalues and the state-feedback eigenvalues, and hence a stable closed loop system can be developed by choosing proper observer and controller separately.

The task of applying a separation principle for nonlinear systems is not as straight forward as for the linear case. The problem being the fact that there are no assurance that the control algorithm, obtained by combining a nonlinear state feedback law with an observer will result in a closed-loop system with satisfactory performance. However, the separation principle has been extended to nonlinear systems in many applications and has often proved to be a successful and stable design method. The problem has been to prove theoretically, that a nonlinear separation principle holds for any nonlinear system. Quite a lot of research has been done on the matter, and nonlinear separation principle has been proved for certain cases, although not in general.

6.1.1 Previous work and methods on nonlinear separation principle

In [12] an observer based control structure for a standard nonlinear model of polymerization reactors is developed. The problem is solved by designing an exponentially converging observer, where the equations are close to those of the extended Kalman filter. The system is proved to stabilize the polymerization reactors by providing a nonlinear separation principle for the case. In this paper, exponential convergence of the estimation error is a key point in the separation principle proof. The separation principle only holds when combining a globally asymptotically stable nonlinear feedback controller, admitting the physical invariant bounded set, with an

exponentially converging high-gain observer. The controlled state then remains in a bounded set. It can be rather difficult to find a globally asymptotically stabilizing controller for the systems, as the sign ambigiouty often cause problems.

In [13] and [14], Khalil and Atassi have thoroughly evaluate the separation principle for stabilization of a class of nonlinear systems. It is proved that the performance of a globally bounded partial state feedback controller of a certain class of nonlinear systems can be recovered by a sufficiently fast high gain observer. The goal for the research is to find a nonlinear separation theorem independent of the state derived, under the least restrictive assumptions possible. Previous results are extended to allow model uncertainties, performance recovery yields asymptotic stability as well as recovery of the region of attraction and trajectories. This distinguish the research from that performed by Teel and Praly [15].

The results in [15] is quite remarkable as it is shown that global stability by state feedback and observability imply semi global stabilizability by output feedback. In contrast to Khalil and Atassi's work, the result of [15] does not allow model uncertainties and only recovery of the asymptotic stability and semi global stabilization property are shown.

The class of system represented in [13] is on the form

$$\dot{x} = Ax + B\phi(x, z, u) \tag{6.1}$$
$$\dot{z} = \varphi(x, z, u) \tag{6.2}$$
$$y = cx \tag{6.3}$$
$$\zeta = q(x, z) \tag{6.4}$$

where

$u \in U \subseteq R^m$ control input
$y \in Y \subseteq R^p$ measured output
$\zeta \in R^s$ measured output
$x \in X \subseteq R^r$ state vector
$z \in Z \subseteq R^l$ state vector

and the system satisfying the following assumptions

Assumption 1: The functions ϕ: $X \times Z \times U \rightarrow R^p$ and φ: $X \times Z \times U \rightarrow R^l$ are locally Lipschitz in their arguments over the domain of interest. In addition, $\phi(0, 0, 0) = 0$, $\varphi(0, 0, 0) = 0$ and $q(0, 0) = 0$.

This assumption guarantees that the origin is the equilibrium of the open loop system. It is also used that if the nonlinear system

$$\dot{X} = f(X) + g(X)u$$
$$y = h(X)$$

has a vector relative degree $(r_1, \cdots, r_p)$, then the system can be transformed into

$$\dot{\xi} = A\xi + B\left[f_1(\xi, z) + g_1(\xi, z)u\right]$$
$$\dot{z} = f_2(\xi, z, u)$$
$$y = C\xi$$

The controller is assumed to be on the form

$$\dot{\vartheta} = \Gamma(\vartheta, x, \xi) \tag{6.5}$$
$$u = \gamma(\vartheta, x, \xi) \tag{6.6}$$

Assumption 2:

1. Γ and γ are locally Lipschitz functions in their arguments over the domain of interest, $\Gamma(0,0,0) = 0$ and $\gamma(0,0,0) = 0$
2. Γ and γ are globally bounded functions of x.
3. The origin ($x = 0$, $z = 0$, $\vartheta = 0$) is an asymptotically stable equilibrium point of the closed-loop system.

A high-gain observer is used

$$\dot{\vartheta} = \Gamma(\vartheta, \hat{x}, \xi) \tag{6.7}$$
$$u = \gamma(\vartheta, \hat{x}, \xi) \tag{6.8}$$
$$\dot{\hat{x}} = A\hat{x} + B\phi_0(\hat{x}, \xi, u) + H(y - C\hat{x}) \tag{6.9}$$

Assumption 3: $\phi_0(\hat{x}, \xi, \gamma(\vartheta, \hat{x}, \xi)$ is locally Lipschitz in its arguments over the domain of interest and globally bounded in x and $\phi_0(0,0,0) = 0$.

The performance recovery can be stated in three points. First, the origin of the closed loop system under feedback is asymptotically stable. Second, the output feedback controller recovers the region of attraction of the state feedback controller in the sense that if R is the region of attraction under state feedback, then for any compact set S in the interior of R, and any compact set $Q \subseteq R^r$, the set $S \times Q$ is included in the region of attraction under output feedback control. Lastly, the

trajectory of (x, z, ϑ) under output feedback approaches the trajectory under state feedback as $\epsilon \rightarrow 0$. In other word, it is boundedness, ultimate boundedness, trajectory of convergence and thereby recovery of asymptotic stability of the origin. This is all proved in [13].

In [14] Khalil and Atassi extend their work on separation principle theory for nonlinear systems. In this study, the attention is on achieving boundedness of trajectories without necessarily convergence with an equilibrium point. It is shown that for a nonlinear system, same as in [13] with the same requirements for globally bounded control law and high gain observer, the output feedback recovers the performance of the state feedback controller. Moreover it renders a compact set of interest positively invariant and asymptotically attractive. Any compact subset of the region of attraction under state feedback can be included in the region of attraction under output feedback. The trajectories also converge to those under state feedback as the observer gain approaches infinity.

Jo and Seo also study the separation principle for nonlinear systems in [16]. Instead of assuming the existence of a Lyapunov function for the observation error, it is assumed existence of a state observer which asymptotically estimates the true state. They show that under the assumption that a nonlinear system has asymptotically stable zero dynamics and is locally detectable, an asymptotic tracking by output feedback control can be achieved. Hence a local separation principle is deduced. This implies that for a nonlinear system, it guarantees that an asymptotically convergent observer can be used with a stabilizing controller to locally stabilize the system. This result is presented under the local detectability condition.

In [17] Cerny and Hrusak present another way of solving the separation problem for nonlinear systems based on dissipative system theory. The dissipative normal is combining two methods. In the first method, the closed loop system structure is represented in a dissipative normal form; a controller is thereafter chosen to fulfill the required closed loop behaviour in order to solve the stabilizing problem for nonlinear systems. In the second method, the error system structure is represented in the dissipative normal form, to solve the state reconstruction problem. The solution of the separation principle problem for nonlinear system can then be found by means of integrating the stabilization and state reconstruction described above. It is embodied in compensation function that guarantees asymptotic stability of the resulting closed loop system.

Assuming a nonlinear system

$$\dot{x}(t) = f\left[x(t), u(t)\right] \tag{6.10}$$

$$y(t) = h\left[x(t)\right] \tag{6.11}$$

The dissipative normal form involves transforming the system so that a function $W\left[x(t)\right]$ fulfills the following conditions

$$w\left[x(t)\right] = \|x(t)\|^2 \tag{6.12}$$

$$L_f\left\{w\left[x(t)\right]\right\} = \beta\left[y(t)\right] \leq 0 \tag{6.13}$$

L_f is the Lie derivation and $w\left[x(t)\right]$ is a measure of the signal energy stored in the system at time t.
Structural asymptotic stability can be imposed by representing the system on the form

$$\dot{x}(t) = \begin{bmatrix} \varphi_1\left[x_1(t)\right] & k_2 & 0 & . & 0 \\ -k_2 & 0 & k_3 & . & . \\ 0 & -k_3 & . & . & 0 \\ . & . & . & . & k_n \\ 0 & . & 0 & -k_n & 0 \end{bmatrix} x(t) \tag{6.14}$$

$$y(t) = \alpha\left[x_i(t)\right] \tag{6.15}$$

where $k_2, \cdots, k_n \neq 0 \in R$ are constants and the nonlinear functions $\varphi_1\left[x_1(t)\right] < 0$ for $x_1(t) \neq 0, \exists \alpha^{-1}\left[y(t)\right]$ and $\alpha\left[x_i(t)\right] = 0 \Leftrightarrow x_1(t) = 0$.

The only equilibrium state $x_e = 0$ will be asymptotically stable and the corresponding $W\left[x(t)\right]$ fulfils the conditions for dissipative normal form (6.12) and (6.13) for any $\varphi_1\left[x_1(t)\right]$, $\alpha\left[x_i(t)\right]$ and $k_2, \cdots, k_n$. The proof can be viewed in [17].

The next step in this method is to design an observer, based on dissipative normal form, which generates the asymptotic estimate $\hat{x}(t)$ of the state x(t) based on input and measurement, such that the following demands are satisfied

$$\dot{\tilde{x}}(t) = \tilde{f}\left[\tilde{x}(t), x(t), \hat{x}(t), u(t), y(t)\right] = \tilde{f}\left[\tilde{x}(t)\right] \tag{6.16}$$

where

$$\tilde{x}(t) = x(t) - \hat{x}(t) \tag{6.17}$$

and the state error convergence condition

$$\lim_{t\to\infty} \tilde{x}(t) = \lim_{t\to\infty} \left[x(t) - \hat{x}(t)\right] = 0 \tag{6.18}$$

The system must be presented on the dissipation normal form

$$\dot{\tilde{x}}^*(t) = \omega_0 \begin{bmatrix} \delta_1^*\left[\tilde{x}_1^*(t)\right] & \delta_2^* & 0 & . & 0 \\ -\delta_2^* & 0 & \delta_3^* & . & . \\ 0 & -\delta_3^* & . & . & 0 \\ . & . & . & . & \delta_n^* \\ 0 & . & 0 & -\delta_n^* & 0 \end{bmatrix} \tilde{x}^*(t) \tag{6.19}$$

where $\delta_1^*[\tilde{x}_1^*(t)]$, ω_0, $\delta_2^*, \cdots, \delta_n^*$ are design parameters with a Lyapunov function $\tilde{V}^*[\tilde{x}^*(t)] = \|\tilde{x}^*(t)\|^2$ related to (6.19) and fulfils

$$L_{\tilde{f}^*}\{[\tilde{x}^*(t)]\} = L_{\tilde{f}^*}\left\{\|\tilde{x}^*(t)\|^2\right\} = 2\omega_0\tilde{x}^*(t)^2\delta_1^*[\tilde{x}^*(t)] \tag{6.20}$$

If the design parameters are properly chosen, the state error system will converge to zero. If $\omega_0 > 0$ and $\delta_1^*[\tilde{x}_1^*(t)] < 0\ \forall\tilde{x}_1^*(t)$, then the error system will be globally asymptotically stable.

The next aim is to propose a controller $u(t) = L[x(t)]$ so that the closed loop system

$$\dot{x}(t) = f\{x(t), L[x(t)]\} \tag{6.21}$$
$$y(t) = h[x(t)] \tag{6.22}$$

is asymptotically stable.

Again the dissipative form is crucial for the presentation, and therefore the closed loop system must be transformed to

$$\dot{x}^*(t) = \nu\begin{bmatrix} f_1^*[x_1^*(t)] & f_2^* & 0 & . & 0 \\ -f_2^* & 0 & f_3^* & . & . \\ 0 & -f_3^* & . & . & 0 \\ . & . & . & . & f_n^* \\ 0 & . & 0 & -f_n^* & 0 \end{bmatrix} x^*(t) \tag{6.23}$$
$$y(t) = x_1^*(t) \tag{6.24}$$

where $f_1^*[x_1^*(t)]$, ν, $f_2^*, \cdots, f_n^*$ are the design parameters. Further suppose that the original open loop system can be transformed to

$$\frac{d}{dt}\begin{bmatrix} \bar{x}_1(t) \\ \vdots \\ \bar{x}_{n-1}(t)\bar{x}_n(t) \end{bmatrix} = \begin{bmatrix} \bar{x}_2(t) \\ \vdots \\ \bar{x}_n(t)\mu[\bar{x}(t), u(t)] \end{bmatrix} \tag{6.25}$$
$$y(t) = \bar{x}_1(t) \tag{6.26}$$

where $\mu[\bar{x}(t), u(t)]$ is a nonlinear function. Then the controller $u(t) = L[x(t)]$ can be derived by using and equivalence relation

$$u(t) = L[x(t)] = \mu^{-1}\{\bar{x}(t), \eta[\bar{x}(t)]\} \tag{6.27}$$
where
$$\eta[\bar{x}(t)] = L_{f^*}^n[x_1^*(t)], \text{ for } x^*(t)T^{-1}[\bar{x}(t)] \tag{6.28}$$

Based on the above steps, a separation principle for nonlinear systems on dissipative form can be presented. A short description of this proof is presented beneath, the full proof can be viewed in [17].

Assume the input control to be

$$u(t) = L\left[\bar{x}(t)\right]|_{\bar{x}(t)=\hat{\bar{x}}(t)} = L\left[\hat{\bar{x}}(t)\right] = \mu^{-1}\left\{\hat{\bar{x}}(t), \eta\left[\hat{\bar{x}}(t)\right]\right\} \tag{6.29}$$

which gives following representation of the closed loop system with observer and feedback control

$$\frac{d}{dt}\begin{bmatrix} \bar{x}_1(t) \\ \vdots \\ \bar{x}_{n-1}(t)\bar{x}_n(t) \end{bmatrix} = \begin{bmatrix} \bar{x}_2(t) \\ \vdots \\ \bar{x}_n(t)\gamma\left[\bar{x}(t), \hat{\bar{x}}(t)\right] \end{bmatrix} \tag{6.30}$$

$$y(t) = \bar{x}_1(t) \tag{6.31}$$

where $\gamma\left[\bar{x}(t), \hat{\bar{x}}(t)\right] = \mu\left\{\bar{x}(t), \mu^{-1}\left\{\hat{\bar{x}}(t), \eta\left[\hat{\bar{x}}(t)\right]\right\}\right\}$. Then, if the previous described methods are combined, the closed loop system can be transformed to dissipation normal form

$$\frac{d}{dt}\begin{bmatrix} x_1^*(t) \\ x_2^*(t) \\ \vdots \\ x_{n-1}^*(t)x_n^*(t) \end{bmatrix} = \begin{bmatrix} f_1^*\left[x_1^*(t)\right]x_1^*(t) + f_2^*x_2^*(t) \\ -f_2^*x_1^*(t) + f_3^*x_3^*(t)\vdots \\ -f_{n-1}^*x_{n-2}^*(t) + f_n^*x_n^*(t) \\ \zeta\left[x^*(t), \hat{x}^*(t)\right] \end{bmatrix} \tag{6.32}$$

$$y(t) = x_1^*(t) \tag{6.33}$$

The system above is the dissipation normal form if and only if

$$\begin{aligned} \zeta\left[x^*(t), \hat{x}^*(t)\right] &= \sum_{i=1}^{n-1} \frac{\partial T_n^{-1}\left[\bar{x}(t)\right]}{\partial \bar{x}_i(t)} L_{f^*}^i\left[x_1^*(t)\right] + \frac{1}{f_n^*}\gamma_1\left[\bar{x}(t)\right] + \frac{1}{f_n^*}\gamma_2\left[\hat{\bar{x}}(t)\right] \\ &= -f_n^*x_{n-1}^*(t) \end{aligned} \tag{6.34}$$

for $\bar{x}(t) = T\left[x^*(t)\right]$ and $\hat{\bar{x}}(t) = \hat{T}\left[\hat{x}^*(t)\right]$.
This condition can only be confirmed if the following assumptions holds

1. The original open loop system in (6.10) and (6.11) can be transformed into the dissipation normal form

$$\dot{x}^*(t) = a^*\left[x^*(t)\right] + b^*\left[x^*(t)\right]u(t) \tag{6.35}$$

$$y(t) = c^*\left[x_1^*(t)\right] \tag{6.36}$$

$$a^*\left[x^*(t)\right] = \begin{bmatrix} a_1^*\left[x_1^*(t)\right] & a_2^* & 0 & . & 0 \\ -a_2^* & 0 & a_3^* & . & . \\ 0 & -a_3^* & . & . & 0 \\ . & . & . & . & a_n^* \\ 0 & . & 0 & -a_n^* & 0 \end{bmatrix} \tag{6.37}$$

2. $f_2^* = a_2^*, f_3^* = a_3^*, \cdots, f_n^* = a_n^*$
3. The compensation function

$$\upsilon\left[\hat{\bar{x}}(t)\right] = -\frac{1}{a_n^*}\gamma_2\left[\hat{\bar{x}}(t)\right] \tag{6.38}$$

$$\tag{6.39}$$

where

$$\gamma_2\left[\hat{\bar{x}}(t)\right] = \mu_1\left[\hat{\bar{x}}(t)\right] - L_{f^*}^n\left[x_1^*(t)\right] \tag{6.40}$$

for $x^*(t) = T^{-1}\left[\bar{x}(t)\right]$ and $\bar{x}(t) = \hat{\bar{x}}(t)$, is added to the proposed controller

$$u(t) = L\left[\hat{\bar{x}}(t)\right] + \upsilon\left[\hat{\bar{x}}(t)\right] \tag{6.41}$$

If the above assumptions hold so that the condition given in (6.34) is fulfilled, then asymptotic stability of the closed loop system is guaranteed, and hence a nonlinear separation principle is proved. The method is exact and does not require any system linearization. Comparing this method with [13],[14] it is an analytic method as no numerical approach is used, but it is also very tedious and depending on having a system that can be transformed to the desired form.

In the work of Loria and Morales [18], another way of approaching the nonlinear separation principle is proposed, based on stability results for cascade systems. Sufficient conditions are given so that an asymptotically stabilizing state feedback controller, implemented using state estimate, implies global asymptotically stability of the closed loop system. The systems having to be transformable into a form affine in the unmeasurable variable. The proof of this relies in a sufficient condition stated in the concept of persistence of excitation. The condition imposed on the globally stabilizing feedback is that it be bounded by a function of order at least 0. It does not vanish asymptotically for large values. The available state feedback need not be bounded. The result yields for time-varying systems and the separation principle is based on analysis results from cascade systems.

Two tools are used to present the main result in the article. First of all, the persistency of excitation is used to prove exponential convergence of the observer error. Second, view the overall closed loop system as a cascade systems on the form

$$\Sigma_1 : \dot{\xi}_1 = f_1(t, \xi_1) + g(t, \xi)\alpha(t, \xi) \tag{6.42}$$

$$\Sigma_2 : \dot{\xi}_2 = f_1(t, \xi_2) \tag{6.43}$$

where all functions satisfies the BRA (Basic regularity assumptions) and $\xi_2 = 0$ implies that $\alpha(t, \xi) \equiv 0 \forall t, \xi_1$. This give ground to the following theorem

Theorem 6.1.1 *Assume that* $\dot{\xi}_1 = f_1(t, \xi_1)$ *and* $\dot{\xi}_2 = f_2(t, \xi_2)$ *are UGAS (Uniformly globally asymptotically stable) and that the cascade system is forward complete and the following assumptions hold*

Assumption 6.1.2 *There is a Lyapunov function* $V(t, \xi_1), \alpha_1, \alpha_2 \in \kappa_\infty$ *and a positive semi definite function* $W(\xi_1)$ *s.t*

$$\alpha_1(|\xi_1|) \leq V(t, \xi_1) \leq \alpha_2(|\xi_1|) \tag{6.44}$$

$$\frac{\partial V}{\partial t} + \frac{\partial V}{\partial \xi_1} f(t, \xi_1) \leq -W(\xi_1) \tag{6.45}$$

Assumption 6.1.3 *There exists* $\lambda, \eta > 0$ *s.t for each* t, ξ_2

$$|\xi_1| \geq \eta \Rightarrow |\frac{\partial V}{\partial \xi_1} g(t, \xi)| \leq \lambda W(\xi_1) \tag{6.46}$$

Assumption 6.1.4 *There exists a* $\theta \in \kappa$ *s.t*

$$|\alpha(t, \xi)| \leq \theta(|\xi_2|) \tag{6.47}$$

then all the solutions of (6.42) are uniformly bounded and the cascade is UGAS.

Considering an affine nonlinear closed loop system on the form

$$\dot{x} = f(t, x) + g(t, x)u \tag{6.48}$$

$$y = h(t, x) \tag{6.49}$$

where the functions satisfies BRA condition

Standing Assumption 6.1.5 *There exists a time varying state feedback* $u = k(t, x)$ *where* $k(\cdot, \cdot)$ *satisfies the BRA s.t*

$$\dot{x} = f(t, x) + g(t, x)k(t, x) \tag{6.50}$$

is UGAS

Standing Assumption 6.1.6 *There exists a matrix* $C \in R^{m \times n}$ *s.t defining the measurable output* $y = Cx$*, the system (6.48) is transformable into the form:*

$$\dot{x} = A(t, y)x + b(t, u, y, x) \tag{6.51}$$

where the function $b(t, u, y, \cdot)$ *satisfies*

$$|b(t, u, y, x) - b(t, u, y, \hat{x})| \leq k_b|\bar{x}| \tag{6.52}$$

where $\bar{x} := x - \hat{x}$ $\forall$ $x, \hat{x} \in R^n$ $\forall$ $t \geq 0$ *,* $u \in R^q$ *and* $y \in R^m$*.*

This leads to following important fact

Theorem 6.1.7 *There exist a C^1 function $V(t,x)$, class κ functions α_1, α_2 and $W(x)$ positive definite s.t*

$$\begin{aligned} \alpha_1(|x|) \leq V(t,x) \leq \alpha_2(|x|) \\ \frac{\partial V}{\partial t} + \frac{\partial V}{\partial x}\left[f(t,x) + g(t,x)k(t,x)\right] \leq -W(x) \\ \left|\frac{\partial V}{\partial x}\right| \leq \alpha(|x|) \end{aligned}$$

and without loss of generality, it can also be assumed that $\alpha(|\cdot|)$ is of the same order of growth as $V(t,\cdot)$ for each t.

The observer proposed for in the article [18] is a persistence of excitation based observer.

$$\dot{\hat{x}} = A(t,y)\hat{x} - L(t,y)C(x-\hat{x}) + b(t,u,y,\hat{x}) \tag{6.53}$$

$L(\cdot,\cdot)$ satisfies BRA. And the estimation error dynamics is represented by

$$\dot{\bar{x}} = A(t,y)\bar{x} - L(t,y)C\bar{x} + b(t,u,y,x) - b(t,u,y,\hat{x}) \tag{6.54}$$

where $\bar{x} = \hat{x} - x$.

Next assumption on the observer gain guarantees that the estimation state error is globally exponentially stable uniformly in y.

Assumption 6.1.8 *There exists a globally bounded positive definite matrix function $P(\cdot)$ s.t, defining*

$$\begin{aligned} \bar{A}(t,y_t) &:= A(t,y_t) - L(t,y_t)C \\ Q(t,y_t) &:= \bar{A}(t,y_t)^T P(t) + P(t)^T \bar{A}(t,y_t) + \dot{P}(t) \end{aligned} \tag{6.55}$$

following yields for all $t \geq 0, y_t \in R^m$

1. *$Q(t,y_t) \leq 0$*
2. *There exist μ and $T > 0$ s.t*

$$\int_t^{t+T} -Q(\tau,y_t)d\tau \geq \mu I > 0 \tag{6.56}$$

3. *There exists a $q_M > 0$ s.t $q_M \geq |Q(t,y_t)|$*

This leads to following proposition

Proposition 6.1.9 *The estimation error dynamics,*

$$\dot{\bar{x}} = A(t,y)\bar{x} + b(t,u,y,\bar{x}+\hat{x}) - b(t,u,y,\hat{x}) \tag{6.57}$$

is exponentially stable, uniformly in y, u, t and $\hat{x}$ if Assumption (6.1.8) holds with sufficiently large $\mu > 0$.

(Proof can be viewed in [18].)

What this proposition actually implies is that the observer error dynamics is exponentially stable uniformly in trajectories $y_t = y(t)$ if the matrix $Q(t, y_t)$ is sufficiently output persistence excitation. It is now possible to propose a separation principle for the closed loop system. By applying the control law $u = k(t, \hat{x})$ the closed loop system in (6.48) gets a cascade structure and becomes

$$\dot{x} = f(t,x) + g(t,x)k(t,x) + g(t,x)\left[k(t,\hat{x}) - k(t,x)\right] \tag{6.58}$$

Further on, the overall closed loop system can be rewritten to

$$\dot{x} = F(t,x) + g(t,x)\bar{\alpha}(t,x,\bar{x}) \tag{6.59}$$
$$\dot{\bar{x}} = A(t,y(t))\bar{x} + b(t,u(t),y(t),x(t)) - b(t,u(t),y(t),\bar{x}-x(t)) \tag{6.60}$$

where $\bar{\alpha}(t,x,\bar{x}) := [k(t,\bar{x}+x) - k(t,x)]$ and $F(t,x) := f(t,x) + g(t,x)k(t,x)$

The standing assumption 6.1.5 implies that $\dot{x} = F(t,x)$ is UGAS, in light of Proposition 6.1.9 the overall closed loop system of (6.59),(6.60) is globally exponentially stable uniformly in the trajectories $y(t)$ and $u(t)$. Thereafter, by defining $\xi := col\,[x,\hat{x}]$ the trajectories of the overall system can be written on the cascade form proposed earlier in (6.42).

$$\dot{\xi}_1 = F_1(t,\xi_1) + G(t,\xi)\alpha(t,\xi) \tag{6.61}$$
$$\dot{\xi}_2 = F_0(t,\xi_2) \tag{6.62}$$

where $G(t,\xi) = g(t,\xi)$, $\alpha(t,\xi) = \bar{\alpha}(t,\xi_1,\xi_2)$ and
$F_0(t,\xi_2) = A(t,y(t))\bar{x} + b(t,u(t),y(t),x(t)) - b(t,u(t),y(t),\bar{x}-x(t))$.

The BRA assumption on $g(\cdot,\cdot)$ and $k(\cdot,\cdot)$ gives the existence of two nondecreasing functions s.t

$$|g(t,x)| \leq \theta_k(|x|)\forall x \in R^n \tag{6.63}$$
$$|k(t,z) - k(t,y)| \leq \theta_k(|z-y|)\forall z,y \in R^n) \tag{6.64}$$

because of this, for each $r > 0$ then $|G(t,\xi)\alpha(t,\xi)| \leq \theta_k(r)\theta_g(|\xi_1|)$. Further on, this leads the main theorem of Loria and Morales work [18].

Theorem 6.1.10 *If there exists a Lyapunov function $V(\cdot,\cdot)$ for the system given in (6.50) satisfying the bounds of theorem 6.1.7 with $W(x) \leq 0$ and constants $q \geq 0$, $c_1, c_2 > 0$ s.t*

$$\int_0^\infty \frac{ds}{\alpha_3(s)\theta_g(s)} = \infty \tag{6.65}$$

$$\frac{|k(t,z)|}{|z|^q} \leq c, \ \forall |z| \geq, \forall t \geq 0 \tag{6.66}$$

then the system (6.48), under the standing assumptions, in closed loop with $u = k(t,\hat{x})$ and the observer proposed in (6.53) under assumption (6.1.8), is said to be uniformly globally asymptotically stable (UGAS), and hence the separation principle for nonlinear system based on cascade structure is presented.

The proof and detailed explanation can be found in [18].

6.1.2 Summary of nonlinear separation principle

The methods presented in the previous chapters are all rather complex and requires strong conditions for the nonlinear separation principle to hold. Many papers and a vast amount of research has been done in this area, without luck in finding a general simple method rule for under what conditions a feedback loop consisting of a nonlinear system with an observer and feedback controller apply the separation principle and therefore can be design separately. Methods have been found and verified for certain cases of nonlinear systems. To sum up the cases presented earlier where separation principle have been proved is the case where the systems are applying

- globally asymptotically stable nonlinear feedback controller admitting physical invariant bounded set combined with an exponentially converging high-gain observer.
- globally bounded control law combined with a sufficiently high gain observer when nonlinearities are only found in measurements
- existence of a state observer which asymptotically estimates the true states. A nonlinear system with asymptotically stable zero dynamics, which is locally detectable, makes it possible with asymptotic tracking by output feedback control. Hence a local separation principle which guarantees asymptotic convergent observer and stabilizing control can be proposed, which in turn locally stabilizes the system.
- observer based on dissipative normal form design combined with a stabilizing controller on dissipative normal form gives an asymptotically stable closed loop system

- cascade structure on overall closed loop system combined with the theory of persistence of excitation to prove exponential converging observer error leads to uniformly globally asymptotically stable system if certain conditions are fulfilled

6.2 EKF stability in general

The Extended Kalman filter was introduced as an approximation of the optimal linear estimator as it was desirable to develop a filter estimator for nonlinear systems. The EKF constructs a linear algorithm that approximates the nonlinear system near the current best estimate. It is assumed that process and observations are linear on the scale of the error in the estimated state. The validity of this assumption is secured by re-linearization about each new state. The problem with this extension of the linear Kalman filter is that optimality of the KF is lost. Although many applications of the EKF proves to be stable and work properly, stability for the general case has proved to be very complex and difficult to state theoretical.

In this chapter previous work and research regarding stability of the EKF are presented, followed by the proof and conditions for the EKF convergence.

6.2.1 Previous work and research on stability for EKF

Since the first successful application on the Apollo program at NASA by the scientist Dr. Stanley F. Schmidt in 1960, the extended Kalman filter has gained more and more popularity. A large amount of literature, research and articles can be found on the theme. The filter have been implemented widely in many areas of signal processing, control and optimization like; adaptive filtering, estimation, prediction, robust control, state observation, system identification, target tracking and many others.

Although the extended Kalman filter has proved superior practical usefulness, the theoretical and mathematical aspects like stability and convergence of the filter has not been investigated as thoroughly as the extended use of the filter should imply. Stability has only been treated for some special cases, like when the state equations are given in a special form, when used as a parameter estimator for linear systems and zero noise case. Only recently has researchers been able to prove general convergence and stability for EKF, though, limited by some rather conservative constraib.

In [19] local convergence of the continuous extended Kalman filter was shown for some very strong conditions. [20] extend this result to yield a larger class of filters where also the strong uniform detectability requirement are shown to be unnecessary. [21] presents an analysis for the discrete-time case while [22] presents an important results which shows the convergence of EKF as an observer for a discrete-time sys-

tem. It is also shown that by small modification of the filter algorithm, the rate of convergence can be prescribed by the designer. This result is studied more closely later in this chapter. [23] investigates the stability for the discrete-time case with nonlinear state and linear output map and by using the results from [21] it is extended to include the stochastic case. In late 90's, an analysis for the general case is presented by [24] with both nonlinear state and output map. Here it is also proved that the EKF is stochastically stable under certain conditions. This result is also more thoroughly presented later in this section. The newest investigation of EKF stability is done by [25]. Here the results of [24] is brought further, in order to relax the conservative conditions for which stability can be established. Also these results will be closer investigated later in this chapter.

Presentation of the most important previous results

In [24], an analysis of the error behaviour for the discrete-time extended Kalman filter for general systems in a stochastic framework is carried through. It is proved that the estimation error remains bounded if the system satisfies the nonlinear observability rank condition and the initial estimation error as well as the disturbing noise terms are small enough. By combining the stability results for the linear Kalman filter and stability analysis for more general nonlinear estimation problems, the error behaviour of the EKF can be analyzed. Suppose a discrete system on the form

$$z_{n+1} = f(z_n, x_n) + G_n w_n \tag{6.67}$$
$$y_n = h(z_n) + D_n v_n \tag{6.68}$$

Z_n is the system state while x_n is the system input. v_n and w_n are uncorrelated zero-mean white noise processes. A state estimator is presented as

$$\hat{z}_{n+1} = f(\hat{z}_n, x_n) + K_n(y_n - h(\hat{z}_n)) \tag{6.69}$$

The functions f and h are assumed to be C^1-functions and can therefore be expanded by the Taylor series to

$$f(z_n, x_n) - f(\hat{z}_n, x_n) = A_n(z_n - \hat{z}_n) + \varphi(z_n, \hat{z}_n, x_n) \tag{6.70}$$
$$h(z_n) - h(\hat{z}_n) = C_n(z_n - \hat{z}_n) + \chi(z_n, \hat{z_n}) \tag{6.71}$$
$$A_n = \frac{\partial f}{\partial z}(\hat{z}_n, x_n)\ ,\ C_n = \frac{\partial h}{\partial z}(\hat{z}_n) \tag{6.72}$$

The estimation error is defined by

$$\zeta_n = z_n - \hat{z}_n \tag{6.73}$$

and

$$\zeta_{n+1} = (A_n - K_n C_n)\zeta_n + r_n + s_n \tag{6.74}$$
$$r_n = \varphi(z_n, \hat{z}_n, x_n) - K_n\chi(z_n, \hat{z_n}),\ \text{and}\ s_n = G_n w_n - K_n D_n v_n \tag{6.75}$$

Applying the following Definitions and Lemmas [24] leads up to the main result of the article

Definition 6.2.1 *The stochastic process ζ_n is said to be exponentially bounded in mean square, if there are real numbers η, $\nu > 0$ and $0 < \vartheta < 1$ s.t*

$$E\left\{\|\zeta_n\|^2\right\} \leq \eta \|\zeta_0\|^2 \vartheta^n + \nu \tag{6.76}$$

holds for every $n \geq 0$.

Definition 6.2.2 *The stochastic process is said to be bounded with probability one, if*

$$sup_{n\geq 0}\|\zeta_n\| < \infty \tag{6.77}$$

holds for probability one.

Lemma 6.2.3 *Assume there is a stochastic process $V_n(\zeta_n)$ as well as real numbers $\underline{v}, \overline{v}, \mu > 0$ and $0 < \alpha \leq 1$ s.t*

$$\underline{v}\|\zeta_n\|^2 \leq v_n(\zeta_n) \leq \overline{v}\|\zeta_n\|^2 \tag{6.78}$$

and

$$E\{V_{n+1}(\zeta_{n+1})|\zeta_n\} - V_n(\zeta_n) \leq \mu - \alpha V_n(\zeta_n) \tag{6.79}$$

are fulfilled for every solution of (6.69). Then the stochastic process is exponentially bounded in mean square.

Definition 6.2.4 *A discrete extended Kalman filter is given by the state estimator (6.69) and the Riccati differential equation*

$$P_{n+1} = A_n P_n A_n^T + Q_n - K_n(C_n P_n C_n^T + R_n)K_n^T \tag{6.80}$$

where A_n and C_n is given in (6.72) and the Kalman gain

$$K_n = A_n P_n C_n^T (C_n P_n C_n^T + R_n)^{-1} \tag{6.81}$$

Q_n and R_n are the covariance noise matrix

$$Q_n = G_n G_n^T \tag{6.82}$$
$$R_n = D_n D_n^T \tag{6.83}$$

The main statement are then given

Theorem 6.2.5 *Considering the nonlinear system given in (6.67) and (6.68) with the extended Kalman filter from 6.2.4. Let the following assumptions hold.*

1. *There are positive real numbers* $\overline{a}, \overline{c}, \underline{p}, \overline{p} > 0$ *s.t the following bounds on various matrices are fulfilled* $\forall n \geq 0$*:*

$$\|A_n\| \leq \overline{a} \tag{6.84}$$
$$\|C_n\| \leq \overline{c} \tag{6.85}$$
$$\underline{p}I \leq P_n \leq \overline{p}I \tag{6.86}$$
$$\underline{q} \leq Q_n \tag{6.87}$$
$$\underline{r}I \leq R_n \tag{6.88}$$

2. A_n *non-singular* $\forall\ n \geq 0$

3. *There are positive real numbers* $\epsilon_\varphi, \epsilon_\chi, \kappa_\varphi, \kappa_\chi > 0$ *s.t the nonlinear functions* φ, χ *in (6.75) are bounded by*

$$\|\varphi(z, \hat{z}, x)\| \leq \kappa_\varphi \|z - \hat{z}\|^2 \tag{6.89}$$
$$\|\chi(z, \hat{z})\| \leq \kappa_\chi \|z - \hat{z}\|^2 \tag{6.90}$$

for $z, \hat{z} \in R^p$ *with* $\|z - \hat{z}\| \leq \epsilon_\varphi$ *and* $\|z - \hat{z}\| \leq \epsilon_\chi$ *respectively.*

Then the estimation error ζ_n *given by (6.73) will be exponentially bounded in mean square and bounded with probability one, provided that the initial estimation error satisfies*

$$\|\zeta_0\| \leq \epsilon \tag{6.91}$$

and the covariance matrices of the noise terms are bounded via

$$G_n G_n^T \leq \delta I \tag{6.92}$$
$$D_n D_n^T \leq \delta I \tag{6.93}$$

for some $\delta, \epsilon > 0$.

The proof of this theorem can be viewed fully in [24].

What is also presented and proved in the article is that the same result yields if the system fulfills following conditions regarding observability and rank:

Theorem 6.2.6 *Considering a nonlinear autonomous system as previous (excluding the process noise* G_n*) with the same Kalman filter presented in Definition 6.2.4. Assuming there are real numbers* $\underline{r}, \underline{q} > 0$ *with*

$$\underline{q}I \leq Q_n \tag{6.94}$$
$$\underline{r}I \leq R_n \tag{6.95}$$

for $n \geq 0$ *and a compact subset* κ *of* R^q*, s.t the following conditions hold*

1. *The nonlinear system satisfies the observability rank condition for every* $z_n \in \kappa$.

2. *The nonlinear functions* f *and* h *are twice continuously differentiable and* $\frac{\partial f}{\partial z}(z) \neq 0$ *holds for every* $z \in \kappa$

3. *The sample paths of* z_n *are bounded with probability one, and* κ *contains these sample paths as well as all points with distance smaller than* ϵ_κ *from these sample paths, where* $\epsilon_\kappa > 0$ *is a real number independent of* n.

Then the estimation error ζ_n *given by (6.73) will be exponentially bounded in mean square and bounded with probability one, provided that the initial estimation error satisfies*

$$\|\zeta_0\| \leq \epsilon \tag{6.96}$$

and the covariance matrices of the noise terms are bounded via

$$D_n D_n^T \leq \delta I \tag{6.97}$$

for some $\delta, \epsilon > 0$.

From this important article, the conclusion is that the estimation error is bounded in mean square and with probability one, if the initial estimation error as well as the disturbances, are small enough. The nonlinearities must be continuous and also the solution of the Riccati equation must remain positive definite and bounded. For autonomous systems it is also shown that the condition on the solution of the Riccati equation can be reduced to a nonlinear observability rank conditions, which can be checked off line.

In [26] convergence analyses of the extended Kalman filter used as an observer for nonlinear deterministic discrete-time systems are carried out. Sufficient conditions for local asymptotic convergence are established here, combined with a method of enlarging the domain of attraction hence improving convergence of EKF by designing the arbitrary matrices in a certain way. By introducing some instrumental matrices α_k and β_k to evaluate the linearity of the model, stability and convergence of the EKF can be controlled in a more accurate way.

The analysis from [26] is taken one step further in [22], where stability is evaluated when EKF is used as an exponential observer for general nonlinear systems. By applying the Lyapunov method, it is proved that under certain conditions the dynamics of the estimation error is exponentially stable. This result is very important when it is desirable to obtain a nonlinear separation type property in the context of feedback stabilization for nonlinear systems as will be investigated in later chapters of this thesis. This article is a continuance of Reif and Unbehauens

previous article on Stochastic stability of the discrete-time EKF. The same system as in their previous article is used, but some new definitions are presented.

$$z_{n+1} = f(z_n, x_n) \tag{6.98}$$
$$y_n = h(z_n) \tag{6.99}$$

Definition 6.2.7 *The different equation* $\zeta_{n+1} = A_n(I - K_nC_n)\zeta_n + r_n$ *(given in (6.69)) has an exponential stable equilibrium point at 0 if there are positive real numbers* $\epsilon, \eta > 0$*, and* $\theta > 1$ *s.t*

$$\|\zeta_n\| \leq \eta\|\zeta_0\|\theta^{-0} \tag{6.100}$$

holds $\forall\ n \geq 0$ *and every solution of* ζ_n *with* $\zeta_0 \in B_\epsilon$*, where* $B_\epsilon = \{v \in \mathbf{R}^q | \|v\| < \epsilon\}$.

Definition 6.2.8 *The observer*

$$\hat{z}_{n+1}^- = f(\hat{z}_n^-, x_n) \tag{6.101}$$
$$\hat{z}_n^+ = \hat{z}_n^- + K_n(y_n - h(\hat{z}_n^-)) \tag{6.102}$$

($\hat{z}_n^-$ *and* $\hat{z}_n^+$ *are the a priori and a posteriori respectively) is an exponential observer if the differential equation (6.69) has an exponentially stable equilibrium at zero.*

Definition 6.2.9 *The deterministic discrete-time EKF is closely related to the one presented in Definition 6.2.4, but taking the a priori and a posteriori states into account, the filter becomes*
Time update:

$$\hat{z}_{n+1}^- = f(\hat{z}_n^+, x_n) \tag{6.103}$$
$$\hat{P}_{n+1}^- = \alpha^2 A_n \hat{P}_n^+ A_n^T + Q \tag{6.104}$$

Linearization:

$$A_n = \frac{\partial f}{\partial z}(\hat{z}_n^+, x_n) \tag{6.105}$$
$$C_n = \frac{\partial h}{\partial z}(\hat{z}_n^-) \tag{6.106}$$

Measurement updates:

$$\hat{z}_n^+ = \hat{z}_n^- + K_n(y_n - h(\hat{z}_n^-)) \tag{6.107}$$
$$P_n^+ = (I - K_nC_n)P_n^- \tag{6.108}$$

Kalman gain:

$$K_n = P_n^- C_n^T (C_n P_n^- C_n^T + R)^{-1} \tag{6.109}$$

where Q and R are symmetric positive definite matrices and $\alpha \geq 1$ is a real number. When $\alpha = 1$ the usual EKF is obtained, else it gives the EKF exponential data weighting. Q and R are usually the covariance noise matrices for the noise term, but when applied as a nonlinear deterministic observer, Q and R are chosen arbitrary symmetric positive definite. The full proof that this system is an exponential observer is shown in [22] by establishing a bound for r_n before applying a well-known formula for matrix inversion and lastly verifying a useful matrix inequality concerning the solution of (6.104) and (6.108).

This leads to the concluding theorem of this article

Theorem 6.2.10 *Consider the discrete-time extended Kalman filter as presented above, which fulfill the assumptions*

1. *There are positive real numbers $\overline{a}, \overline{c}, \underline{p}, \overline{p} > 0$ s.t the following bounds on various matrices are fulfilled $\forall n \geq 0$:*

$$\|A_n\| \leq \overline{a} \tag{6.110}$$
$$\|C_n\| \leq \overline{c} \tag{6.111}$$
$$\underline{p}I \leq P_n^- \leq \overline{p}I \tag{6.112}$$
$$\underline{p}I \leq P_n^+ \leq \overline{p}I \tag{6.113}$$
$$\tag{6.114}$$

2. *A_n non-singular $\forall$ $n \geq 0$*

3. *There are positive real numbers $\epsilon_\varphi, \epsilon_\chi, \kappa_\varphi, \kappa_\chi > 0$ s.t the nonlinear functions φ, χ in (6.75) are bounded by*

$$\|\varphi(z, \hat{z}^+, x)\| \leq \kappa_\varphi \|z - \hat{z}^+\|^2 \tag{6.115}$$
$$\|\chi(z, \hat{z}^-)\| \leq \kappa_\chi \|z - \hat{z}^-\|^2 \tag{6.116}$$

   for $z, \hat{z}^+, \hat{z}^- \in R^p$ with $\|z - \hat{z}^+\| \leq \epsilon_\varphi$ and $\|z - \hat{z}^-\| \leq \epsilon_\chi$ respectively.

Then the extended Kalman filter is an exponential observer. In other words, the constant θ for the exponential error decay in (6.100) satisfies $\theta > \alpha$.

This theorem is proved by employing a standard Lyapunov-function technique for differential equations.

In his doctoral thesis from 2004, Knut Rapp did a quite thoroughly investigation of the EKF stability problem. The aim of this thesis was to take the previous stability proofs even further by easing the conditions under which the Kalman filter can be proved stable. The results of his investigation states that stability can be proved without requiring the matrix $H_k = \frac{\partial h}{\partial z}|_{\hat{z}=\hat{z}_{k,k-1}}$ to be bounded in norm, provided that the Hessian $\frac{\partial^2 h}{\partial z^2}|_{\hat{z}=\hat{z}_{k,k-1}}$ is bounded $\forall z \in R$. [25] This is valid as long as

- Lower and upper bounds of Kalman gain matrix K_k and the matrix $(I-K_kH_k)$ are as tight as possible
- When choosing filter tuning matrix Q_k stability properties must be taken into consideration. This is crucial for obtaining theoretical stability of EKF.
- Since approximation in EKF is only valid locally, the initial error must be bounded.

What has been proved earlier in the studies of EKF stability are that the results are very conservative. The stability properties are dependent on initial error and noise processes, which have proved to be very small. Knut Rapp [25] comes to the same conclusion in his thesis, but he also states that the results can be improved significantly by proper choice of filter tuning matrix Q and by applying tight upper bounds on the Kalman gain and $(I - K_kH_k)$ matrix. This yields also for the general nonlinear case, although the system gets more vulnerable for noise, or more sensitive.

In the next section the stability proof of [25] are presented.

6.2.2 General stability proof of EKF

The model used in this analysis has nonlinear terms in both state and output combined with white zero mean process noise w_k and measurement noise v_k, and covariance matrices $E\left[w_k w_k^T\right] = Q_k$ and $E\left[v_k v_k^T\right] = R_k$.

$$x_{k+1} = f(x_k) + w_k \tag{6.117}$$
$$y_k = h(x_k) + v_k \tag{6.118}$$

The extended Kalman filter has the form

$$\hat{x}_{k,k} = \hat{x}_{k,k-1} + K_k\left[y_k - h(\hat{x}_{k,k-1})\right] \tag{6.119}$$
$$P_{k,k} = \left[I - K_kH_k\right]P_{k,k-1} \tag{6.120}$$
$$H_k = \left[\frac{\partial h}{\partial x}\right]_{\hat{c}=\hat{x}_{k,k-1}} \tag{6.121}$$

with the time update

$$\hat{x}_{k,k-1} = f(\hat{x}_{k-1,k-1}) \tag{6.122}$$
$$P_{k,k-1} = F_{k-1}P_{k-1,k-1}F_{k-1}^T + Q_k \tag{6.123}$$
$$F_k = \left[\frac{\partial f}{\partial x}\right]_{\hat{c}=\hat{x}_{k,k}} \tag{6.124}$$

where F_k is non-singular $\forall k \geq 0$ and the filter gain matrix is as usual given by

$$K_k = P_{k,k-1}H_k^T\left[H_kP_{k,k-1}H_k^T + R_k\right]^{-1} \tag{6.125}$$

R_k and Q_k are assumed bounded from below throughout the analysis, where $\overline{r}I \leq R_k$ and $\overline{q}I \leq Q_k \ \forall k \geq 0$, where $\overline{r}, \overline{q} > 0$.

The error in filtered state and predicted state can as before be represented by

$$e_{k,k} = x_k - \hat{x}_{k,k} \tag{6.126}$$
$$e_{k,k-1} = x_k - \hat{x}_{k,k-1} \tag{6.127}$$

By applying the same method of expansion as before previous and rearranging the equation it now becomes

$$e_{k,k} = \tilde{F}_k e_{k-1,k-1} + n_k + l_k \tag{6.128}$$
$$e_{k,k-1} = F_{k-1} e_{k-1,k-1} + w_{k-1} + \theta_f^-(x, \hat{x}) \tag{6.129}$$

Where $\theta_f^-(x, \hat{x})$ is the remainder term at time $k-1$ and

$$\tilde{F}_k = [I - K_k H_k] F_{k-1} \tag{6.130}$$
$$n_k = [I - K_k H_k] w_{k-1} - K_k v_k \tag{6.131}$$
$$l_k = [I - K_k H_k] \theta_f^-(x, \hat{x}) + K_k \phi_h(x, \hat{x}) \tag{6.132}$$

The stability proof for this system is based up on the Lyapunov method. The assumptions presented in [24] are still necessary.

$$\|F_k\| \leq f \tag{6.133}$$
$$p_1 I \leq P_{k,k} \leq p_2 I \tag{6.134}$$
$$p_1 I \leq P_{k,k-1} \leq q_2 I \tag{6.135}$$
$$\frac{\overline{\sigma}(H_k^T)}{\underline{\sigma}(H_k^T)} \leq h \tag{6.136}$$

$\overline{\sigma}(H_k^T)$ and $\underline{\sigma}(H_k^T)$ denotes the largest and smallest singular value in the H_k^T matrix. To prove conditions for stability two lemmas giving some properties of the system have to be presented

Lemma 6.2.11 *Assume that F_k is non-singular $\forall k > 0$ and the conditions above are fulfilled. Then there exist a real number $0 < \gamma < 1$ s.t*

$$\tilde{F}_k^T P_k^{-1} \tilde{F}_k \leq (1 - \gamma) P_{k-1}^{-1} \tag{6.137}$$

Lemma 6.2.12 *If the condition given by (6.136) holds, then an upper bound for the norm of the Kalman gain matrix is given by*

$$\|K_k\| \leq h \frac{q_2}{q_1} \tag{6.138}$$

The proof of these lemmas can be viewed in [25]. These Lemmas leads to the main theorem and proof of EKF stability.

Theorem 6.2.13 *Assume that the bounds given above are fulfilled and that f_k is non-singular $\forall k \geq$, assume further that there exist an $\overline{\epsilon}$ s.t*

$$\|e_{k-1,k-1}\| \leq \overline{\epsilon} \tag{6.139}$$

which implies $\|x_k - \hat{x}_{k,k-1}\| \leq \epsilon_1(\overline{\epsilon})$, where

$$\epsilon_1(\overline{\epsilon}) = a\overline{\epsilon} + \overline{w}$$

Moreover, assume that

$$\|\phi(x_k, \hat{x}_{k,k-1})\| \leq \varphi\|x_k - \hat{x}_{k,k-1}\|^2 \tag{6.140}$$

and

$$\|\theta(x_k, \hat{x}_{k,k})\| \leq \vartheta\|x_k - \hat{x}_{k,k-1}\|^2 \tag{6.141}$$

holds for $\|x_k - \hat{x}_{k,k-1}\|^2 \leq \epsilon_1(\overline{\epsilon})$ and $\|x_k - \hat{x}_{k,k}\|^2 \leq \epsilon_1(\overline{\epsilon})$ respectively.
Then there exists a constant $\epsilon > 0$ s.t the solution of the error model (6.128) is:

1. *Locally exponentially stable if the initial error satisfies $\|e_{0,0}\| \leq \epsilon$, $\overline{w} = \overline{v} = 0$*
2. *Bounded by*

$$\|e_{k,k}\|^2 \leq \frac{p_2}{p_1}(1+\xi)^k\|e_{0,0}\|^2 - \frac{p_2}{\xi}\rho(\overline{w}, \overline{v}, \epsilon) \tag{6.142}$$

if the initial error satisfies $\|e_{0,0}\| \leq \epsilon$ and $\overline{w}, \overline{v}$ are sufficiently small. Here $\xi \in (-1, 0)$ is a constant and $\rho(\overline{w}, \overline{v}, \epsilon) > 0 \; \forall \; k \geq 0$ is a function to be defined later.

The proof of this theorem follows underneath is based on Lyapunov stability and is derived by [25].

Proof Let V: $R^n \to R$ be a positive square Lyapunov function defined by

$$V(e_{k-1}) = e_{k-1}^T P_{k-1}^{-1} e_{k-1} \tag{6.143}$$

$$\Downarrow$$

$$\frac{1}{p_2}\|e_{k-1}\|^2 \leq V(e_{k-1}) \leq \frac{1}{p_1}\|e_{k-1}\|^2 \tag{6.144}$$

Then

$$\begin{aligned}\Delta V :&= e_k^T P_k^{-1} e_k - e_{k-1}^T P_{k-1}^{-1} e_{k-1} \\ &= (\tilde{F} e_{k-1} + n_k + l_k)^T P_k^{-1} (\tilde{F} e_{k-1} + n_k + l_k) - e_{k-1}^T P_{k-1}^{-1} e_{k-1} \\ &= e_{k-1}^T \left[\tilde{F}_k^T P_k^{-1} \tilde{F}_k - P_{k-1}^{-1} \right] e_{k-1} + n_k^T P_k^{-1} n_k + l_k^T P_k^{-1} (2\tilde{F}_k e_{k-1} + l_k) \\ &+ 2 n_k^T P_k^{-1} (\tilde{F}_k e_{k-1} + l_k) \end{aligned} \tag{6.145}$$

Applying Lemma 6.2.11 gives

$$\Delta V \leq -\gamma V(e_{k-1}) + l_k^T P_k^{-1} (2\tilde{F}_k e_{k-1} + l_k) + 2 n_k^T P_k^{-1} (\tilde{F}_k e_{k-1} + l_k) + n_k^T P_k^{-1} n_k \tag{6.146}$$

By considering the second term, it holds that

$$\begin{aligned}&\| l_k^T P_k^{-1} (2\tilde{F}_k e_{k-1} + l_k) \| \leq \| P_k^{-1} \| (\| \theta_f^-(x, \hat{x})^T \left[I - K_k H_k \right]^T \| + \\ &\| \phi_h(x, \hat{x})^T K_k^T) (\| 2\tilde{F}_k e_{k-1} \| + \| \left[I - K_k H_k \right] \theta_f^-(x, \hat{x}) \| + \| K_k \phi_h(x, \hat{x}) \|)\end{aligned} \tag{6.147}$$

Using $\| e_{k,k-1} \| \leq \vartheta \| e_{k-1,k-1} \|^2 + f \| e_{k-1,k-1} \| + \overline{w}^2$ gives

$$\| l_k^T P_k^{-1} (2\tilde{F}_k e_{k-1,k-1} + l_k) \| \leq \overline{\varphi} \| e_{k-1,k-1} \|^3 + \overline{w} W_1(\overline{w}, \overline{e}) \tag{6.148}$$

where

$$\begin{aligned}\overline{\varphi} = &\frac{1}{q_1^2 p_1} \Big[h^2 \varphi^2 \vartheta^2 q_2^2 (\vartheta \overline{\epsilon}^5 + 4\overline{\epsilon}^4) + 2h\varphi\vartheta^2 q_2 \overline{\epsilon}^3 (3h\varphi f^2 q_2 + \vartheta p_2) \\ &+ (2(p_2\vartheta + h f^2 q_2 \vartheta) + q_1) 2h f q_2 \vartheta \varphi \overline{\epsilon}^2 + (4h f^2 q_1 q_2 \vartheta \varphi + (p_2 \varphi + h f^2 q_2 \varphi)^2) \overline{\epsilon} \Big] \\ &+ \frac{2f}{q_1 p_1} (p_2 \vartheta + h f^2 q_2 \varphi)\end{aligned} \tag{6.149}$$

and

$$\begin{aligned}W_1(\overline{w}, \overline{\epsilon}) = &\frac{1}{q_1 p_1} \Big[2h\varphi\overline{\epsilon} \frac{q_2}{q_1} \overline{w} (3h q_2 \vartheta (2f\overline{\epsilon}^2 + \vartheta \overline{\epsilon}^3) + f q_1 + (p_2 \vartheta + 3h q_2 f^2 \varphi) \overline{\epsilon}) \\ &+ h^2 \varphi^2 \frac{q_2^2}{q_1} \overline{w}^2 (\overline{w} + 4(\vartheta \overline{\epsilon}^2 + f\overline{\epsilon})) + 4h\varphi\overline{\epsilon}^2 \frac{q_2}{q_1 p_1} \big[f^2 + f\vartheta\overline{\epsilon}(1 + \frac{p_2}{q_1}) \\ &+ h\varphi\overline{\epsilon} \frac{q_2}{q_1} (f\vartheta\overline{\epsilon}(2+f)\vartheta^2\overline{\epsilon}^2 + f^3) \big] \Big]\end{aligned} \tag{6.150}$$

The Lyapunov inequality now becomes

$$\Delta V \leq -\gamma V(e_{k-1}) + \overline{\varphi} \| e_{k-1,k-1} \|^3 + n_k^T P_k^{-1} (\tilde{F}_k e_{k-1} + l_k) + \overline{w} W_1(\overline{w}, \overline{\epsilon}) \tag{6.151}$$

for $\|e_{k-1,k-1}\| \leq \overline{\epsilon}$.

Choosing

$$\epsilon = min\Big(\overline{\epsilon}, \frac{\gamma}{\psi p_2 \overline{\varphi}}\Big) \tag{6.152}$$

where $\psi > 1$, gives for $\|e_{k-1,k-1}\| \leq \epsilon$

$$\overline{\varphi}\|e_{k-1,k-1}\|\|e_{k-1,k-1}\|^2 \leq \frac{\gamma}{\psi p_2 \overline{\varphi}}\|e_{k-1,k-1}\|^2 \leq \frac{\gamma}{\psi} V(e_{k-1}) \tag{6.153}$$

and this makes

$$\Delta V \leq \frac{\gamma(1-\psi)}{\psi} V(e_{k-1}) + n_k^T P_k^{-1} n_k + 2n_k^T P_k^{-1}(\tilde{F}_k e_{k-1} + l_k) + \overline{w} W_1(\overline{w}, \overline{\epsilon}) \tag{6.154}$$

for $\|e_{k-1,k-1}\| \leq \epsilon$.

The next terms to consider are the $n_k^T P_k^{-1} n_k$ and the $2n_k^T P_k^{-1}(\tilde{F}_k e_{k-1} + l_k)$. The inequalities presented in (6.2.11), (6.134), (6.135) leads to the following inequality

$$\|n_k^T P_k^{-1} n_k\| \leq \|P_k^{-1}\|\|n_k\|^2 \leq \frac{1}{p_1}(\|I - K_k H_k\|\overline{w} + \|K_k\|\overline{v})^2 \leq \frac{1}{q_1^2 p_1}(p_2\overline{w} + hq_2\overline{v})^2 \tag{6.155}$$

and

$$\begin{aligned} &\|2n_k^T P_k^{-1}(\tilde{F}_k e_{k-1} + l_k)\| \leq 2\|n_k^T P_k^{-1}\|\|\tilde{F}_k e_{k-1} + l_k\| \\ &\leq \frac{2}{q_1 p_1}(p_2\overline{w} + q_2 h\overline{v}) \times (f\frac{p_2}{q_1}\|e_{k-1}\| + \vartheta\frac{p_2}{q_1}\|e_{k-1}\|^2 + h\varphi\frac{q_2}{q_1}\|e_{k,k-1}\|^2) \end{aligned} \tag{6.156}$$

by substituting for $\|e_{k,k-1}\|$ and adding it to the inequalities above

$$\|2n_k^T P_k^{-1}(\tilde{F}_k e_{k-1} + l_k)\| + \|n_k^T P_k^{-1} n_k\| \leq (p_2\overline{w} + hq_2\overline{v}) W_2(\overline{w}, \overline{v}, \epsilon) \tag{6.157}$$

and

$$\begin{aligned} W_2(\overline{w}, \overline{v}, \epsilon) = \frac{1}{q_1^2 p_1} \times \Big[&2(fq_2\epsilon + p_2\vartheta\epsilon^2 + hq_2\varphi(\vartheta^2\epsilon^4 + 2f\vartheta\epsilon^3 \\ &+ (2\vartheta + f^2)\epsilon^2 + 2f\overline{w}\epsilon + \overline{w}^2)) + p_2\overline{w} + hq_2\overline{v}\Big] \end{aligned} \tag{6.158}$$

This takes us further in the proof of Theorem 6.2.13 and

$$\Delta V \leq \frac{\gamma(1-\psi)}{\psi} V(e_{k-1}) + \rho(\overline{w}, \overline{v}, \epsilon) \tag{6.159}$$

where

$$\rho(\overline{w}, \overline{v}, \epsilon) = \overline{w} W_1(\overline{w}, \epsilon) + (p_2 \overline{w} + h q_2 \overline{v}) W_2(\overline{w}, \overline{v}, \epsilon) \tag{6.160}$$

Since $0 < \gamma < 1$ and $\psi > 1$

$$\xi := \frac{\gamma(1-\psi)}{\psi} \in (-1, 0) \tag{6.161}$$

Using this and the inequality from (6.159) it can be shown that starting at k = 0 gives

$$\begin{aligned}
v(e_{1,1}) &\leq (1-\xi) V(e_{0,0}) + \rho(\overline{w}, \overline{v}, \epsilon) \\
v(e_{2,2}) &\leq (1-\xi) V(e_{1,1}) + \rho(\overline{w}, \overline{v}, \epsilon) \\
&\leq (1-\xi)^2 V(e_{0,0}) + (1 + (1+\xi)) \rho(\overline{w}, \overline{v}, \epsilon) \\
&\vdots \\
v(e_{k,k}) &\leq (1-\xi)^k V(e_{0,0}) + \sum_{n=0}^{k} (1+\xi)^n \rho(\overline{w}, \overline{v}, \epsilon)
\end{aligned} \tag{6.162}$$

This further implies that

$$\|e_{k,k}\|^2 \leq \frac{p_2}{p_1} (1+\xi)^k \|e_{0,0}\|^2 - \frac{p_2}{\xi} \rho(\overline{w}, \overline{v}, \epsilon) \tag{6.163}$$

The condition of (6.140) can be relaxed to $\|\phi(x_k, \hat{x}_{k,k-1})\| \leq \varphi \|x_k - \hat{x}_{k,k-1}\|$ if Input-to-state stability is assumed. See [25]. This will simplify the W_1 and W_2 functions, although another term $p_2 f \vartheta (2 + h\varphi q_2 / q_1)$ will be included in (6.159). This term will be small if the nonlinearities are small. This builds-up under the intuitive conclusions from previous work, which states that the EKF will be stable if the nonlinearities are small and the filter is initialized reasonably.

6.2.3 Summary of EKF stability

To sum up the all the results and research done on the topic of EKF stability it is seen that:

1. The estimation error for stochastic discrete-time system is bounded if the system satisfies

- the observability rank condition for autonomous systems, otherwise the solution of the Riccati equations need to remain positive definite and bounded
- initial estimation error is small
- noise term is small
- continuous nonlinearities
- Jacobie matrix of the output must be bounded although this bound has been relaxed to only acquire finite ratio between largest and smallest singular value of H_k as long as the norm of the Hessian matrix of the function $h(x_k)$ are finite for any $x \in R^n$

2. The extended Kalman filter is an exponential observer if the assumptions from Theorem 6.2.5 holds.

3. Local asymptotic convergence can be improved, under mild conditions, when EKF is used as an observer for nonlinear deterministic discrete-time systems by

   - properly choosing the arbitrary matrix R_k
   - introducing instrumental matrices to evaluate the linearity of the model to control both stability and convergence of the EKF.

Chapter 7

EKF Convergence for ESMO

7.1 Convergence of the extended Kalman filter

In this section the result presented previous from [22] and [24] will be used to analyze stability properties to the nonlinear ESMO satellite system with extended Kalman filter. The equations and system matrices are given in (2.61) and Appendix A, the goal is to prove that the Kalman filter in (2.80-2.86) is exponentially stable according to [22]. This result will be used further in this thesis to prove that a nonlinear separation principle yields for ESMO in order to combine the filter with a stabilizing feedback controller.

Several properties and assumptions need to be fulfilled for Theorem 6.2.5 to yield for ESMO. The estimation error ξ_k will be exponentially bounded if:

1.
$$\|A_k\| \leq \overline{a} \tag{7.1}$$
$$\|C_k\| \leq \overline{c} \tag{7.2}$$
$$\underline{p}I \leq P_k \leq \overline{p}I \tag{7.3}$$
$$\underline{q}I \leq Q_k \tag{7.4}$$
$$\underline{r}I \leq R_k \tag{7.5}$$

   for all time steps k, where $\overline{a}, \overline{c}, \underline{p}, \overline{p} > 0$ are real numbers.

2. A_k nonsingular for every $k \geq 0$.

3. there are positive real numbers $\epsilon_\varphi, \epsilon_\chi, \kappa_\varphi, \kappa_\chi > 0$ s.t the nonlinear functions φ, χ in (2.78) and (2.79) are bounded by

$$\|\varphi(x, \hat{x}^+, x)\| \leq \kappa_\varphi \|x - \hat{x}^+\|^2 \tag{7.6}$$
$$\|\chi(x, \hat{x}^-)\| \leq \kappa_\chi \|x - \hat{x}^-\|^2 \tag{7.7}$$

   for $x, \hat{x}^+, \hat{x}^- \in R^p$ with $\|x - \hat{x}^+\| \leq \epsilon_\varphi$ and $\|x - \hat{x}^-\| \leq \epsilon_\chi$ respectively.

provided that the initial estimation error $\|\xi_0\| \leq \epsilon$ and that the noise terms are bounded via

$$G_n G_n^T \leq \delta I \tag{7.8}$$
$$D_n D_n^T \leq \delta I \tag{7.9}$$

for some $\delta, \epsilon > 0$.

7.1.1 Constraints on the linearized system matrix

The linearized system matrix F_k is given in (2.66). The constraints required on this matrix is that the norm of it must have an upper bound smaller or equal to the largest singular value in the matrix and in addition the matrix must be non-singular, but this will be investigated later. The ∞-norm of F_k, $\|F_k\|_\infty = \max_i \sum_{j=1}^{n} |f_{ij}|$. By studying F_k it can be seen that the if all the variable defining the matrix are bounded for all k, then the matrix norm will be bounded for all k.

The variables in question are:

k_x, k_y, k_z- constants
ω_0- constant
a_{ij} - constant from reaction wheel allocation matrix
c_{ij}- variable from rotation matrix always within the unit circle
i_w- constant
W_w- chosen input, therefor assumed limited
η^*- operating point always within the unit circle
ϵ^*- operating point always within the unit circle
ω_{ob}^{b*}- operating point

From this it can be seen that all the variables of the linearized system matrix are bounded except for the ω_{ob}^{b*} term. η^* and ϵ^* are bounded in the unit circle since they describe angles, and maximum angle will be 360°. The other variables are all constants and therefore bounded.

The key point in this part will be to prove that ω_{ob}^{b*} will be bounded. The principle of extended Kalman filter is that it re-linearize the system for every new state estimate. This means that there will be a new operating point for every new estimate. The angular velocity operating point for every step of the Kalman filter loop has to be bounded to prove that the norm of F_k is upper bounded. The operating point fed into the linearizing algorithm is depending on the last estimate and the error between measurement and last estimate, times the Kalman gain. The equation for this is $\omega_{ob}^{b*} = \omega_{ob,k+1}^{b} = \omega_{ob,k}^{b} + K_k(q_{measured} - q_k)$.From this equation it can be concluded that as long as the measurement is bounded, and that the Kalman gain

is bounded and the angular velocity estimate used as the operating point will also be bounded. And hence, all elements of F_k are bounded and therefore it is proved that $\|F_k\| \leq \overline{f}$.

The same constraints yields for the output matrix H_k, but as this is assumed linear and constant for ESMO, no further investigation of boundedness is required.

Figure 7.1 shows graphical values of $\|F_k\|$, and it can be seen here, that the maximum single value goes toward a constant.

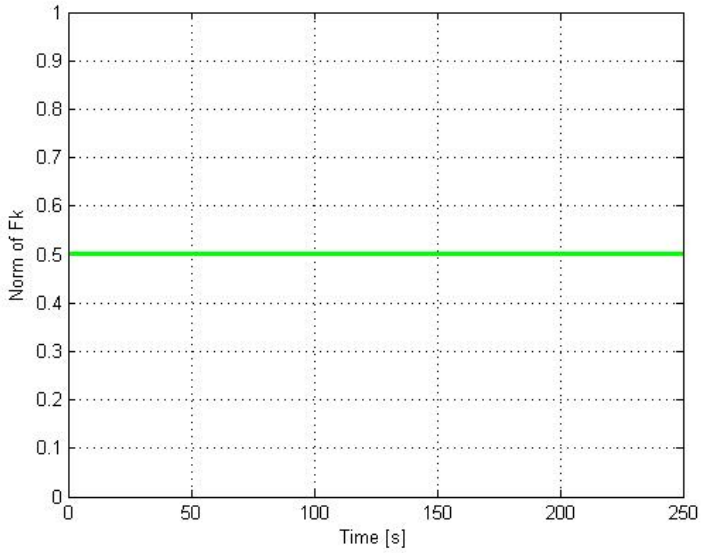

Figure 7.1: Graphical value of $\|F_k\|$

7.1.2 Constraints on the error covariance

The last property from assumption one in Theorem 6.2.5 is that error covariance P_k is both upper and lower bounded. To prove this, the result in Lemma 4.1 [24] can be used:

Consider a solution P_n for $n \geq 0$ of the Riccati difference equation (given in (6.80)) which gives the error covariance of in the extended Kalman filter, and let the following assumptions hold.

1. *There are real numbers $\underline{q}, \overline{q}, \underline{r}, \overline{r} > 0$ such that Q_n, R_n in (6.80) are bounded by*

$$\underline{q}I \leq Q_n \leq \overline{q}I \tag{7.10}$$

$$\underline{r}I \leq R_n \leq \overline{r}I \tag{7.11}$$

2. *A_n, C_n satisfy the uniform observability condition.*

3. Initial condition P_0 is positive definite.

Then there are real numbers $\underline{p}, \overline{p} > 0$ such that the solution of (6.80) is bounded via

$$\underline{p}I \leq P_n \leq \overline{p}I \tag{7.12}$$

for every $n \geq 0$.

The first assumption require bounds on the noise matrices R_k and Q_k. From (A.5) Q_k is given as a constant 6×6 matrix, hence Q_k is bounded and (7.10) holds. R_k is the measurement noise matrix given by

$$\mathbf{R}_k = diag(\sigma^2_{v_{2,k-1}} \ \sigma^2_{v_{3,k-1}} \ \sigma^2_{v_{4,k-1}}) \tag{7.13}$$

where $\sigma^2_{v_{i,k-1}}$ is updated with each new estimate and given by

$$\sigma^2_{v_{k-1}} = \begin{bmatrix} \epsilon^T \left[\epsilon_n^2\right] \\ \eta \left[\epsilon_n^2\right] + S(\epsilon) \left[\epsilon_n^2\right] \end{bmatrix} \tag{7.14}$$

since both η and ϵ are limited by the unit circle, each new estimate ϵ_n will also apply the same bound which gives $\sigma^2_{v_{i,k-1}}$ a maximum value of $[1 \ 2]^T$, R_k and minimum value of $[-1 - 2]^T$, R_k will therefor be both upper and lower bounded and (7.10) are fulfilled. This result also proves that the bounds assumed in (7.4) and (7.5)

Figure 7.2 shows graphical the lower and upper bounds respectively of R_k from simulations.

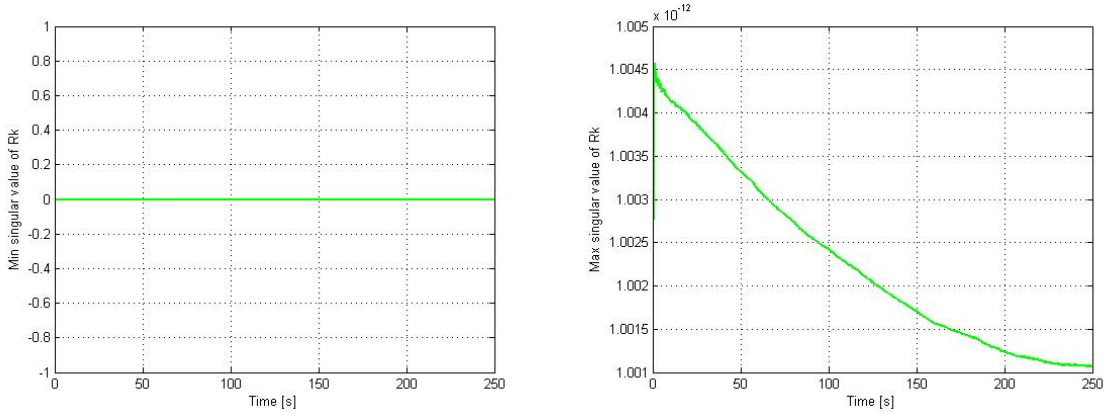

Figure 7.2: Lower and upper bounds on R_k

The next assumptions says that F_k, H_k must satisfy the uniform observability con-

dition. In other words,

$$O_k = \begin{bmatrix} H_k \\ H_k F_k \\ H_k F_k^2 \\ \vdots \end{bmatrix} \tag{7.15}$$

must have full rank for every $n > 0$.

$$O_k = \begin{bmatrix} 1 & 0 & 0 & 0 & 0 & 0 & 0 \\ 0 & 1 & 0 & 0 & 0 & 0 & 0 \\ 0 & 0 & 1 & 0 & 0 & 0 & 0 \\ 0 & 0 & 0 & 0 & 0 & 0 & 0 \\ 0 & -\frac{1}{2}\omega^b_{ob,x} & -\frac{1}{2}\omega^b_{ob,y} & -\frac{1}{2}\omega^b_{ob,z} & -\frac{1}{2}\epsilon_1 & -\frac{1}{2}\epsilon_2 & -\frac{1}{2}\epsilon_3 \\ \frac{1}{2}\omega^b_{ob,x} & 0 & -\frac{1}{2}\omega^b_{ob,z} & \frac{1}{2}\omega^b_{ob,y} & \frac{1}{2}\eta & \frac{1}{2}\epsilon_3 & -\frac{1}{2}\epsilon_2 \\ \frac{1}{2}\omega^b_{ob,y} & \frac{1}{2}\omega^b_{ob,z} & 0 & -\frac{1}{2}\omega^b_{ob,x} & -\frac{1}{2}\epsilon_3 & \frac{1}{2}\eta & \frac{1}{2}\epsilon_1 \end{bmatrix} \tag{7.16}$$

By only doing the first two rows of multiplication it can be seen that the linearized system will be observable for every $n > 0$ as O_k has full column rank. This is confirmed by extensive simulations in Matlab.

The third objective that needs to be fulfilled for P_k is that P_0 is positive definite. P_0 is in this study chosen arbitrarily, and as used in previous simulations, P_0 is given as

$$P_0 = \begin{bmatrix} 10^{-6} & 0 & 0 & 0 & 0 & 0 \\ 0 & 10^{-6} & 0 & 0 & 0 & 0 \\ 0 & 0 & 10^{-6} & 0 & 0 & 0 \\ 0 & 0 & 0 & 10^{-10} & 0 & 0 \\ 0 & 0 & 0 & 0 & 10^{-10} & 0 \\ 0 & 0 & 0 & 0 & 0 & 10^{-10} \end{bmatrix} \tag{7.17}$$

One condition for positive definiteness is $det(A) \neq 0$. $det(P_0) = 1.0000e-048 \neq 0$ and P_0 is therefor positive definite.

All the conditions for P_k to be bounded are thereby complied and the first condition for exponential boundedness of estimation error is fulfilled.

Figure 7.3 shows lower and upper bounds for P_k graphical through simulation.

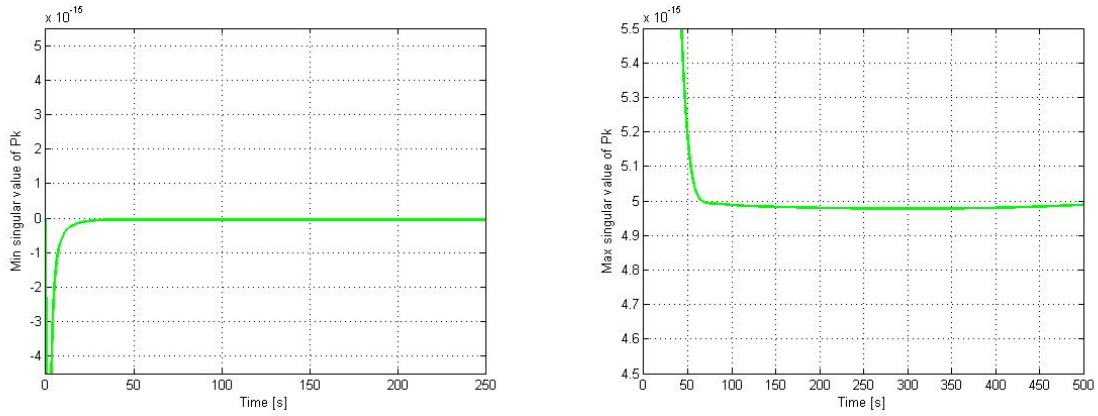

Figure 7.3: Lower and upper bounds on P_k

7.1.3 Nonsingular linearized system matrix

F_k nonsingular is another constraint on the system to state exponentially observer characteristics. In linear algebra, a n-by-n (square) matrix A is called invertible or non-singular if there exists a n-by-n matrix B such that $AB = BA = I_N$, another property of a nonsingular matrix is that $det(a) \neq 0$ and the $rank(A) = n$. If one of these properties are true, then all of them are true and the matrix is nonsingular. For the ESMO matrix F_k these properties have to yield for all time steps k and different x^*, and can therefore be quite difficult to prove, but by studying the equations for each element in F_k, it can be seen that the matrix will have full rank $(rank(F_k) = n)$ for all x^* as long as $x^* \neq 0$ as each row of elements are unique. x^* will never equal zero as $\eta = 1$ when $\boldsymbol{\epsilon}$ and $\boldsymbol{\omega} = 0$.

Because of the very complex F_k matrix, the singularity is also tested and assured nonsingular through simulations by taking the determinant of the matrix for every single step in the estimation process. See figure 7.4.

7.1.4 Lipschitz bounded nonlinear functions

The last condition to secure exponentially bounded estimation error, is the assumption that the norm of the nonlinear functions φ and χ given in (2.78) and (2.79) are nonlinear limited by some kind of parabola also known as a Lipschitz function. This can easily be shown for ESMO by applying some mathematical tricks and tools like the triangle inequality. First we have that

$$\varphi(z_k, \hat{z}_k, x_k) = (I + \frac{1}{2}F_k^2\Delta^2 + \frac{1}{3!}F_k^3 \ldots)(z_k - \hat{z}_k) \tag{7.18}$$

$$\chi(z_k, \hat{z}_k) = 0 \tag{7.19}$$

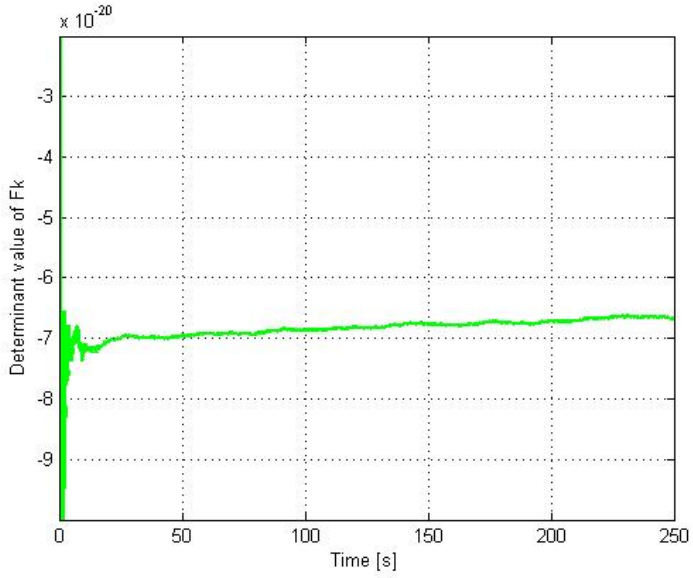

Figure 7.4: Determinant of F_k for $k > 0$

since $\chi(z_k, \hat{z}_k) = 0$ the bound on χ is always fulfilled. Further we investigate the norm of φ.

$$\|\varphi(z_k, \hat{z}_k, x_k)\| = \|(I + \frac{1}{2}F_k^2\Delta T^2 + \frac{1}{3!}F_k^3\Delta T^3 \ldots)(z_k - \hat{z}_k)\| \tag{7.20}$$

$$\leq \|z_k - \hat{z}_k\|\|I + \frac{1}{2}F_k^2\Delta T^2 + \frac{1}{3!}F_k^3\Delta T^3 \ldots\| \tag{7.21}$$

$$\leq \|z_k - \hat{z}_k\|(\|I\| + \|\frac{1}{2}F_k^2\Delta T^2\| + \|\frac{1}{3!}F_k^3\Delta T^3\| \ldots) \tag{7.22}$$

since

$$\|I\| = 1 \tag{7.23}$$

$$\|\frac{1}{2}F_k^2\Delta T^2\| = c_1 \cdot \|F_k^2\| \tag{7.24}$$

$$\|\frac{1}{2}F_k^3\Delta T^3\| = c_2 \cdot \|F_k^3\| \tag{7.25}$$

c_1 and c_2 are positive constant, and then using the fact that

$$\|A\|_\infty = max_i \sum_j |a_{ij}| = constant \tag{7.26}$$

if all elements of matrix A are bounded.

Then, since F_k has been proved bounded for each $k > 0$

$$\|F_k^2\| = constant \tag{7.27}$$
$$\|F_k^3\| = constant \tag{7.28}$$
$$\vdots \tag{7.29}$$

and it can be stated that

$$\|z_k - \hat{z}_k\|(\|I\| + \|\frac{1}{2}F_k^2\Delta T^2\| + \|\frac{1}{3!}F_k^3\Delta T^3\|\ldots) = C\|z_k - \hat{z}_k\| \leq \kappa_\varphi\|z_k - \hat{z}_k\| \tag{7.30}$$

where C is a positive constant.

It is thereby proved that the linear function φ is bounded by a Lipschitz function assumed that $\|z_k - \hat{z}_k\| \leq \epsilon_\varphi$ where ϵ_φ is a real positive number larger than zero.

All the constraint of Theorem 6.2.5 is thereby fulfilled.

7.2 Conclusion of convergence for EKF

From the above analysis it is proved that all the conditions mentioned by [24] for the estimation error ξ_n to be exponentially bounded with probability one are fulfilled. But this theorem proof is only valid if initial estimation error is smaller than a given ϵ and that the noise terms in the system are bounded by a constant δ. In other words, noise and initial estimation error must be adequately small. Estimates of the value for δ and ϵ can be found and compared to simulations, these estimates often turns out to be very conservative.

Although it can be very difficult to prove that initial estimation error and noise terms are adequately small, these assumptions need not be fulfilled for the filter to work as an exponential observer. According to [22] it is sufficient that assumption 1, 2 and 3 of theorem 6.2.5 holds. These assumptions are the same assumptions proved valid for ESMO in the previous segment. It can therefore be concluded that the extended Kalman filter used on ESMO is an exponential observer.

Chapter 8

Nonlinear Separation Principle on ESMO

In this chapter the main objective is to apply a nonlinear separation principle on the closed loop ESMO where the exponentially bounded observer is combined with the feedback control law. Limited literature and research can be found where extended Kalman filter is used in a nonlinear separation principle. The properties established in the previous chapter will be important to prove that a nonlinear separation principle can in fact be established, even with an extended Kalman filter as the observer. The first task will be to investigate stability of the proposed controllers, then an analysis of the overall characteristics of the system when combining these controllers with the EKF will be carried through.

8.1 Stability of feedback controllers

Before it is possible to analyze the overall stability, or convergence of the satellite system, with both feedback controller and exponentially converging controller, it is crucial to determine the stability characteristic of the feedback controllers. In this section the proposed controllers from chapter 3.1 are being examined. The goal is to achieve global asymptotic stability, a state that is very difficult to achieve for quaternion based attitude controllers because of multiple equilibrium points. Stability of the same feedback controllers were analyzed in [8] and [9], and the same methods and strategies will be used in the following subsections to prove GAS of the proposed feedback controllers for ESMO.

8.1.1 GAS of Model-independent PD controller

In this section the result from [8] is used to show that the PD controller using unit quaternion is globally asymptotic stabilizing for a class of desired trajectories.

Theorem 8.1.1 *: Consider the following PD control law:*

$$\tau = k_p \mathbf{q} - k_v \boldsymbol{\Delta\omega} \tag{8.1}$$

where k_p and k_v are positive scalar constants. $\boldsymbol{\Delta}\omega = \omega_{ib}^b - \omega_{ib}^d$ is the angular velocity error where ω_{ib}^b is the angular velocity of the body relative the inertial frame given in body frame notations and ω_{ib}^d is the desired angular velocity relative inertial frame given in body frame notations. Let

$$\rho_1 \equiv \|\dot{\omega}_{ib}^d\| + \|\omega_{ib}^d\|^2. \tag{8.2}$$

If $\rho_1 \in L_2[0,\infty) \cap L_\infty[0,\infty)$, then $\mathbf{q}$ and $\boldsymbol{\Delta}\omega \to 0$ as $t \to \infty$.

The theorem yields as long as the desired trajectory is in L_2. In other words, there are rather large limitations on the controller. But still it will be very useful for operations where the problem is to move from the initial attitude to a goal attitude with certain desired transient response or for the case where the set point ω_{ib}^d is zero. For these cases the L_2 requirement is trivially satisfied and the zero equilibrium will be GAS.

To prove this theorem the direct Lyapunov method is used, proposing a Lyapunov candidate based on kinetic energy error, an artificial potential energy and a product term of angular momentum and the position error. The proof in short will be presented beneath, for the full version of the stability proof, see [8].

Proof The proposed Lyapunov candidate

$$V = (k_p + ck_v)((\eta - 1)^2 + \boldsymbol{\epsilon} \cdot \boldsymbol{\epsilon}) + \frac{1}{2}\boldsymbol{\Delta\omega} \cdot I\boldsymbol{\Delta\omega} - c\boldsymbol{\epsilon} \cdot \boldsymbol{I\Delta\omega} \tag{8.3}$$

$$V \geq \begin{bmatrix} \|\boldsymbol{\epsilon}\| \\ \|\boldsymbol{\Delta\omega}\| \end{bmatrix}^T P_c \begin{bmatrix} \|\boldsymbol{\epsilon}\| \\ \|\boldsymbol{\Delta\omega}\| \end{bmatrix} = \mathbf{x}^T \cdot P_c \cdot \mathbf{x} \tag{8.4}$$

and

$$P_c = \frac{1}{2}\begin{bmatrix} 2(k_p + ck_v) & c\|I\| \\ c\|I\| & \mu_I \end{bmatrix} \tag{8.5}$$

μ_I is defined as $inf_{\|v\|=1} v \cdot \mathbf{I}v$ which is positive. P_c will be positive definite if c is sufficiently small.

$$\begin{aligned} \dot{V} =& -ck_p\|\boldsymbol{\epsilon}\|^2 - k_v\|\boldsymbol{\Delta\omega}\|^2 + (\boldsymbol{\Delta\omega} - c\boldsymbol{\epsilon}) \cdot (-\boldsymbol{\omega}_{ib}^d \times \boldsymbol{I}\boldsymbol{\omega}_{ib}^d - \mathbf{I}\dot{\boldsymbol{\omega}}_{ib}^d) \\ & - c\boldsymbol{\Delta\omega} \cdot \boldsymbol{I}(\frac{1}{2}\boldsymbol{\Delta\omega} \times \boldsymbol{\epsilon} - \frac{1}{2}\eta\boldsymbol{\Delta\omega} + \boldsymbol{\omega}_{ib}^d \times \boldsymbol{\epsilon}) \\ & - c\boldsymbol{\epsilon} \cdot (\boldsymbol{\Delta\omega} \times \boldsymbol{I}\boldsymbol{\Delta\omega} + (\boldsymbol{\omega}_{ib}^d \times \mathbf{I} - \boldsymbol{I}\boldsymbol{\omega}_{ib}^d\times)\boldsymbol{\Delta\omega}) \\ \leq& - x^T Q_c x + w^T x \\ \leq& - \lambda\|x\|^2 + \rho\|x\| \end{aligned} \tag{8.6}$$

$$Q_c \equiv \begin{bmatrix} ck_p & \frac{3}{2}\|I\|\gamma_d \\ \frac{3}{2}\|I\|\gamma_d & k_v - 2c\|I\| \end{bmatrix} \tag{8.7}$$

$$w \equiv \|I\|(\|\dot{\boldsymbol{\omega}}^d_{ib}\| + \|\boldsymbol{\omega}^d_{ib}\|^2) \begin{bmatrix} 1 \\ c \end{bmatrix} \tag{8.8}$$

$$\rho \equiv \sqrt{1+c^2}\|I\|(\|\dot{\boldsymbol{\omega}}^d_{ib}\| + \|\boldsymbol{\omega}^d_{ib}\|^2) \tag{8.9}$$

where $\gamma_d \equiv \sup_{t\geq 0}\|\boldsymbol{\omega}^d_{ib}\|$ and $\lambda \equiv \lambda_{min}(Q_c)$ which is the minimum eigenvalue of Q_c. P_c and Q_c in this proof is depending on the constant c to be small enough for positive definiteness. This c is not implemented in the control law and can therefor be chosen arbitrarily small enough.

Further on, by taking the integral on both sides, moving some of the components

$$\lambda \int_0^t \|x(s)\|^2 ds - \int_0^t \rho(s)\|x(s)\|^2 \leq V_0 \tag{8.10}$$

and then applying Schwarz inequality and using assumption that $\rho_1 \in L_2$

$$\lambda\|x\|^2_{L_2} \leq V_0 + \|\rho\|_{L_2}\|x\|_{L_2} \tag{8.11}$$

which then gives a bound on the $\|x\|_{L_2}$

$$\|x\|_{L_2} \leq \left[\frac{1}{\lambda}\left(V_0 + \frac{\|\rho\|^2_{L_2}}{4\lambda}\right)\right]^{1/2} + \frac{\|\rho\|_{L_2}}{2\lambda} \tag{8.12}$$

From this it is showed that $x \in L_2[0,\infty)$ and by substituting (8.12) into (8.10) it follows that V is uniformly bounded along the trajectory in t. From the satellite equations of motion, $\dot{x}$ will also be uniformly bounded, and therefore x is uniformly continuous. From Barbalat's Lemma 4.3.6, it can therefore be stated that $x(t) \to 0$ as $t \to \infty$ hence the controller is GAS according to [8].

8.1.2 GAS of Model-Dependent PD controller

Model-dependent controller is taken from [8] and [27] and is very useful when good tracking performance is crucial, but high gains cannot be used because of constraints on the system. The control law is described in section 3.1.2 and can be proved globally asymptotically stable as the model independent PD controller above.

Theorem 8.1.2 *:Consider the following controll law*

$$\boldsymbol{\tau} = k_p\boldsymbol{\epsilon} - k_d\boldsymbol{\Delta\omega} + \boldsymbol{I}\frac{d\boldsymbol{\omega}^b_{ob}}{dt} + \boldsymbol{\omega}^b_{ob} \times \boldsymbol{I}\boldsymbol{\omega}^b_{ob} \tag{8.13}$$

If $k_v > \gamma_I \gamma_d$ where $\gamma_I = \|I\|$ and $\gamma_d \equiv \sup_{t\geq 0} \|\boldsymbol{\omega}_{ib}^d\|$ as before, then $\boldsymbol{\epsilon}(t) \to 0$ and $\boldsymbol{\Delta\omega} \to 0$ as $t \to \infty$. If $\eta \to +1$, as $t \to \infty$, then the convergence is of exponential rate and the system is globally stable. A sufficient condition for this is

$$\frac{1}{2}\boldsymbol{\Delta\omega}(0) \cdot \boldsymbol{I}\boldsymbol{\Delta\omega}(0) < 2k_p(1+\eta(0)) \tag{8.14}$$

The proof of this theorem is simular to the proof of Theorem 8.1.1. Considering the same Lyapunov candidate as given in (8.3). By taking the derivative along the solution and then substitute in the control law the derivative of V becomes

$$\dot{V} \leq -x^T Q_c x \tag{8.15}$$

where Q_c is

$$Q_c = \begin{bmatrix} ck_p & \frac{1}{2}\gamma_d\gamma_I c \\ \frac{1}{2}\gamma_d\gamma_I c & k_v - \gamma_I\gamma_d - \gamma_I c \end{bmatrix} \tag{8.16}$$

If k_v now satisfies $k_v > \gamma_I\gamma_d$, then there exists a range of c sufficiently small so that Q_c is positive definite. Barbalat's theorem 4.3.6 then states that $x(t) \to 0$ as $t \to \infty$.

The next thing is to prove exponential rate of convergence. Here the problem of multiple equilibriums is treated so that global stability can be stated instead of only local.

When $\|\boldsymbol{\epsilon}\| \to 0$, η will go to either +1 or -1. The problem is to figure out which equilibrium the system tends to, or alternatively, force the system to one of them. Suppose that $\eta \to +1$, then there exists some finite time T such that $\eta(t) \geq 0$ for all $T \geq 0$. Since $|\eta| \leq 1$, for $t \geq T$

$$\|\boldsymbol{\epsilon}\|^2 = 1 - \eta^2 \geq 1 - \eta \geq (1-\eta)^2 \tag{8.17}$$

Then it can be showed that

$$\|\boldsymbol{\epsilon}\|^2 = \frac{1}{2}\|\boldsymbol{\epsilon}\|^2 + \frac{1}{2}\|\boldsymbol{\epsilon}\|^2 \geq \frac{1}{2}(\|\boldsymbol{\epsilon}\|^2 + (1-\eta)^2) \tag{8.18}$$

and then there will exists a $\lambda > 0$ for all $t \geq T$ such that

$$\dot{V} \leq -\lambda V \tag{8.19}$$

and hence , $\|\boldsymbol{\epsilon}\|, \boldsymbol{\Delta\omega} \to 0$ exponentially.

If on the other hand $\eta \to -1$, such a conclusion cannot be stated. In this case as

$$V \to 4(k_p + ck_v)$$

and if

$$V(0) < 4(k_p + ck_v) \tag{8.20}$$

the situation with $\eta \to -1$ cannot occur since V is non increasing. This therefor gives the condition for V(t) exponentially converging to zero

$$\frac{1}{2}\boldsymbol{\Delta\omega}(0) \cdot \boldsymbol{I}\boldsymbol{\Delta\omega}(0) < k_p(4 - (1 - \eta(0))^2 - \|\epsilon(0)\|^2) = 2k_p(1 + \eta(0)) \tag{8.21}$$

8.1.3 Comments to PD controller

It is shown in [8] that the case where $\eta = -1$ corresponds to an unstable equilibrium and is therefore clearly undesirable. Any small perturbation will cause a rotation of 360° to $\eta = +1$. But as described previous, this situation is avoided when (8.14) is satisfied by either choosing k_p large enough or $\boldsymbol{\Delta\omega} = 0$. By combining the globally non-singular parameterization with the global stability analysis tool of Lyapunov's direct method, global asymptotic stability is proved for both the model-dependent and the model-independent PD controller. It is the choice of Lyapunov function that is most crucial in the proof of the above controllers.

It is important to be aware that the control laws presented above does not create a continuous, globally asymptotically stable vector field on $SO(3) \times R^3$, as this is not possible since implementation would require memory as the sign ambiguity in $\mathbf{q}$ cannot be resolved from the attitude kinematic equation. However, on $S(3) \times R^3$, where $S(3)$ is the unit sphere in R^4 where the quaternion lies, a globally asymptotically stable vector field in the closed-loop can be found. This means that as the kinematic equation for the system, the unit quaternion representation must be used. See [8].

8.1.4 GAS of Robust controller

The global asymptotically stable robust controller proposed in section 3.1.3 is analyzed thoroughly in [9], main results and proofs will be presented in this thesis too, as it is a very significant part of the overall nonlinear separation principle later in this chapter.

The control law is given by equation (3.6), where G_p is symmetric and positive definite matrix fulfilling $0 < \lambda_{max}(G_p) \leq 2\gamma$ and γ is a positive constant, then the overall feedback loop system of ESMO (or any other satellite) has two equilibrium points at $(\boldsymbol{\epsilon} = 0, \boldsymbol{\omega} = 0, \eta = 1)$, and $(\boldsymbol{\epsilon} = 0, \boldsymbol{\omega} = 0, \eta = -1)$. Proof of this can be seen in [9].

By looking at the parameterization where

$$\eta = \cos(\frac{\phi}{2}) \tag{8.22}$$

If applying the equilibrium points to (8.22), then $\eta = 1 \Rightarrow \phi = 0$, while $\eta = -1 \Rightarrow \phi = 2\pi$ in other words, there is only one equilibrium point in the physical space. The desired equilibrium space will therefore be $(\boldsymbol{\epsilon} = 0, \boldsymbol{\omega} = 0, \eta = 1)$. Therefore, $\beta = (\eta - 1)$ are defined, to make the origin of the state space converge to the desired equilibrium space. The system equation for $\dot{\eta}$ and $\dot{\epsilon}$ in (2.6) can then be rewritten to

$$\dot{\beta} = -\frac{1}{2}\boldsymbol{\omega}^T\boldsymbol{\epsilon} \tag{8.23}$$

$$\dot{\boldsymbol{\epsilon}} = \frac{1}{2}(S(\boldsymbol{\epsilon}) + (\beta + 1))\boldsymbol{\omega} \tag{8.24}$$

and the system in (2.6) can now be expressed as

$$\dot{x} = f(x, u) \text{ , where } x = (\beta, \boldsymbol{\epsilon}, \omega_{ob}^b) \tag{8.25}$$

By using this rewritten model, the initial orientation given by $(\beta(0), \boldsymbol{\epsilon}(0))$ can always be defined in such a way that $-1 \leq \beta \leq 0$ corresponding to $0 \leq \eta(0) \leq 1$, which is equal to $|\phi| \leq \pi$, and the positive equilibrium point is chosen.

The control law will now be rewritten to

$$u = -\frac{1}{2}\left[(\boldsymbol{\epsilon} \times \boldsymbol{\epsilon} + (\beta + 1)\boldsymbol{I})G_p - \gamma\beta\boldsymbol{I}\right]\boldsymbol{\epsilon} - G_r\boldsymbol{\omega} \tag{8.26}$$

Now the following theorem establish global asymptotic stability of the physical equilibrium state

Theorem 8.1.3 *Suppose G_p and G_r are symmetric and positive definite, and that $0 < \lambda_{max}G_p \leq 2\gamma$. Then the closed loop system given by rotational equation of motion $J\dot{\omega} + \omega \times (J\omega) = \tau$, (8.23), (8.24) and (8.26) is globally asymptotically stable.*

Proof Consider the positive definite and radially unbounded Lyapunov function

$$V = \boldsymbol{\omega^T J\omega} + \boldsymbol{\epsilon^T G_p \epsilon} + \gamma\beta^2 \tag{8.27}$$

The derivative of V is

$$\dot{V} = 2\boldsymbol{\omega}^T\left[-S(\boldsymbol{\omega}) \times (\boldsymbol{J\omega}) + u\right] + \boldsymbol{\epsilon}^T\boldsymbol{G_p}(\boldsymbol{\omega} \times \boldsymbol{\epsilon} + (\beta + 1)\boldsymbol{\omega}) - \gamma\beta\boldsymbol{\omega}^T S(\boldsymbol{\epsilon}) \tag{8.28}$$

Substituting for u, rearranging and simplifying

$$\dot{V} = -2\boldsymbol{\omega}^T\boldsymbol{G}_r\boldsymbol{\omega} \tag{8.29}$$

which is negative semi definite.

To prove negative semi definiteness it is necessary to investigate the Lyapunov function at $\dot{V} = 0$, this occurs only when $\boldsymbol{\omega} = 0$, and therefore two equilibrium points will be present, namely for $\boldsymbol{\epsilon} = \boldsymbol{\omega} = 0, \beta = 0$ and $\boldsymbol{\epsilon} = \boldsymbol{\omega} = 0, \beta = -2$. As before, these two equilibrium points represents the same physical equilibrium state.

From (8.27) it is verified that any small perturbation in β from the equilibrium point $\beta = -2$ ($\eta = -1$) will cause a decrease in the value of V. This means that the equilibrium point with $\beta = -2$ corresponds to an isolated equilibrium point such that $\dot{V} = 0$ at that exact point, and $\dot{V} < 0$ in the neighbourhood of that point.

Previously it is shown that $\dot{V}$ is negative everywhere in the feasible state space except at the two equilibrium points. That is if the initial conditions lies anywhere in the state space except at the equilibrium corresponding to $\beta = -2$, then the system will asymptotically approach the origin. When at the equilibrium point corresponding to $\beta = -2$ at $t = 0$, the system will stay there for all $t > 0$. It can derby be concluded by La Salle's theorem (4.3.3) that the system is globally asymptotically stable. [9]

8.2 Stability of overall feedback loop

In the previous section global asymptotic stability of a selection control laws for ESMO has been explored. In chapter 7, exponentially convergence of the extended Kalman filter ((2.80)-(2.84)) was proved. The aim of this section is to present the main result of this thesis, namely a nonlinear separation principle for the combined closed-loop system of equation of motion and kinematic equations for ESMO (2.61), the extended Kalman filter proposed for ESMO and the above GAS control laws.

In chapter 6.1, a lot of previous work, methods, constraints, and principles yielding several special cases of nonlinear separation principle was presented. None of these presented work has tried to combine an extended Kalman filter with a control law, but as the filter has proved to be acting like a exponentially observer for the system, some of the thesis previous derived for other systems may yield.

In [12], stability of polymerization reactors using I/O Linearization and a high gain observer is presented. Here a nonlinear separation principle is derived, based on exponentially converging observer combined with a globally asymptotically stable nonlinear feedback controller admitting the physical state space as a positively invariant bounded set. From Theorem 8.1.1, 8.1.2 and 8.1.3 and the following proofs, it is quite clear that these controllers fulfill the requirement of the controller in [12]. From Chapter 7 the extended Kalman filter is proved exponentially converging and it is therefore possible to propose a nonlinear separation principle for ESMO based

upon the work done in [12] transformed into discrete time

Theorem 8.2.1 ***Nonlinear Separation Principle for ESMO:***

For the system Ξ_k given by

$$z_{k+1} = \phi_k z_k + \Gamma_k u_k$$
$$\hat{z}_{k+1} = \phi_k + \Gamma_k \hat{u}_k + K_k(y_k - h(\hat{z}_k))$$

K_k given by the equations for Kalman gain, depending on P_k

If the controller u_k is globally asymptotically stable, such that z_k in Ξ remains in a compact set Ω for all $k > 0$, where the compact set Ω contains the equilibrium point of the controller u_k, and if the estimation error $\xi_n = z_k - \hat{z}_k$ converges exponentially to zero for all $k > 0$, (i.e an exponential observer), then, for all initial state values $z_0 \in \Omega$, the system Ξ is globally asymptotically stable (GAS) for all $z_0 \in \Omega$, $\forall$ $\hat{x}_0 \in R^n$, $\forall P_0 > 0$. And therefore, the observer and the controller can be designed separately as long as they fulfil the requirement stated in this theorem.

Proof When an exponential observer like the proposed EKF is used, the estimation error will tend to zero and is therefore bounded. The error covariance P_k which the Kalman gain K_k depends on is given by the Riccati equation and is proved bounded from above and below in Chapter 7 and hence the state $(\xi_k, \hat{z}_k, P_k)$ of Ξ remains in a compact set along any trajectory.

Let $\Lambda = \{\xi_k, \hat{z}_k, P_k, k \geq 0\}$ be a semi trajectory of the closed loop combined system Ξ. This semi trajectory, laying in a compact set as stated above, has a nonempty ω-limit set. Let $(\bar{\xi}, \bar{z}, \bar{P})$ be an element of the considered ω-limit set of Λ. Since $\xi_k \to 0$ $\Rightarrow \bar{\xi} = 0$. Let $\{0, \hat{z}_k, P_k, k \geq 0\}$ be a semitrajectory starting at $k = 0$ from $(0, \bar{z}, \bar{P})$. Since ω-limit set is positively invariant (La Salle), it follows that $\{0, \hat{z}_k, P_k, k \geq 0\}$ belongs to the considered ω-limit set of Λ. By using the closed-loop stability assumption and exponentially convergence $\hat{z}_k \to z_k^* = \psi^(z_k^*)$, so there are points at which $\xi_k = 0$ and $\hat{z}_k = z_k^*$ in the ω-limit set of Λ as the set is closed.

Then, let $(0, \bar{z}^*, \bar{P})$ be an element of ω-limit and again following the same procedure, letting $\{0, z_k^*, P_k, k \geq 0\}$ be a semitrajectory starting at $k = 0$ from $(0, z_k^*, \bar{P})$ belonging to a ω-limit set of Λ. The dynamics of P_k is given by (2.82) and (2.84) (which are based upon the Riccati equation. The linearized system is proved to be observable in section 7.1.2 and therefor knows that $P_k \to P^*$ which is the unique positive-definite solution of the algebraic Riccati equation. Therefor, $(0, \bar{z}^*, P^*)$ belongs to the ω-limit set of Λ. It follows , under the assumption of (local) asymptotic stability of Ξ_k, that Λ enters in a finite time into the basin of attraction of $(0, \bar{z}^*, P^*)$. Hence Ξ_k is globally asymptotically stable on $\Omega \times R^N \times P_k^+$

The last part of the proof states local asymptotic stability of Ξ_k, by letting N be

the invariant manifold defined by $N = \{(\xi, \hat{z}, P)|\xi = 0\}$. The nonlinear dynamics on N are given by subsystem

$$\Xi_N\{\hat{z}_{k+1} = \phi_k + \Gamma_k \hat{u}_k + K_k(y_k - h(\hat{z}_k))$$
$$K_k \text{ given by the equations for Kalman gain, depending on } P_k$$

where the system Ξ_N is triangular and both the subsystems are asymptotically stable. Using the (local) asymptotic stability results of Vidyasagar [28], it is deduced that the nonlinear dynamics on N are asymptotically stable. Since the estimation error is exponentially converging, it can be concluded that Ξ_k is (local) asymptotically stable. And hence, it is proved that the overall closed loop system is globally asymptotically stable.

8.3 Discussion

In this chapter the stability of the proposed controllers in Chapter 3.1 are analyzed and proved to be GAS. The convergence result from Chapter 7 is then combined with GAS feedback controllers and GAS stability of the overall feedback-loop combining controller and observer is stated as a nonlinear separation principle.

The nonlinear separation principle proposed is general and holds for all systems combining GAS control law with an exponentially converging observer as the controlled state always will remain in a bounded set when this requirement are fulfilled.

The theorem and proof is based upon the results presented in [12], where nonlinear separation principle is deduced for the polymerization reactors in continuous time using a high-gain observer and a GAS feedback law. The main difference in this thesis is that the theorem is proposed for a satellite system attitude determination where extended Kalman filter is used as an observer combined with a GAS feedback law.

Chapter 9

Simulations

The simulation chapter here consists of five sections where simulations with the three presented controllers are carried out in each section, followed by a section where response to different steps are compared for the three controllers and then a discussion of the results. The same Simulink model is used in each section, only the controller part differs. For simplicity, a single star sensor is used in the simulations for measurements, and the attitude is estimated in the extended Kalman filter block. Continuing, the estimated states are used as input to the respective feedback controller. A general wish for attitude determination is accuracy of 0.001° about all axes and for tracking no upper bound for tracking error is given, but as always best possible accuracy is to be desired.

Simulations are done with different proportional and derivative gains, to get a rough picture of how sensitive the controller is and how it behaves when large or small gains are applied. It is also done simulations for different step sizes, to see how large steps the controller is capable of following.

9.1 Overall Simulink diagram

The overall simulink model can be seen in Figure 9.1. The model parameters are given in table 9.1, and is decided from ESMO statement of propose and previous values used in ESEO. All the initial values for of EKF is given in table 9.2.
The controller calculates a 3×1 torque vector which has to be distributed to the four reaction wheels in some way. An optimal distribution of control torque is derived by Fossen [29].

$$u = \tau A^{\diamond},\ A^{\diamond} = A^T(AA^T)^{-1} \tag{9.1}$$

A is the allocation matrix given in (A.1) and $A^{\diamond}$ is the Moore - Penrose pseudo inverse matrix.

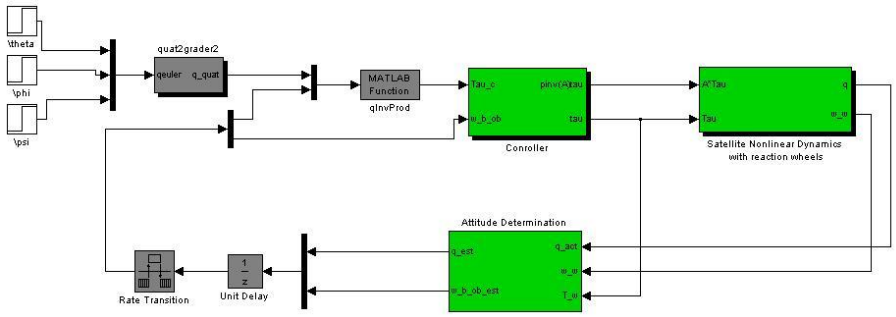

Figure 9.1: Overall feedback loop

Parameter	Value
Satellite Inertia	$\text{diag}(22.0,\ 32.3,\ 34.7)[kgm^2]$
Actuator Inertia	$\text{diag}(1,\ 1,\ 1,\ 1)\cdot 10^{-2}\,[kgm^2]$
Moon radius	$1736\,[km]$
Moon mass	$7.35 \cdot 10^{22}$
Universal Gravity Gradient G	$6.6742 \cdot 10^{-11}\left[\frac{m^3}{kgs^2}\right]$
Orbit velocity ω_0	$0.9683 \cdot 10^{-3}$

Table 9.1: Initial satellite values

Parameter	Value
ΔT	0.05
q_{noise}	$1 \cdot 10^{-12}$
ω_{noise}	$1 \cdot 10^{-8}$
$star_{noise}$	$1 \cdot 10^{-12}$
Q	$\text{diag}\ (q_{noise}^2, q_{noise}^2, q_{noise}^2, \omega_{noise}^2, \omega_{noise}^2, \omega_{noise}^2)$
R	$[star_{noise}\ star_{noise}\ star_{noise}]^T$
H	$[\boldsymbol{I}_{3\times 3}\mathbf{0}_{3\times 3}]$
GG	$\Delta T \cdot eye(6)$
$P_{k,0}$	$\text{diag}(1 \cdot 10^{-6}, 1 \cdot 10^{-6}, 1 \cdot 10^{-6}, 1 \cdot 10^{-10}, 1 \cdot 10^{-10}, 1 \cdot 10^{-10})$
$q_{k,0}$	$[5\ 5\ 5]\,[deg]$ (converted into quaternions)
$\omega_{k,0}$	$[0.0005\ 0.0005\ 0.0002]\,[rad/s]$

Table 9.2: Initial EKF values

9.2 PD model independent

The PD-controller given in equation (3.5) is simulated in this section. The first simulations shows tracking error and estimation error when exposed to a 5° step in reference value. Later sections will have a closer look at tracking qualities.

In figure 9.2 and figure 9.3 the gains are $K_p = 3 \cdot eye(3)$ and $K_d = 5 \cdot eye(3)$ and the figure shows tracking and estimation errors, both overall and zoom on steady state

response.

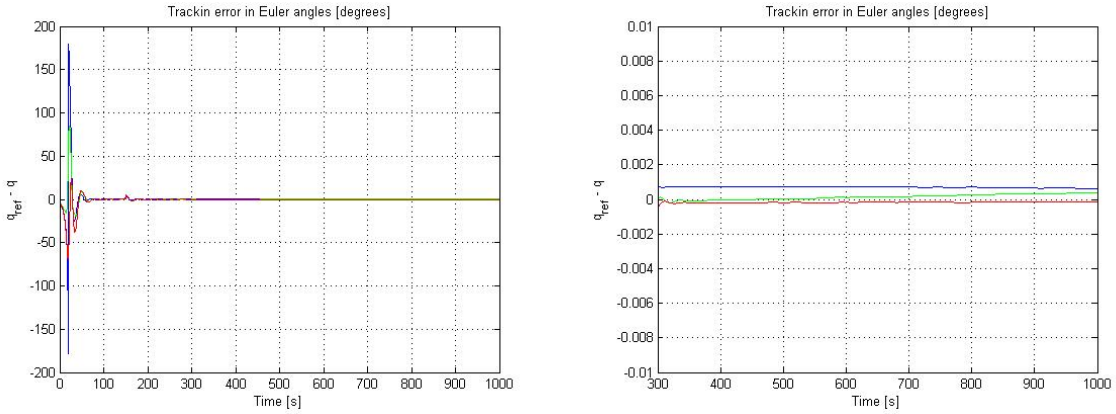

Figure 9.2: PD: Tracking error in Euler angles, small gains

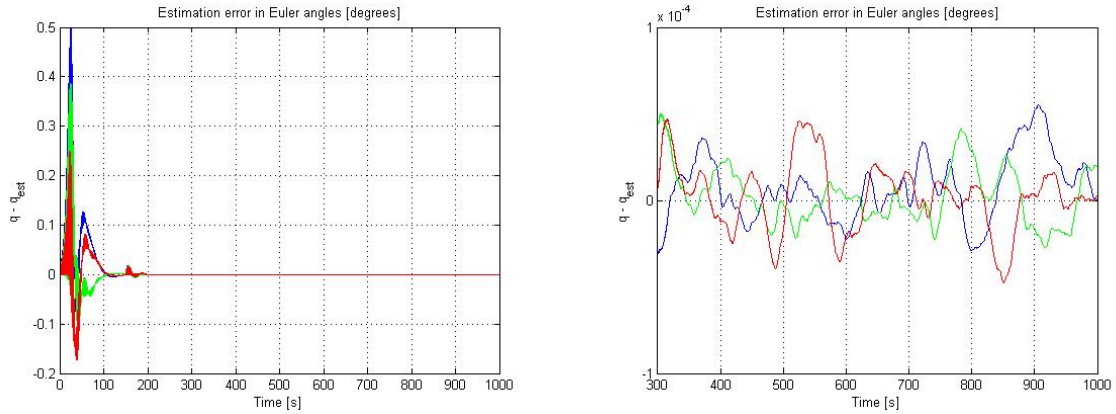

Figure 9.3: PD: Estimation error in Euler angles, small gains

From the figures using small gain it is clear that after the initial oscillations, the system will soon stabilize the attitude around the reference. The 5° step is happening at time t = 150sec. Only a small difference at this exact step can be seen on the graph. A small deviation on about 0.0015° in the steady state can be seen. The estimation error is in the neighborhood of 10^{-4}°, which is well withing the requirement.

Figure 9.4 and figure 9.5 shows the tracking and estimation error with gains $K_p = 30 \cdot eye(3)$ and $K_d = 50 \cdot eye(3)$.

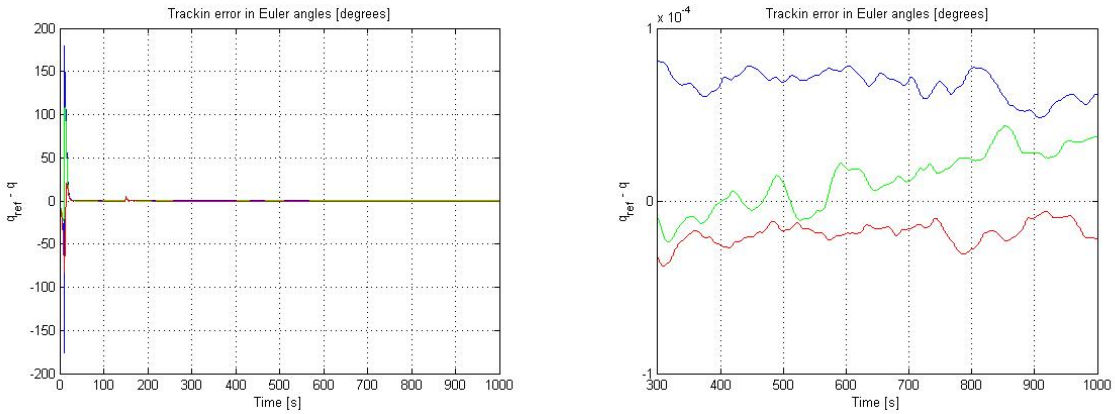

Figure 9.4: PD: Tracking error in Euler angles, medium gains

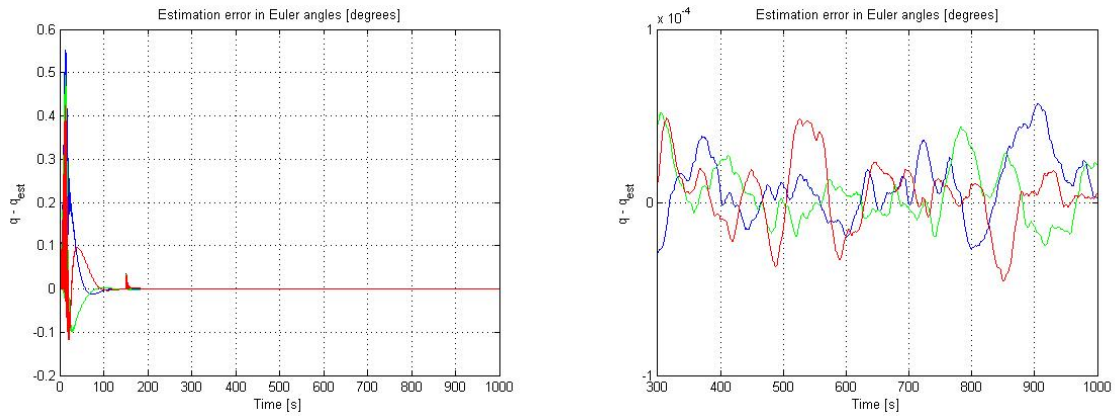

Figure 9.5: PD: Estimation error in Euler angles, medium gains

When increasing the gain ten times, the tracking deviation decreases considerably to around 10^{-4} and the inital response are slightly smoothed. Estimation error almost unchanges.

Even larger gains are imposed in figure 9.6 and figure 9.7, here the gains are set to $K_p = 60 \cdot eye(3)$ and $K_d = 100 \cdot eye(3)$ which is close to maximum gains, as the system start to oscillate for larger gains.

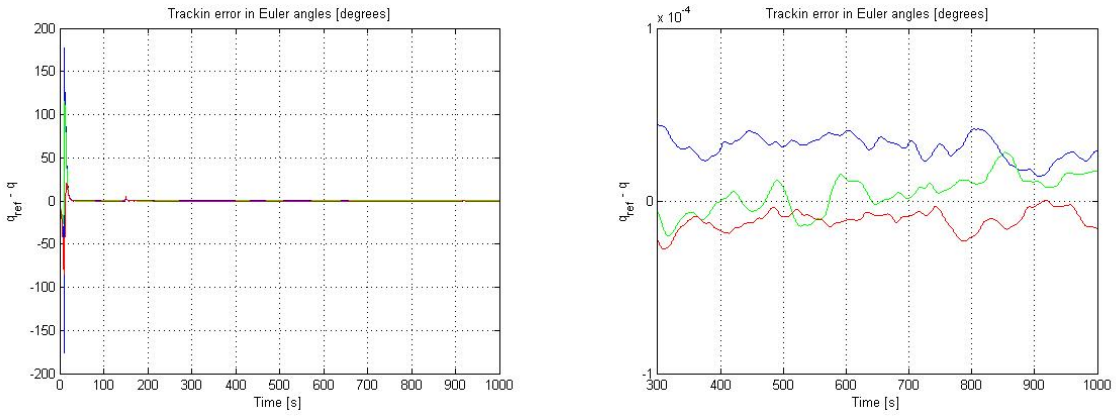

Figure 9.6: PD: Tracking error in Euler angles, large gains

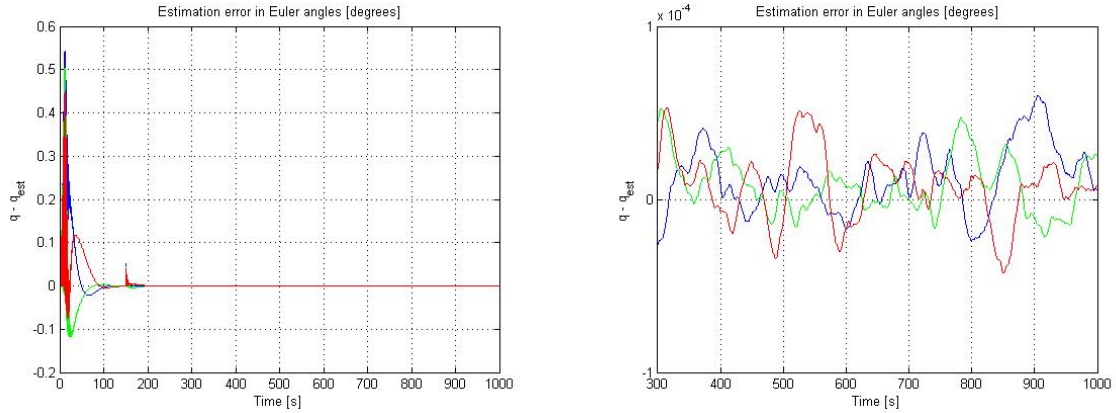

Figure 9.7: PD: Estimation error in Euler angles, large gains

In this last simulations for PD control, the gains are set close to maximum, higher gains makes the system diverge (tested in simulations). The tracking error is once more decreased and smoothed, while estimation error remains the same.

9.3 PD model dependent

The model dependent PD controller is a nonlinear controller given in equation (3.5). When PD-model dependent controller is used, constraints on S_d is applied to force the system into desired equilibrium point. $S_d > \alpha \|I\| \cdot \sup_{t \geq 0} \|\boldsymbol{\omega}_{ib}^d\|$. S_d is therefore chosen to be two times this constraint.

Figure 9.8 and figure 9.9 shows the tracking and estimation error with gains $S_p = 3$ and $S_d = 22.2$. The figure shows tracking and estimation errors, both overall and zoom on steady state response.

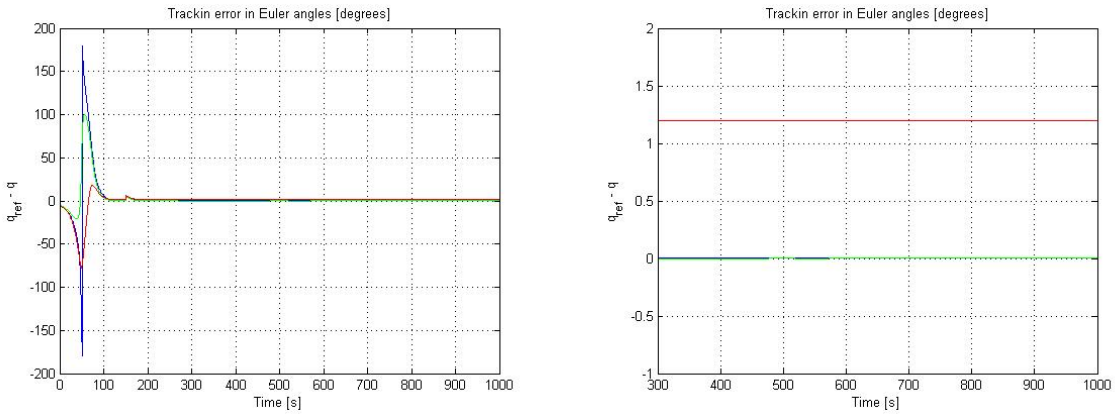

Figure 9.8: MdPD: Tracking error in Euler angles, small gains

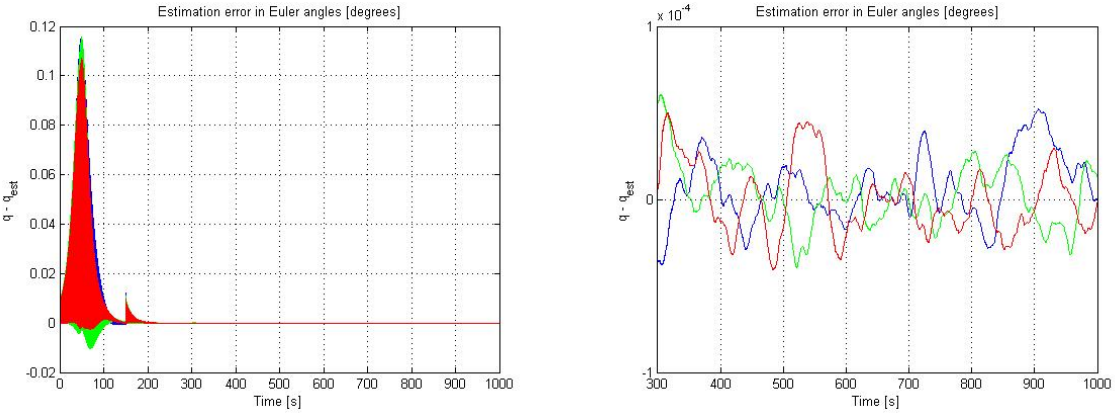

Figure 9.9: MdPD: Estimation error in Euler angles, small gains

For the model dependent controller when small gains are used, the initial response is smoother than for the regular PD controller, although there still is a singularity (because of Euler angles), before the system settles down at the reference attitude. The tracking deviation, however, is larger than for the PD controller with one of the attitude angles settling at 1.2° from the reference. The estimation error is oscillating in the beginning, but settles down quite nicely in the end.

Larger gains are imposed in figure 9.10 and figure 9.11, here the gains are set to $S_p = 30$ and $S_d = 222$.

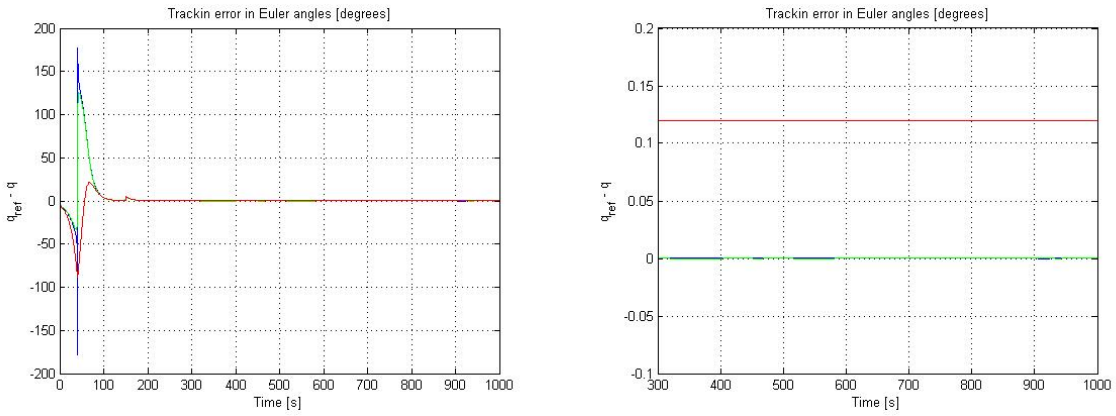

Figure 9.10: MdPD: Tracking error in Euler angles, medium gains

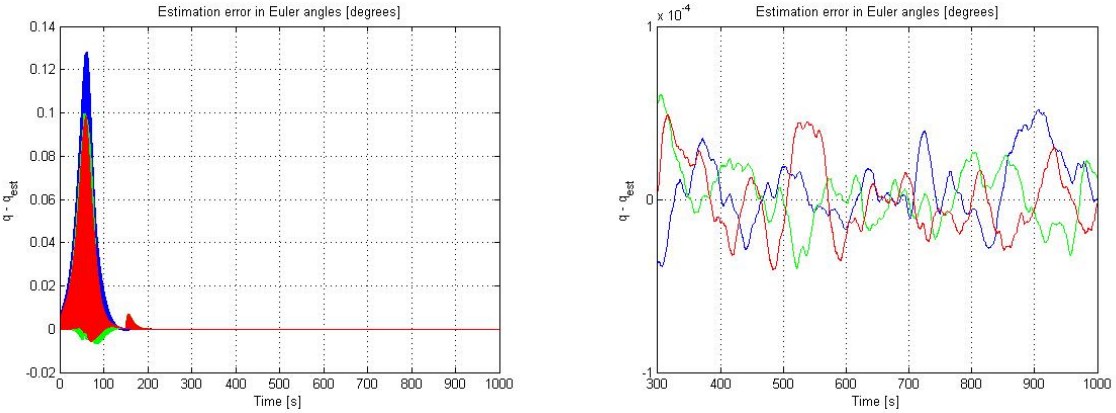

Figure 9.11: MdPD: Estimation error in Euler angles, medium gains

When the gains are increased ten times, the tracking deviation is decreased ten times to 0.12°, the tracking improves for higher gains. Estimation error is still good.

In figure 9.12 and figure 9.13 the gains are $S_p = 45$ and $S_d = 333$, these gains are close to maximum gains before the system starts to oscillate.

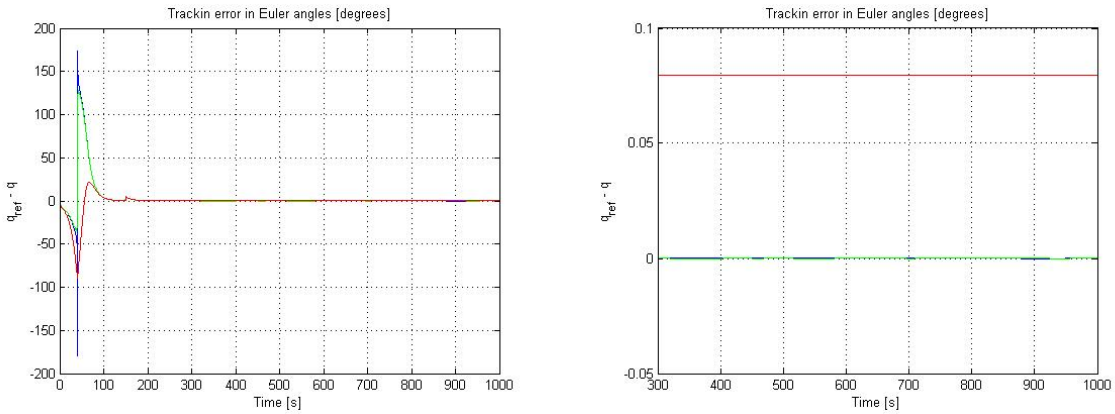

Figure 9.12: MdPD: Tracking error in Euler angles, large gains

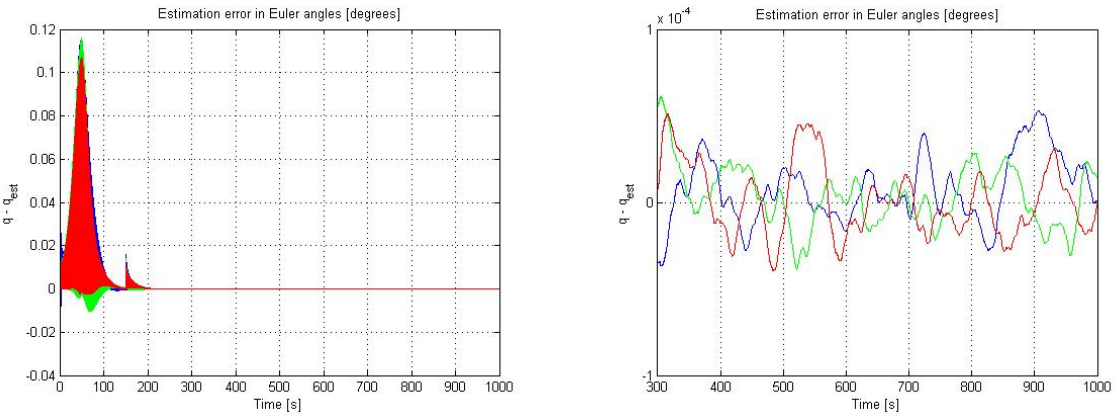

Figure 9.13: MdPD: Estimation error in Euler angles, large gains

The tracking error is yet again reduced and is now showing rather good tracking properties, with only 0.075° deviation. The estimation error remains unchanged with the gain increase.

9.4 Robust Control

In this section the results from the robust controller in (3.6) are given. This controller is also nonlinear. The constraints for this controller is that $\lambda_{max}(G_p) \leq 2\gamma$.

In figure 9.14 and figure 9.15 the gains are $G_p = 0.5 \cdot eye(3)$ and $G_r = 2 \cdot eye(3)$ and $\lambda = 1.2$ and the figure shows tracking and estimation errors, both overall and zoom on steady state response.

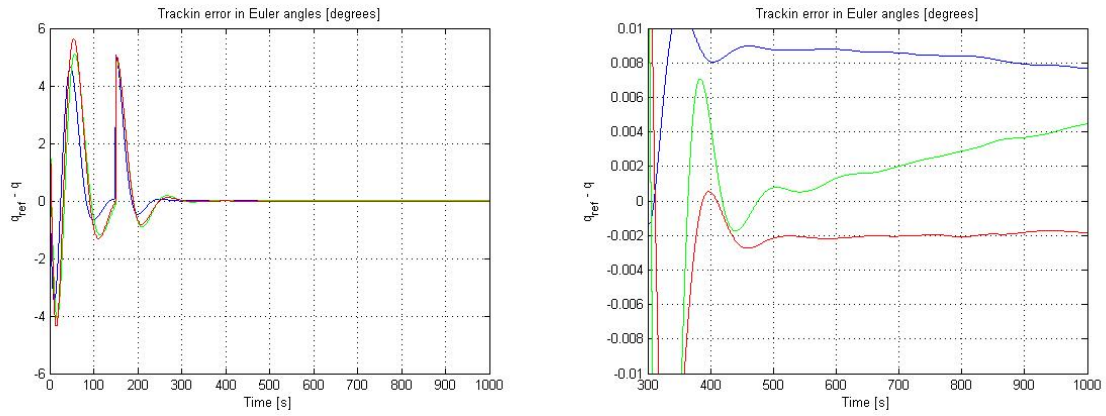

Figure 9.14: Robust: Tracking error in Euler angles, small gains

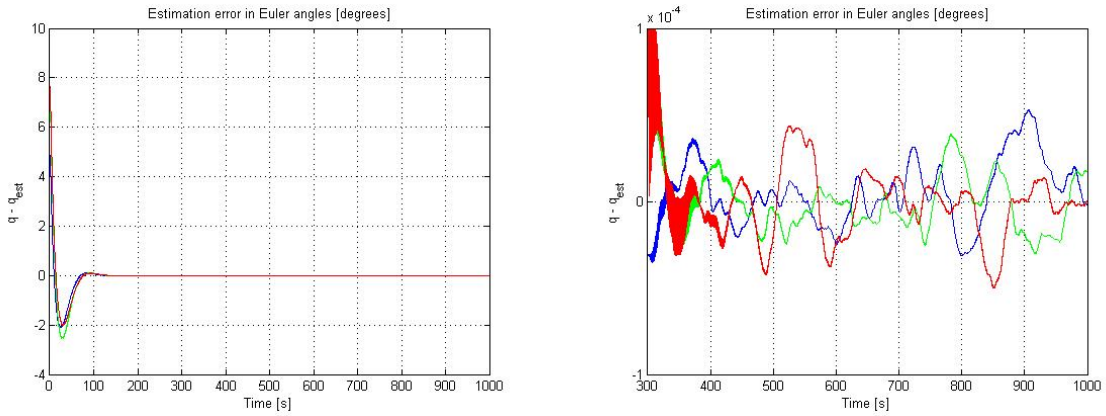

Figure 9.15: Robust: Estimation error in Euler angles, small gains

The results when using the robust controller shows a rather good response as the initial oscillations are reduced from $\pm 180°$ to only $\pm 5°$. Even for very small gains the deviation is limited and within $0.01°$ steady state deviation and the estimation error response is also much smoother and calmer than for the PD controllers.

Figure 9.16 and figure 9.17 shows the tracking and estimation error with gains $G_p = 5 \cdot eye(3)$ and $G_r = 20 \cdot eye(3)$ and $\lambda = 12$.

When the gains in the robust controller are increased ten times, the performance of the controller improves just as much. The initial response is now completely smooth and nice, and when the step is applied, the system is back to steady state after short period of time. The estimation error is not as smooth as the tracking error initially, but looking closer at the graph, the peak error after reference change is $7 \cdot 10^{-3}$, which is well within the requirement of $0.01°$ accuracy.

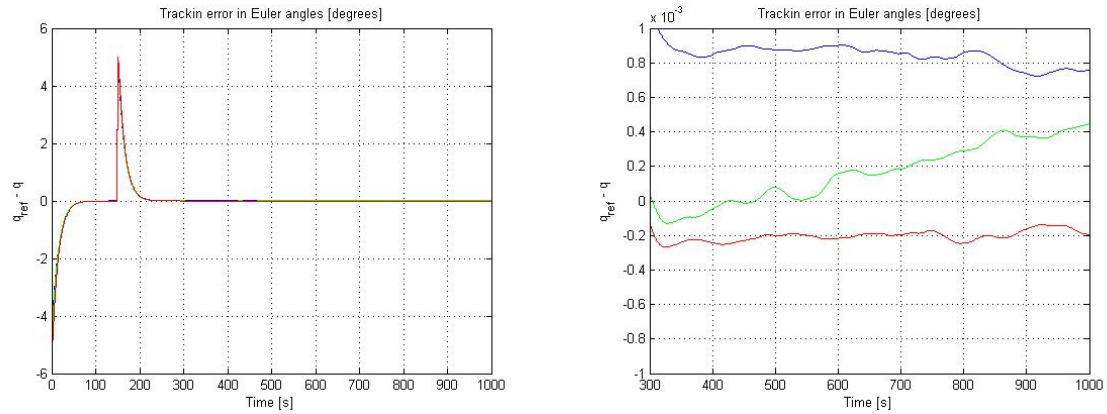

Figure 9.16: Robust: Tracking error in Euler angles, medium gains

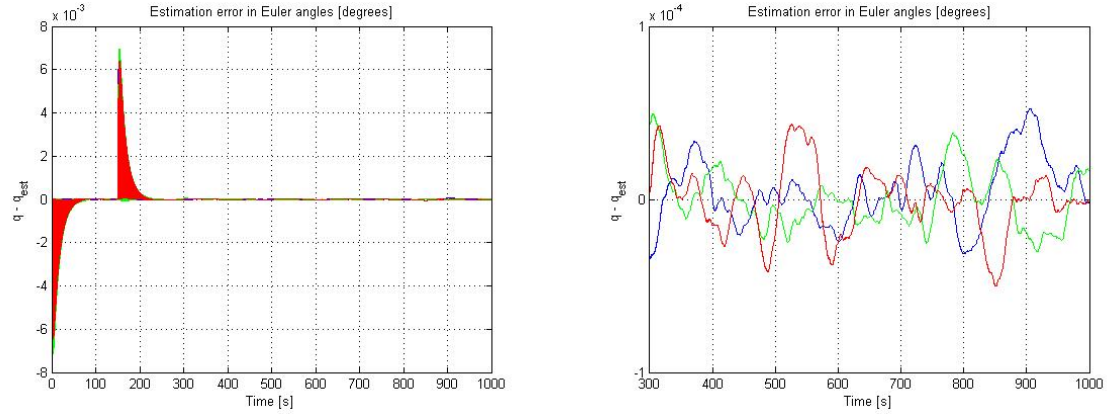

Figure 9.17: Robust: Estimation error in Euler angles, medium gains

Larger gains are imposed in figure 9.18 and figure 9.19, here the gains are set to $G_p = 20 \cdot eye(3)$ and $G_r = 80 \cdot eye(3)$ and $\lambda = 48$ which is close to maximum gains, as the system start to oscillate for larger gains.

By increasing the gains close to maximum, the best result is achieved. The steady state deviation is within 10^{-4}, showing a smooth and relatively quick response. The estimation error shows even smaller peaks initially and the steady state deviation is still within 10^{-4} as before.

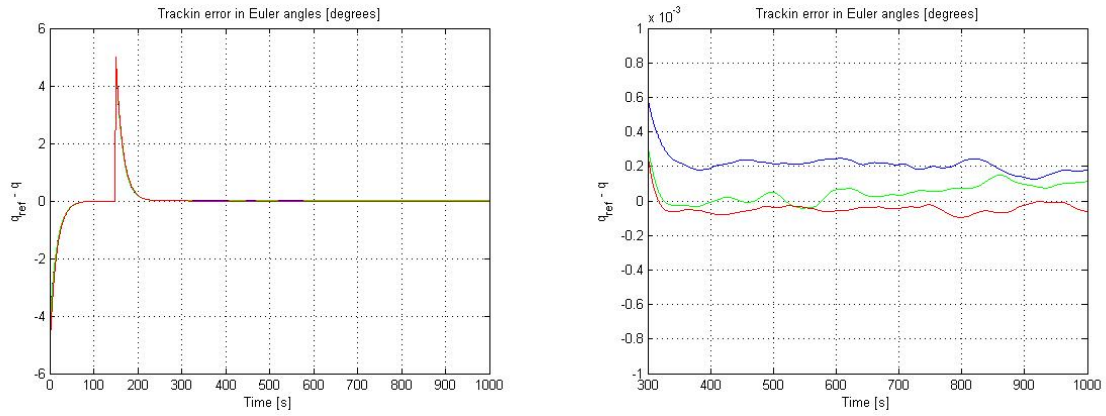

Figure 9.18: Robust: Tracking error in Euler angles, large gains

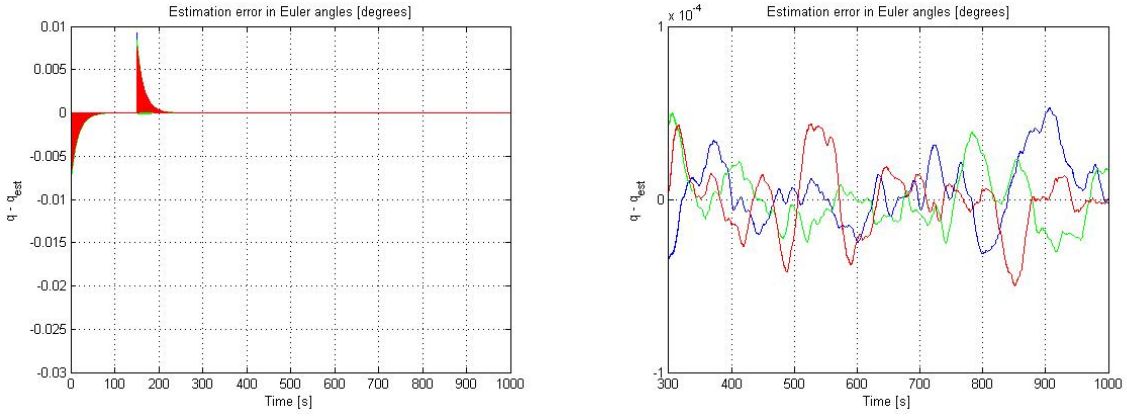

Figure 9.19: Robust: Estimation error in Euler angles, large gains

9.5 Comparing tracking qualities

The three controllers are here exposed for different reference steps; $\begin{bmatrix}20 & 40 & 80\end{bmatrix}$. The response, time and steady state deviation are then compared to see which controller have the best properties.

Figure 9.20 shows the result when applying 20° step on system with PD, model-dependent PD and robust controller respectively. In figure 9.21 the same response is presented when 40° step is applied, followed by 9.22 where the simulations are carried out with 80° step.

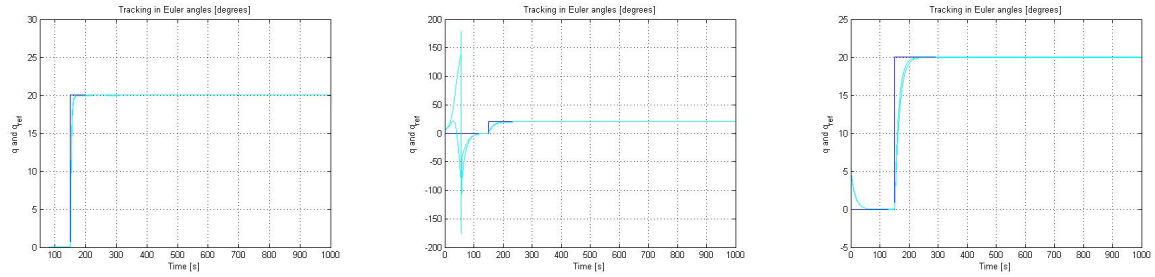

Figure 9.20: PD, mPD and Robust controller, reference vs attitude with 20° step

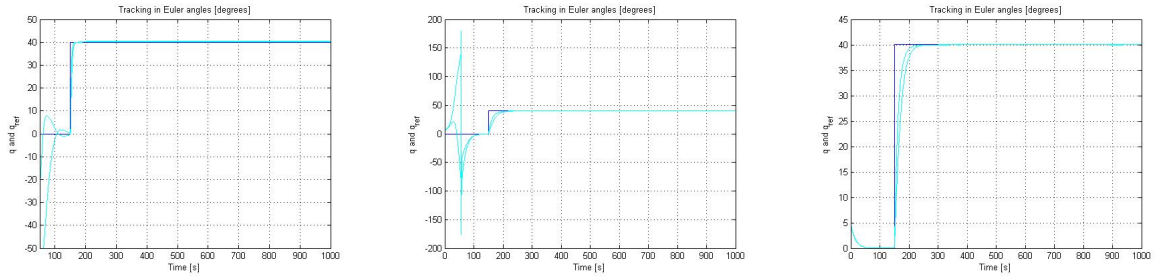

Figure 9.21: PD, mPD and robust controller, reference vs attitude with 40° step

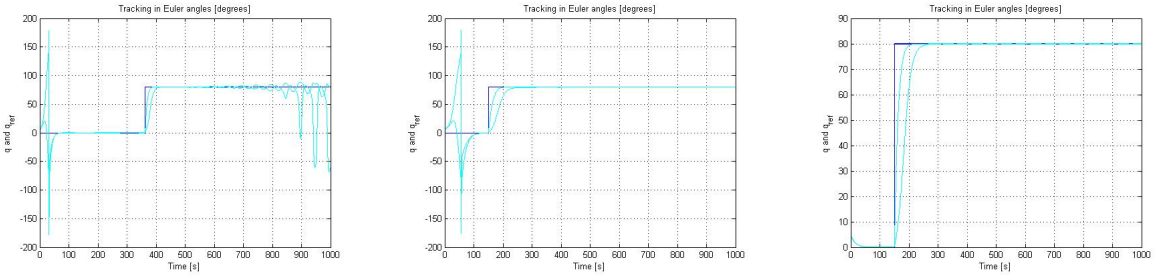

Figure 9.22: PD, mPD and Robust controller, reference vs attitude with 80° step

Taking a closer look at the steady state responses for the model dependent PD controller and the robust controller it is clear that very large step introduce some problems for the controllers. The model-dependent PD controller shows rather large deviation and small oscillations, while the robust controller shows sign of marginal stability as it oscillates around the reference value.

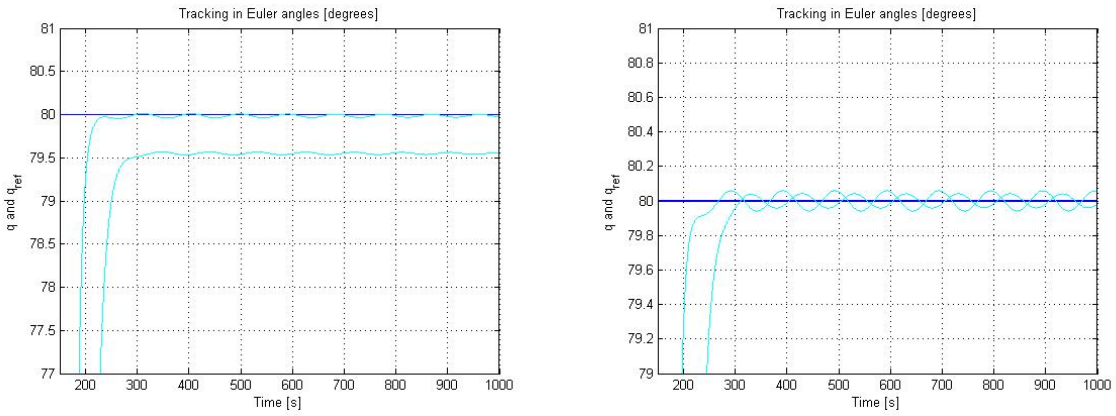

Figure 9.23: mPD and Robust controller, ref vs attitude with 80° step close up

9.6 Discussion and comparing

The aim for the simulations carried out in this chapter has been to prove that the theoretically derived results previous in this thesis, also yields in practice. It has not been the task of this thesis to derive the most successful controller or to get the best tracking for the satellite, the choice of controllers are based upon stabilizing qualities in order to prove a nonlinear separation principle. When that is said, simulations are done with the three controllers to decide which controller fulfills the requirement of a satellite on a moon mission best. Properties that are important for a space mission is accurate attitude determination (within 0.001deg), best possible tracking performance, easy to implement, robust, computational cheap and solid.

It is clear from the above simulation results, that introducing feedback in the attitude determination loop preserve the stability of the open loop system. The attitude estimation process is unconcerned with the controller choice and produces estimates well within the requirement for 0.001° for all three controllers. The tracking properties on the other hand vary to some extent between the three controllers.

The independent PD controller gives good results and it is simple and easy to implement. It is proved stable and the gain scheduling is done off-line which leads to small computational cost, it is also the most used controller, and has been used successfully in countless of operations and systems. As a tracking controller, the simple PD gives small deviations in steady state, however initially, quite high oscillations occur before settling at the reference. It also look as though the controller destabilize the system for very high gains, and since it does not incorporate any system terms it will not react to large changes in the system, and the gains might be very wrong for the system if this occur. It also had larger problems with high reference change than the other two controllers.

The model-dependent PD controller is more complex than the the simple PD controller, but it still results in relatively small tracking error, though larger deviation than the simple PD controller. It is proved stable as long as the constraint on the gains are fulfilled and it incorporates the system states which is suppose to give good response even when high gains cannot be applied to the system. The controller proves that it can handle both high gains and large changes in reference. Although it is stable when these events occur, the tracking quality is not as good as for the other controllers. It is on the other hand, robust against changes and would probably stand better against the harsh environment where ESMO is going than the PD. On the other hand, it is very computational heavy, even when the gains are computed offline and will therefore require a much more powerful software system than the PD controller.

Lastly, the robust controller proves to give by far, the most precise and smooth attitude tracking. The initial response is smooth and nice and it follows the changes in reference both fast and exact. The deviation is small even for small gains and it respond well to large changes in reference, although for 90° it start oscillate slightly, but still showing stable characteristic. It is also quite simple, though more complex than the PD controller but this is accounted for by being more resistible and adoptable to changes in the model and the environment. The only constraint for stability is that the gain is smaller than two times a constant γ.

Based upon the above simulation and discussion, it is clear that the system remains stable when feedback is incorporated as the theory imply. If choosing a controller for ESMO based upon the above simulations and discussion, the robust controller would probably be the best choice as this controller shows the best simulations result in all the tests, both for small and large gains and small and large changes in reference. It is also robust and tough, and will probably work well in the harsh and though environment in space.

Chapter 10

Concluding Remarks and Recommendations

10.1 Conclusion

Attitude determination for a vehicle in space is a very important element when planning a space mission. Being able to control the attitude is another very important part of the attitude subsystem, in order to steer the satellite into desired attitude and position for the satellite to be able to fulfill its mission objectives. As the controller is introduced, the system is transformed into a closed-loop, which might have totally different characteristic than the open loop. The needs to study the stability of the overall system therefor becomes important, especially when combined with an observer for state estimation.

Three different controllers are proposed for the closed loop system of ESMO. All three controllers are proved globally asymptotically stable. The extended Kalman filter is proved exponentially converging and combined with the globally stabilizing control laws, a nonlinear separation principle is proposed for ESMO. This principle guarantees that as long as the observer is exponentially converging and the feedback law is GAS, then the observer and controller can be designed separately and the total system will still be GAS.

Through simulations, the different controllers are tested and simulated for different gains and different steps in reference. The plots show how the tracking and estimation error reacts to feedback. All the controllers give remarkable good response, the estimation error is within 10^{-4} for all three controllers independent of the gain. The tracking error varies between the controllers, different gains and step changes. Overall, based on tracking qualities, robustness, computational cost and implementation issues, the best choice for ESMO, based on the simulation and analysis in this thesis is the robust controller. It is accurate, cheap, robust, GAS and resistible to changes, which is suitable for a lightweight, budget space satellite.

10.2 Further work

As the stability of the closed loop system is established with an extended Kalman filter as observer, it would be useful to compare the results with other types of observers to see what implementation have the best characteristics when both cost, size and accuracy are being considered.

A more thoroughly study on the choice of controller and tuning of these controllers would also be interesting as to propose the most optimal solution for ESMO.

Bibliography

[1] Håvard Lund. Reaction wheels in tetrahedron. Master's thesis, Narvik University College, 2005.

[2] Stian Simonsen. Attitude determination for the esmo satellite using kalman filter. Master's thesis, Narvik University College, 2006.

[3] Karianne Tønne. Attitude determination for esmo: Extended kalman filter. Preliminary project for master thesis, 2006.

[4] Olav Egeland and Jan Tommy Gravdahl. *Modeling and Simulation for Automatic Control*. Marine Cybernetics, Trondheim, Norway, 2002.

[5] Erik Kyrkjebø. Satellite attitude determination - three axis attitude determination using magnetometers and star trackers. Master's thesis, NTNU, Norwegian University of Science and Technology, 2000.

[6] Bernt Ove Sunde. Sensor modeling and attitude determination for microsatellite. Master's thesis, Norwegian University for Technology and Science, 2006.

[7] Thomas Bak. *Spacecraft Attitude Determination - a Magnetometer Approach*. PhD thesis, Aalborg University, 1999.

[8] John Ting-Yung Wen and Kenneth Kreutz-Delgado. The attitude control problem. *IEEE Transaction on Automatic Control*, 36:1148 – 1162, 1991.

[9] A.G. Kelkar S.M. Joshi and J.T.-Y. Wen. Robust attitude stabilization of spacecraft using nonlinear quaternion feedback. *IEEE Transaction on automatic control*, 40:1800 – 1803, 1996.

[10] Hassan K. Khalil. *Nonlinear Systems*. Pearson Education International Inc., USA, 2000.

[11] Mohinder S. Grewal and Angus P. Andrews. *Kalman Filtering: Theory and Practice*. John Wiley & Sons, Inc., USA, 2001.

[12] F. Viel, E. Buvelle, and J. P. Gauthier. Stability of polymerization reactors using i/o linearization and an high-gain observer. *Automatica, Vol 31*, 31:971–984, 1995.

[13] Ahmed N. Atassi and Hassan K. Khalil. A separation principle for the stabilization of a class of nonlinear systems. *IEEE Transaction on Automatic control*, 44:1672 – 1687, 1999.

[14] Ahmed N. Atassi and Hassan K. Khalil. A separation principle for the stabilization of a class of nonlinear systems. *IEEE Transaction on Automatic control*, 46:742 – 746, 2001.

[15] Andrew Teel and Laurent Praly. Global stabilization and observability imply semi-global stabilizability by output feedback. *System Control Letter*, 22:313 – 325, 1994.

[16] Nam H. Jo and Jin H. Seo. Local separation principle for non-linear systems. *International Journal of Control*, 73:292 – 302, 2000.

[17] Vaclav Cerny and Josef Hrusak. Separation principle for a class of non-linear systems. *ukjent*, ukjent:ukjent, 2005.

[18] Antonio Loria, Thos I. Fossen, and Elena Panteley. A separation principle for dynamic positioning of ships: Theoretical and experimental results. *IEEE Control System Technology*, 8:332 – 343, 2000.

[19] A. Bensoussan, J.S. Baras, and M.R. James. Dynamic observers as asymptotic limits for recursive filters: special cases. *SIAM Journal of Applied Mathematics*, 48:1147–1158, 1988.

[20] A.J Krener. *The convergence of the extended Kalman filter*. Directions in Mathematical Systems and Theory, 2003.

[21] Y. Song and J.W. Grizzle. The extended kalman filter as a local asymptotic observer for discrete-time nonlinear systems. *Journal of Mathematical Systems, Esimatian and Control*, 5:59–78, 1995.

[22] Konrad Reif and Rolf Unbehauen. Stochastic stability of the discrete-time extended kalman filter. *IEEE Transaction on Signal Processing*, 47:2324–2328, 1999.

[23] B.F. La Scala, R.R. Bitmead, and M.R. James. Conditions for stability of the extended kalman filter and their applications to the frequency tracking problem. *Mathematics of Control, Signals and Systems*, 8:1–26, 1995.

[24] S. Gunther, K. Reif, E. Yaz, and R. Unbehauen. The extended kalman filter as an exponential observer for nonlinear systems. *IEEE Transaction on Automatic control*, 44:714–728, 1999.

[25] Knut Rapp. *Nonlinear estimation and control in the iron ore pelletizing process: An application and analysis of the Extended Kalman filter*. PhD thesis, Norwegian University of Science and Technology, NTNU, 2004.

[26] M. Boutayeb, H. Rafaralahy, and M. Darouach. Convergence analysis if the extended kalman filter used as an observer for the nonlinear deterministic discrete-time systems. *IEEE Transaction on Automatic control*, 42:581–586, 1997.

[27] Ola-Erik Fjellstad and Thor I. Fossen. Comments on ẗhe attitude control problem*:* *IEEE Transaction on Automatic Control*, 39:699 – 700, 1994.

[28] M. Vidyasagar. On the stabilization of nonlinear systems using state detection. *IEEE Transaction on automatic control*, 25:504 – 509, 1980.

[29] Thor I. Fossen. *Guidance and control of ocean vehicles*. John Wiley & Sons, New York, 1994.

Appendix A

System Parameters

A.1 System matrices and paramters

$$\mathbf{A_{wheels}} = \begin{bmatrix} a_{11} & a_{12} & a_{13} & a_{14} \\ a_{21} & a_{22} & a_{23} & a_{24} \\ a_{31} & a_{32} & a_{33} & a_{34} \end{bmatrix} = \begin{bmatrix} \frac{\sqrt{1}}{3} & \frac{\sqrt{1}}{3} & -\frac{\sqrt{1}}{3} & -\frac{\sqrt{3}}{3} \\ \frac{\sqrt{2}}{3} & -\frac{\sqrt{2}}{3} & 0 & 0 \\ 0 & 0 & -\frac{\sqrt{2}}{3} & \frac{\sqrt{2}}{3} \end{bmatrix} \tag{A.1}$$

$$\mathbf{I}_w = \begin{bmatrix} i_1 & 0 & 0 & 0 \\ 0 & i_2 & 0 & 0 \\ 0 & 0 & i_3 & 0 \\ 0 & 0 & 0 & i_4 \end{bmatrix} = \begin{bmatrix} 10^{-3} & 0 & 0 & 0 \\ 0 & 10^{-3} & 0 & 0 \\ 0 & 0 & 10^{-3} & 0 \\ 0 & 0 & 0 & 10^{-3} \end{bmatrix} \tag{A.2}$$

$$I_{inertia} = \begin{bmatrix} I_x & 0 & 0 \\ 0 & I_y & 0 \\ 0 & 0 & I_z \end{bmatrix} = \begin{bmatrix} 22 & 0 & 0 \\ 0 & 32.3 & 0 \\ 0 & 0 & 34.7 \end{bmatrix} \tag{A.3}$$

Measurement matrix can be assumed constant

$$\mathbf{H}_k = \begin{bmatrix} \mathbf{I}_{3\times3} & \mathbf{0}_{3\times3} \end{bmatrix} \tag{A.4}$$

Noise matrices for the Kalman filter

$$Q_k = \begin{bmatrix} 10^{-12} & 0 & 0 & 0 & 0 & 0 \\ 0 & 10^{-12} & 0 & 0 & 0 & 0 \\ 0 & 0 & 10^{-12} & 0 & 0 & 0 \\ 0 & 0 & 0 & 10^{-8} & 0 & 0 \\ 0 & 0 & 0 & 0 & 10^{-8} & 0 \\ 0 & 0 & 0 & 0 & 0 & 10^{-8} \end{bmatrix} \tag{A.5}$$

$$E_k = \begin{bmatrix} \Delta T & 0 & 0 & 0 & 0 & 0 \\ 0 & \Delta T & 0 & 0 & 0 & 0 \\ 0 & 0 & \Delta T & 0 & 0 & 0 \\ 0 & 0 & 0 & \Delta T & 0 & 0 \\ 0 & 0 & 0 & 0 & \Delta T & 0 \\ 0 & 0 & 0 & 0 & 0 & \Delta T \end{bmatrix} \tag{A.6}$$

A.2 The linearized velocity part

$$\mathbf{F}_{vel} = \begin{bmatrix} b_{11} & b_{12} & b_{13} & b_{14} & b_{15} & b_{16} & b_{17} \\ b_{21} & b_{22} & b_{23} & b_{24} & b_{25} & b_{26} & b_{27} \\ b_{31} & b_{32} & b_{33} & b_{34} & b_{35} & b_{36} & b_{37} \end{bmatrix} \tag{A.7}$$

$$\begin{aligned} b_{11} &= 2k_x\omega_0(\eta\omega_y + \epsilon_1\omega_z) + 2\omega_0(\eta\omega_y - \epsilon_1\omega_z) + k_x(\eta c_{33} - \epsilon_1 c_{23}) \\ &+ \frac{1}{I_x}(2i_w\omega_0(a_{21} + a_{22} + a_{23} + a_{24})(-\epsilon_3(a_{11} + a_{12} + a_{13} + a_{14}) - \eta(a_{21} + a_{22} + a_{23} + a_{24}) \\ &+ \epsilon_1(a_{31} + a_{32} + a_{33} + a_{34}) + a_{21}\omega_{w,1} + \frac{1}{2\omega_0}(\omega_{w,2} + \omega_{w,3} + \omega_{w,4}))(c_{32}\omega_0 - \omega_z) \\ &- 2\epsilon_1\omega_0 e_2 + 2i_w\omega_0(a_{31} + a_{32} + a_{33} + a_{34})(\epsilon_3(-a_{11} - a_{12} - a_{13} - a_{14}) + \eta(-a_{21} - a_{22} - a_{23} - a_{24}) \\ &- \epsilon_1(a_{31} + a_{32} + a_{33} + a_{34}) + \frac{1}{2\omega_0}(\omega_{w,1} + a_{32}\omega_{w,2} + \omega_{w,3} + \omega_{w,4}))(\omega_x - c_{22}\omega_0) - 2\epsilon_2\omega_0 e_3) \end{aligned} \tag{A.8}$$

$$\begin{aligned} b_{12} &= -2k_x\omega_0(\epsilon_3\omega_y + \epsilon_2\omega_z) + 2\omega_0(\epsilon_2\omega_z - \epsilon_3\omega_y) + k_x(\epsilon_3 c_{33} - \epsilon_2 c_{23}) \\ &+ \frac{1}{I_x}(2i_w\omega_0(a_{21} + a_{22} + a_{23} + a_{24})(-\epsilon_2(a_{11} + a_{12} + a_{13} + a_{14}) + \epsilon_1(a_{21} + a_{22} + a_{23} + a_{24}) \\ &+ \eta(a_{31} + a_{32} + a_{33} + a_{34}) + a_{21}\omega_{w,1} + \frac{1}{2\omega_0}(\omega_{w,2} + \omega_{w,3} + \omega_{w,4}))(\omega_z - c_{32}\omega_0) \\ &- 2\eta\omega_0 e_2 + 2i_w\omega_0(a_{31} + a_{32} + a_{33} + a_{34})(-\epsilon_2(a_{11} + a_{12} + a_{13} + a_{14}) + \epsilon_1(a_{21} + a_{22} + a_{23} + a_{24}) \\ &+ \eta(a_{31} + a_{32} + a_{33} + a_{34}) + \frac{1}{2\omega_0}(\omega_{w,1} + \omega_{w,2} + \omega_{w,3} + \omega_{w,4}))(\omega_x - c_{22}\omega_0) - 2\epsilon_1\omega_0 e_3) \end{aligned} \tag{A.9}$$

$$\begin{aligned} b_{14} &= 2k_x\omega_0(\epsilon_1\omega_y - \eta\omega_z) + 2\omega_0(\epsilon_1\omega_y + \eta\omega_z) + k_x(\epsilon_1 c_{33} + \eta c_{23}) \\ &+ \frac{1}{I_x}(2i_w\omega_0(a_{21} + a_{22} + a_{23} + a_{24})(-\eta(a_{11} + a_{12} + a_{13} + a_{14}) + \epsilon_3(a_{21} + a_{22} + a_{23} + a_{24}) \\ &+ \epsilon_2(a_{31} + a_{32} + a_{33} + a_{34}) + a_{21}\omega_{w,1} + \frac{1}{2\omega_0}(\omega_{w,2} + \omega_{w,3} + \omega_{w,4}))(\omega_z - c_{32}\omega_0) \\ &+ 2\epsilon_2\omega_0 e_2 + 2i_w\omega_0(a_{31} + a_{32} + a_{33} + a_{34})(-\eta(a_{11} + a_{12} + a_{13} + a_{14}) + \epsilon_3(a_{21} + a_{22} + a_{23} + a_{24}) \\ &+ \epsilon_2(a_{31} + a_{32} + a_{33} + a_{34}) + \frac{1}{2\omega_0}(\omega_{w,1} + \omega_{w,2} + \omega_{w,3} + \omega_{w,4}))(\omega_x - c_{22}\omega_0) - 2\epsilon_3\omega_0 e_3) \end{aligned} \tag{A.10}$$

$$\begin{aligned} b_{15} &= \frac{1}{I_x}(i_w(a_{21}(\omega_{w,1} + a_{11}) + a_{22}(\omega_{w,2} + a_{12}) + a_{23}(\omega_{w,3} + a_{13}) + a_{24}(\omega_{w,4} + a_{14}))(c_{23}\omega_0 - \omega_z) \\ &+ (i_w(a_{31}(\omega_{w,1} + a_{11}) + a_{32}(\omega_{w,2} + a_{12}) + a_{33}(\omega_{w,3} + a_{13}) + a_{34}(\omega_{w,4} + a_{14})))(\omega_y - c_{23}\omega_0)) \end{aligned} \tag{A.11}$$

$$\begin{aligned} b_{16} &= k_x\omega_z - c_{32}\omega_0 + \frac{1}{I_x}(i_w(a_{21}(\omega_{w,1} + a_{21}) + a_{22}(\omega_{w,2} + a_{22}) + a_{23}(\omega_{w,3} + a_{23}) \\ &+ a_{24}(\omega_{w,4} + a_{24}))(c_{32}\omega_0 - \omega_z) + (i_w(a_{31}(\omega_{w,1} + a_{21}) + a_{32}(\omega_{w,2} + a_{22}) + a_{33}(\omega_{w,3} + a_{23}) \\ &+ a_{34}(\omega_{w,4} + a_{24})))(\omega_y - c_{22}\omega_0) + e_3) \end{aligned} \tag{A.12}$$

$$\begin{aligned} b_{17} &= k_x\omega_y + c_{22}\omega_0 + \frac{1}{I_x}(i_w(a_{21}(\omega_{w,1} + a_{31}) + a_{22}(\omega_{w,2} + a_{32}) + a_{23}(\omega_{w,3} + a_{33}) \\ &+ a_{24}(\omega_{w,4} + a_{34}))(c_{32}\omega_0 - \omega_z) + (i_w(a_{31}(\omega_{w,1} + a_{31}) + a_{32}(\omega_{w,2} + a_{32}) + a_{33}(\omega_{w,3} + a_{33}) \\ &+ a_{34}(\omega_{w,4} + a_{34})))(\omega_y - c_{22}\omega_0) - e_2) \end{aligned} \tag{A.13}$$

$$
\begin{aligned}
b_{21} &= 2k_y\omega_0(\epsilon_2\omega_z - \eta\omega_x) + 2\omega_0(\epsilon_2\omega_z + \eta\omega_x) + k_y(\epsilon_3 c_{33} - \epsilon_1 c_{13}) \\
&+ \frac{1}{I_y}(2i_w\omega_0(a_{11}+a_{12}+a_{13}+a_{14})(-\epsilon_3(a_{11}+a_{12}+a_{13}+a_{14}) - \eta(a_{21}+a_{22}+a_{23}+a_{24}) \\
&+ \epsilon_1(a_{31}+a_{32}+a_{33}+a_{34}) + \frac{1}{2\omega_0}(\omega_{w,1}+\omega_{w,2}+\omega_{w,3}+\omega_{w,4}))(\omega_z - c_{32}\omega_0) \\
&+ 2\epsilon_1\omega_0 e_1 + 2i_w\omega_0(a_{31}+a_{32}+a_{33}+a_{34})(-\epsilon_3(a_{11}+a_{12}+a_{13}+a_{14}) - \eta(a_{21}+a_{22}+a_{23}+a_{24}) \\
&+ \epsilon_1(a_{31}+a_{32}+a_{33}+a_{34}) + \frac{1}{2\omega_0}(\omega_{w,1}+a_{32}\omega_{w,2}+\omega_{w,3}+\omega_{w,4}))(\omega_y - c_{22}\omega_0) - 2\epsilon_3\omega_0 e_3)
\end{aligned} \tag{A.14}
$$

$$
\begin{aligned}
b_{22} &= 2k_y\omega_0(\epsilon_1\omega_z + \epsilon_3\omega_x) + 2\omega_0(\epsilon_3\omega_x - \epsilon_1\omega_z) + k_y(-\eta c_{33} - \epsilon_2 c_{13}) \\
&+ \frac{1}{I_y}(2i_w\omega_0(a_{11}+a_{12}+a_{13}+a_{14})(-\epsilon_2(a_{11}+a_{12}+a_{13}+a_{14}) + \epsilon_1(a_{21}+a_{22}+a_{23}+a_{24}) \\
&+ \eta(a_{31}+a_{32}+a_{33}+a_{34}) + \frac{1}{2\omega_0}(\omega_{w,1}+\omega_{w,2}+\omega_{w,3}+\omega_{w,4}))(\omega_z - c_{32}\omega_0) \\
&+ 2\eta\omega_0 e_1 + 2i_w\omega_0(a_{31}+a_{32}+a_{33}+a_{34})(-\epsilon_2(a_{11}+a_{12}+a_{13}+a_{14}) + \epsilon_1(a_{21}+a_{22}+a_{23}+a_{24}) \\
&+ \eta(a_{31}+a_{32}+a_{33}+a_{34}) + \frac{1}{2\omega_0}(\omega_{w,1}+a_{32}\omega_{w,2}+\omega_{w,3}+\omega_{w,4}))(\omega_y - c_{22}\omega_0) - 2\epsilon_2\omega_0 e_3)
\end{aligned} \tag{A.15}
$$

$$
\begin{aligned}
b_{23} &= 2k_y\omega_0(\eta\omega_z + \epsilon_2\omega_x) + 2\omega_0(\epsilon_2\omega_x - \eta\omega_z) + k_y(\epsilon_1 c_{33} + \epsilon_3 c_{13}) \\
&+ \frac{1}{I_y}(2i_w\omega_0(a_{11}+a_{12}+a_{13}+a_{14})(-\epsilon_1(a_{11}+a_{12}+a_{13}+a_{14}) - \epsilon_2(a_{21}+a_{22}+a_{23}+a_{24}) \\
&+ \epsilon_3(a_{31}+a_{32}+a_{33}+a_{34}) + \frac{1}{2\omega_0}(\omega_{w,1}+\omega_{w,2}+\omega_{w,3}+\omega_{w,4}))(\omega_z - c_{32}\omega_0) \\
&- 2\epsilon_3\omega_0 e_1 + 2i_w\omega_0(a_{31}+a_{32}+a_{33}+a_{34})(-\epsilon_1(a_{11}+a_{12}+a_{13}+a_{14}) - \epsilon_2(a_{21}+a_{22}+a_{23}+a_{24}) \\
&+ \epsilon_3(a_{31}+a_{32}+a_{33}+a_{34}) + \frac{1}{2\omega_0}(\omega_{w,1}+a_{32}\omega_{w,2}+\omega_{w,3}+\omega_{w,4}))(\omega_y - c_{22}\omega_0) - 2\epsilon_1\omega_0 e_3)
\end{aligned} \tag{A.16}
$$

$$
\begin{aligned}
b_{24} &= 2k_y\omega_0(\epsilon_3\omega_z - \epsilon_1\omega_x) - 2\omega_0(\epsilon_1\omega_x + \epsilon_3\omega_z) + k_y(\eta c_{13} - \epsilon_2 c_{33}) \\
&+ \frac{1}{I_y}(2i_w\omega_0(a_{11}+a_{12}+a_{13}+a_{14})(-\eta(a_{11}+a_{12}+a_{13}+a_{14}) + \epsilon_3(a_{21}+a_{22}+a_{23}+a_{24}) \\
&+ \epsilon_2(a_{31}+a_{32}+a_{33}+a_{34}) + \frac{1}{2\omega_0}(\omega_{w,1}+\omega_{w,2}+\omega_{w,3}+\omega_{w,4}))(\omega_z - c_{32}\omega_0) \\
&- 2\epsilon_2\omega_0 e_1 + 2i_w\omega_0(a_{31}+a_{32}+a_{33}+a_{34})(-\eta(a_{11}+a_{12}+a_{13}+a_{14}) + \epsilon_3(a_{21}+a_{22}+a_{23}+a_{24}) \\
&+ \epsilon_2(a_{31}+a_{32}+a_{33}+a_{34}) + \frac{1}{2\omega_0}(\omega_{w,1}+a_{32}\omega_{w,2}+\omega_{w,3}+\omega_{w,4}))(\omega_y - c_{22}\omega_0) - 2\eta\omega_0 e_3)
\end{aligned} \tag{A.17}
$$

$$
\begin{aligned}
b_{25} &= -k_y\omega_z + c_{32}\omega_0 + \frac{1}{I_y}(i_w(a_{11}(\omega_{w,1}+a_{11}) + a_{12}(\omega_{w,2}+a_{12}) + a_{13}(\omega_{w,3}+a_{13}) \\
&+ a_{14}(\omega_{w,4}+a_{14}))(\omega_z - c_{32}\omega_0) + (i_w(a_{31}(\omega_{w,1}+a_{11}) + a_{32}(\omega_{w,2}+a_{12}) + a_{33}(\omega_{w,3}+a_{13}) \\
&+ a_{34}(\omega_{w,4}+a_{14})))(c_{22}\omega_0 - \omega_x) - e_3)
\end{aligned} \tag{A.18}
$$

$$
\begin{aligned}
b_{26} &= \frac{1}{I_y}(i_w(a_{11}(\omega_{w,1}+a_{21}) + a_{12}(\omega_{w,2}+a_{22}) + a_{13}(\omega_{w,3}+a_{23}) + a_{14}(\omega_{w,4}+a_{24}))(\omega_z - c_{23}\omega_0) \\
&+ (i_w(a_{31}(\omega_{w,1}+a_{21}) + a_{32}(\omega_{w,2}+a_{22}) + a_{33}(\omega_{w,3}+a_{23}) + a_{34}(\omega_{w,4}+a_{24})))(c_{23}\omega_0 - \omega_x))
\end{aligned} \tag{A.19}
$$

$$
\begin{aligned}
b_{27} &= -k_y\omega_y - c_{12}\omega_0 + \frac{1}{I_y}(i_w(a_{11}(\omega_{w,1}+a_{31}) + a_{12}(\omega_{w,2}+a_{32}) + a_{13}(\omega_{w,3}+a_{33}) \\
&+ a_{14}(\omega_{w,4}+a_{34}))(\omega_z - c_{32}\omega_0) + (i_w(a_{31}(\omega_{w,1}+a_{31}) + a_{32}(\omega_{w,2}+a_{32}) + a_{33}(\omega_{w,3}+a_{33}) \\
&+ a_{34}(\omega_{w,4}+a_{34})))(c_{12}\omega_0 - \omega_x) + e_1)
\end{aligned} \tag{A.20}
$$

$$
\begin{aligned}
b_{31} &= 2k_z\omega_0(\epsilon_2\omega_y - \epsilon_1\omega_x) + 2\omega_0(\epsilon_2\omega_y + \epsilon_1\omega_x) + k_z(\epsilon_3 c_{23} + \eta c_{13}) \\
&+ \frac{1}{I_z}(2i_w\omega_0(a_{11}+a_{12}+a_{13}+a_{14})(-\epsilon_3(a_{11}+a_{12}+a_{13}+a_{14}) - \eta(a_{21}+a_{22}+a_{23}+a_{24}) \\
&+ \epsilon_1(a_{31}+a_{32}+a_{33}+a_{34}) + \frac{1}{2\omega_0}(\omega_{w,1}+\omega_{w,2}+\omega_{w,3}+\omega_{w,4}))(c_{22}\omega_0 - \omega_y) \\
&+ 2\eta\omega_0 e_1 + 2i_w\omega_0(a_{31}+a_{32}+a_{33}+a_{34})(-\epsilon_3(a_{11}+a_{12}+a_{13}+a_{14}) - \eta(a_{21}+a_{22}+a_{23}+a_{24}) \\
&+ \epsilon_1(a_{31}+a_{32}+a_{33}+a_{34}) + \frac{1}{2\omega_0}(\omega_{w,1}+a_{32}\omega_{w,2}+\omega_{w,3}+\omega_{w,4}))(c_{12-\omega_y}\omega_0) - 2\epsilon_3\omega_0 e_2)
\end{aligned} \tag{A.21}
$$

$$
\begin{aligned}
b_{32} &= 2k_z\omega_0(\epsilon_1\omega_y + \epsilon_2\omega_x) + 2\omega_0(\epsilon_1\omega_y - \epsilon_2\omega_x) + k_z(\epsilon_3 c_{13} - \eta c_{23}) \\
&+ \frac{1}{I_z}(2i_w\omega_0(a_{21}+a_{22}+a_{23}+a_{24})(-\epsilon_1(a_{11}+a_{12}+a_{13}+a_{14}) - \epsilon_2(a_{21}+a_{22}+a_{23}+a_{24}) \\
&+ \epsilon_3(a_{31}+a_{32}+a_{33}+a_{34}) + a_{21}\omega_{w,1} + \frac{1}{2\omega_0}(\omega_{w,2}+\omega_{w,3}+\omega_{w,4}))(c_{22}\omega_0 - \omega_y) \\
&+ 2\epsilon_2\omega_0 e_1 + 2i_w\omega_0(a_{31}+a_{32}+a_{33}+a_{34})(-\epsilon_1(a_{11}+a_{12}+a_{13}+a_{14}) - \epsilon_2(a_{21}+a_{22}+a_{23}+a_{24}) \\
&+ \epsilon_3(a_{31}+a_{32}+a_{33}+a_{34}) + \frac{1}{2\omega_0}(\omega_{w,1}+\omega_{w,2}+\omega_{w,3}+\omega_{w,4}))(c_{12}\omega_x - \omega_0) - 2\epsilon_1\omega_0 e_2)
\end{aligned} \tag{A.22}
$$

$$
\begin{aligned}
b_{33} &= 2k_z\omega_0(\eta\omega_y - \epsilon_3\omega_x) + 2\omega_0(\eta\omega_y + \epsilon_3\omega_x) + k_z(\epsilon_1 c_{23} + \epsilon_2 c_{13}) \\
&+ \frac{1}{I_z}(2i_w\omega_0(a_{11}+a_{12}+a_{13}+a_{14})(-\epsilon_1(a_{11}+a_{12}+a_{13}+a_{14}) - \epsilon_2(a_{21}+a_{22}+a_{23}+a_{24}) \\
&+ \epsilon_3(a_{31}+a_{32}+a_{33}+a_{34}) + \frac{1}{2\omega_0}(\omega_{w,1}+\omega_{w,2}+\omega_{w,3}+\omega_{w,4}))(c_{22}\omega_0 - \omega_y) \\
&+ 2\epsilon_2\omega_0 e_1 + 2i_w\omega_0(a_{31}+a_{32}+a_{33}+a_{34})(-\epsilon_1(a_{11}+a_{12}+a_{13}+a_{14}) - \epsilon_2(a_{21}+a_{22}+a_{23}+a_{24}) \\
&+ \epsilon_3(a_{31}+a_{32}+a_{33}+a_{34}) + \frac{1}{2\omega_0}(\omega_{w,1}+a_{32}\omega_{w,2}+\omega_{w,3}+\omega_{w,4}))(c_{12}\omega_0 - \omega_x) - 2\epsilon_1\omega_0 e_2)
\end{aligned} \tag{A.23}
$$

$$
\begin{aligned}
b_{34} &= 2k_z\omega_0(\eta\omega_x + \epsilon_3\omega_y) + 2\omega_0(\epsilon_3\omega_y - \eta\omega_x) + k_z(\epsilon_1 c_{13} - \epsilon_2 c_{23}) \\
&+ \frac{1}{I_z}(2i_w\omega_0(a_{11}+a_{12}+a_{13}+a_{14})(-\eta(a_{11}+a_{12}+a_{13}+a_{14}) + \epsilon_3(a_{21}+a_{22}+a_{23}+a_{24}) \\
&+ \epsilon_2(a_{31}+a_{32}+a_{33}+a_{34}) + \frac{1}{2\omega_0}(\omega_{w,1}+\omega_{w,2}+\omega_{w,3}+\omega_{w,4}))(c_{22}\omega_0 - \omega_y) \\
&- 2\epsilon_1\omega_0 e_1 + 2i_w\omega_0(a_{11}+a_{12}+a_{13}+a_{14})(-\eta(a_{11}+a_{12}+a_{13}+a_{14}) + \epsilon_3(a_{21}+a_{22}+a_{23}+a_{24}) \\
&+ \epsilon_2(a_{31}+a_{32}+a_{33}+a_{34}) + \frac{1}{2\omega_0}(\omega_{w,1}+a_{32}\omega_{w,2}+\omega_{w,3}+\omega_{w,4}))(c_{12}\omega_0 - \omega_x) - 2\eta\omega_0 e_2)
\end{aligned} \tag{A.24}
$$

$$
\begin{aligned}
b_{35} &= -k_z\omega_y - c_{22}\omega_0 + \frac{1}{I_z}(i_w(a_{11}(\omega_{w,1}+a_{11}) + a_{12}(\omega_{w,2}+a_{12}) + a_{13}(\omega_{w,3}+a_{13}) \\
&+ a_{14}(\omega_{w,4}+a_{14}))(c_{22}\omega_0 - \omega_y) + (i_w(a_{21}(\omega_{w,1}+a_{11}) + a_{22}(\omega_{w,2}+a_{12}) + a_{23}(\omega_{w,3}+a_{13}) \\
&+ a_{24}(\omega_{w,4}+a_{14})))(\omega_x - c_{12}\omega_0) + e_2)
\end{aligned} \tag{A.25}
$$

$$
\begin{aligned}
b_{36} &= -k_z\omega_x + c_{12}\omega_x + \frac{1}{I_z}(i_w(a_{11}(\omega_{w,1}+a_{21}) + a_{12}(\omega_{w,2}+a_{12}) + a_{13}(\omega_{w,3}+a_{13}) \\
&+ a_{14}(\omega_{w,4}+a_{24}))(c_{22}\omega_0 - \omega_y) + (i_w(a_{21}(\omega_{w,1}+a_{21}) + a_{22}(\omega_{w,2}+a_{22}) + a_{23}(\omega_{w,3}+a_{23}) \\
&+ a_{24}(\omega_{w,4}+a_{24})))(\omega_x - c_{12}\omega_0) - e_1)
\end{aligned} \tag{A.26}
$$

$$
\begin{aligned}
b_{37} &= \frac{1}{I_z}(i_w(a_{11}(\omega_{w,1}+a_{31}) + a_{12}(\omega_{w,2}+a_{32}) + a_{13}(\omega_{w,3}+a_{33}) + a_{14}(\omega_{w,4}+a_{34}))(c_{22}\omega_0 - \omega_y) \\
&+ (i_w(a_{21}(\omega_{w,1}+a_{21}) + a_{22}(\omega_{w,2}+a_{22}) + a_{23}(\omega_{w,3}+a_{23}) + a_{24}(\omega_{w,4}+a_{24})))(\omega_x - c_{12}\omega_0))
\end{aligned} \tag{A.27}
$$

Appendix B

CD Contents

Folder	File	Description
Common for all	euler2q.m	compute quat. from euler angles
Common for all	q2euler.m	computes euler angles from quat.
Common for all	qInvProduct.m	computes inverse quat. product
Common for all	qProduct.m	computes quat. product
Common for all	Rquat.m	computes the rotation matrix
Common for all	Sk_matrix.m	creates the skew symmetric matrix
Common for all	init.m	initialisation of the ESMO satellite
Common for all	lin.m	computes the linearaized **F** matrix
Common for all	nonlin.m	computes the nonlinear propagation
Common for all	plotter.m	plots the tracking and estimation errors
Common for all	initStarEKF.m	initalize the single star EKF
Common for all	starEKF.m	the discrete EKF
PD	PDcontrol.mdl	ESMO with PD controller
M.PD	mPDcontrol.mdl	ESMO with Model dependent PD controller
Robust	Robust.mdl	Simulink model with robust controller